Università degli Studi di Milano
Facoltà di Scienze Matematiche, Fisiche e Naturali
Dipartimento di Scienze della Terra "Ardito Desio"
Scuola di Dottorato "Terra, Ambiente e Biodiversità"
Dottorato di Ricerca in Scienze della Terra
Ciclo XXV – Raggruppamento disciplinare GEO/09

Chromite: from the mineral to the commodity

PhD Thesis

Maria Pedrotti
Matr. N. R08693

Tutore
Prof. Giovanni Grieco

Anno Accademico
2011-2012

Coordinatore
Prof. Elisabetta Erba

A chi mi vuole bene,
mi stima e crede in me

Index

Abstract

Chromite belongs to the spinel group with the general chemical formula XY_2O_4, where X and Y represent divalent and trivalent metal ions, respectively. Four types of chromite ore deposits occur as either lode or secondary deposits. Lode chromite ore deposits comprise stratiform and podiform deposits, whereas secondary chromite ore deposits comprise laterite and placer deposits.

Chromite is an important industrial mineral used in the refractory industry. Moreover it is the only industrial source of chromium for chemical and metallurgical industries and to be marketed as a valuable commodity it requires very demanding quality parameters that differ according to the kind of application. Chromite ore cannot be usually sold as it is and, therefore, some kind of ore beneficiation is required in order to separate chromite from gangue minerals. The most commonly used beneficiation methods for chromite ores are the gravity methods, such as the shaking table, jig, spiral and Reichert cone methods.

The present work deals with the geologic studies that, coming after prospection, lead to the evaluation of the chromite ore quality and to planning and/or improvement of beneficiation plants.

The quality of chromite ore deposits, in order to rank them for possible exploitation, was studied in five deposits of Madagascar (Andriamena, Antanimbary, North Befandriana, North Belobaka and North Toamasina), in collaboration with UT Group s.r.l., for the development of chromite mining in the country. The basic geological, mineralogical and geochemical study of the deposits led to the reconstruction of genetic models for each of them. This was the starting point for a more detailed study on the quality of the chromite ore. The five most important chromite ore localities, investigated for this work, are all characterized by outcropping chromitite bodies hosted within mafic/ultramafic intrusions of probable Neoproterozoic to Cambrian age. Metamorphism and alteration affected, at different degrees, all chromitites, but never completely obliterate their primary characters. Chromitite host rocks are peridotite, orthopyroxenite or orthoamphibolite, while primary gangue phases are orthopyroxene, olivine, rare plagioclase, ilmenite, rutile, pyrrhotite and pentlandite. Secondary assemblage comprises serpentine, talc, Cr-chlorite, tremolitic to actinolitic amphibole and magnetite. Geologic, textural, mineralogical and mineral chemistry data are compatible with an ophiolite origin for North Befandriana chromitites and a layered intrusion origin for Andriamena, North Toamasina, North Belobaka and Antanimbary chromitites. These latter show differences that can be related to a different position of the chromitite bodies within the stratigraphic sequence of a layered intrusion. North Befandriana is a high quality deposit that could be exploited without any beneficiation of the ore, Andriamena needs beneficiation to reach market standard, Antanimbary and North Belobaka is low quality for metallurgical or chemical use but could be a good prospect for refractory market. Finally North Toamasina chromite ore is not suitable for any market even after beneficiation.

An innovative study of geologic processes that can affect chromite ore beneficiation was applied to Vavdos chromite deposit (Greece) hosted in the Vavdos ultramafic massif belonging to the Halkidiki ophiolite of the Circum-Rhodope orogenic belt. Here metamorphic modification of chromite led to redistribution of Cr_2O_3 from chromite to silicates. The effect of the redistribution is to lower the efficiency of gravity plants as Cr_2O_3 contained in silicate phases will be preferentially discharged into the tailing during enrichment. The influence of this process that is widespread in chromite ores, on chromite enrichment was evaluated quantitatively. Generally accepted assumption that chromite ores do host Cr only in chromite is misleading as metamorphosed chromite ores host significative amounts of Cr in gangue phases and especially in Cr-chlorite. This study, of a completely metasomatized chromite ore, shows that about 3 wt% of total Cr_2O_3 in the rock is hosted in Cr-chlorite; while only about 0.2 wt% of total Cr_2O_3 is hosted in serpentine. As Cr-chlorite can host even more Cr_2O_3 than at Vavdos, and as the deepest alteration of chromite due to metasomatism occurs for ores containing about 34% chromite, the amount of Cr_2O_3 redistributed within the gangue can be even higher than at Vavdos, especially in low grade disseminated ores, where probably about 5-6% of Cr_2O_3 can be hosted in the gangue, a value that could rise to 7-8 wt% for high Cr_2O_3 Cr-chlorite. The effect of this wrong assumption is a mistake in the calculation of plant efficiency that will be overestimated. Mistakes due to redistribution of Cr_2O_3 during metamorphism can be easily avoided through mineralogical analysis that can detect the

presence of Cr-chlorite in the ore. Planning of beneficiation in Cr-chlorite-bearing chromite ores requires additional investigation, concerning Cr_2O_3 content in Cr-chlorite and Cr-chlorite amount in the ore.

A procedure to evaluate efficiency and results of gravity chromite enrichment plants was tested on Brieville enrichment plant (Madagascar), which belongs to Kraomita Malagasy mining company. Here a detailed study of chromite sand quality parameters at each step within the plant together with the measuring of all sand flow rates led to the reconstruction of separation efficiency at each step of chromite processing. The results of grain size, XRD, XRF, EMP and grain counting analyses together with separation efficiency (SE) and liberation degree (LD) evaluation allow to conclude that Brieville plant does not properly work due to the low sorting of sands feeding shaking tables that negatively affects their separation efficiency. Moreover the low degree of liberation of chromite, especially in the coarsest grain sizes, negatively affects the re-cycling process of mix materials. Plant efficiency and quality of final product can be improved by: moving the Cr_2O_3-enriched mixes to the concentrate and the Cr_2O_3-depleted mixes to the waste; grinding to finer grain size the overall feed of shaking tables and the mixes that will be re-cycled and substituting hydrosizers with screens. The first change, that does not involve any additional operational cost, has been effectively applied to the plant just after publication of the present study. The other changes involve additional operational costs and require a detailed economic analysis before being applied to the plant.

Finally a completely new technology for high performance beneficiation of chromite sand that leads to the production of chromite refractory sands was tested. For this work chromite concentrate sand from Krasta enrichment plant (Albania) was used. The innovative beneficiation plant of Omega Foundry Machinery LTD. comprises a drum magnet and the new Inclined Fluidised Separator that uses an air cushion as the fluidizing agent during gravity driven grain separation. Refractory chromite sand chemical and technical requirements are the most demanding in chromite market and no chromite ore can attain them by simple crushing and grinding. On the other hand usual enrichment methodologies either cannot meet the required parameters or have a very low refractory sand recovery. The combination of drum magnet and Inclined Fluidised Separator in the Omega Foundry Machinery LTD. pilot plant not only produces a good quality refractory sand, but the result is reached with a high recovery, making of this plant an optimal solution for the production of refractory chromite sand. The Inclined Fluidised Separator is particularly performing as it combines a very high recovery of silica in the waste with an increase of the grain size of concentrate.

Chapter 1

Chromite: history, geology, uses and report of chromium market

1.1 Introduction

World chromite supply has come under severe pressure over the past year driven by robust demand for ferrochrome used in ferroalloy production, ultimately used to make stainless steel.

With the metal industry hungry for raw material, residual supplies that typically serve non-metallurgical markets (known as "special grades" for the refractory, chemical, and foundry sectors) are selling out.

Over 90% of the world's chromite production is converted into ferrochrome for metallurgical applications, a figure that dwarfs supply to non-metallurgical markets. Out of a total global chromite annual output of about 19 Mt, the refractory industry accounts for about 1% while 3% each is consumed in the foundry and chemical industries.

Given that most chromite is produced by vertically integrated ferrochrome producers, the amount of material available to supply non-metallurgical markets is dictated by the fluctuating requirements of the metallurgical industry.

1.2 History

Chromium is one of the "newer" elements, celebrating the 200th anniversary of its discovery in 1997. It was about 1760 when the chromium-bearing mineral crocoite from deposits in the Ural Mountains was recognized in Europe. However, it was not until 1797-98 that chromium was isolated by Nicolas-Louis Vauquelin, a professor of chemistry at the Paris École des Mines. Chromium was discovered later than other metals because it does not appear terrestrially as a native metal, and it is strongly bonded in the minerals in which it occurs. The wide variety of colorful compounds derivable from crocoite led Vauquelin to name the newly discovered element chromium, a name derived from χρομα (chroma), the Greek name for color. Crocoite, also called Siberian red lead, was found to produce a yellow pigment that became popular. Thus paint became the first commercial application of chromium. Chromium was soon discovered in chromite, a much more common mineral, also from the Ural Mountains.

Chromium is primarily used in the metallurgical industry as an alloying element in steel. Chromium confers properties on the alloy that are not achievable with base metals alone. The most common use of chromium is with iron to make stainless steel, an iron-chromium alloy. Chromium confers oxidation resistance to stainless steel, making it "stainless." Stainless steel, in addition to being commonly found in home and commercial kitchens, is an important engineering alloy used throughout industry in machinery, containers, and pipes. Chromium is also used in chemicals for a variety of purposes.

1.3 Geology

1.3.1 Mineralogy

The most important chromium-bearing mineral is chromite, which is the only ore of chromium. It is in the spinel group with the general chemical formula XY_2O_4, where X and Y represent divalent and trivalent metal ions, respectively. The six end-member compositions that combine to form chromite are hercynite ($FeAl_2O_4$), spinel

($MgAl_2O_4$), Fe-chromite ($FeCr_2O_4$), magnesiochromite ($MgCr_2O_4$), magnetite (Fe_3O_4), and magnesioferrite ($MgFe_2O_4$). Thus, the general formula is $(Mg,Fe)(Cr,Al)_2O_4$. At high temperatures (>1200 °C) and low oxygen fugacity, the conditions under which chromite first forms, there is complete solid solution between Mg and Fe and between Cr and Al. Other elements found in lesser amounts are Ti, Zn, Ni, V, Mn, and Co.

Ions in spinel-group minerals form a close-packed, cubic, face-centered lattice that imparts a relatively high density; the typical specific gravity of commercial chromite product is 4.5 to 4.8 g/cm^3. The mineral chromite is black with a metallic to dull luster and yields a dark brown streak, distinguishing it from other black spinel-group-minerals, which typically have a white streak (e.g., magnetite). The mineral chromite is opaque to slightly translucent in thin section, depending on the amount of trivalent ion present; it is opaque if it contains very little Fe^{3+} but slightly translucent if it contains more than a few percent of Fe^{3+}. Chromite with very low amounts of Fe^{3+} is nonmagnetic; higher amounts of Fe^{3+} make it weakly magnetic. Hardness is typically 5.5 to 6.5 on the Mohs scale. Chromite normally does not show cleavage and exhibits conchoidal to uneven fracture.

1.3.2 Chromite ore deposit types

Four types of chromite ore deposits occur as either lode deposits or secondary deposits. Lode chromite ore deposits comprise stratiform and podiform deposits, whereas secondary chromite ore deposits comprise laterite and placer deposits.

Ultramafic and mafic magmas can be oversaturated in respect of chromite by several petrogenetic processes such as: i) magma mixing; ii) assimilation of country rocks; iii) pressure decrease. Exsolved solid chromite or chromite melt is concentrated by orthomagmatic segregation processes, which reach from quiet gravitational setting to dynamic flow channels. Ore deposits occur either in layered mafic intrusions where tabular seams prevail (stratiform chromite or Bushveld Type), or in the mantle section of ophiolites (podiform chromite or Alpine Type). Chromites of these two main metallogenic settings display a different composition and chemical evolution controlled by the pseudo stratigraphic position (Figure 1). Trace elements provide illuminating constraints on chromite petrogenesis (Pagé & Barnes 2009). A third setting of chromite deposits is concentrically zoned ultramafic ring intrusions of the Ural-Alaska Type (Augé et al. 2005). In the Ural Mountains, these intrusions were the source of historically very significant placers of chromite and platinum. Some Archean komatiitic intrusions host minor chromite deposits (Rollinson 1997, Prendergast 2008). Significant genetic settings of chromite deposits include:

- stratiform chromite in layered mafic intrusion (e.g. Bushveld);
- podiform chromite within dunite pods of the mantle section of ophiolites;
- stratiform chromite in ultramafic cumulates of igneous intrusion in ophiolites (e.g. Philippines);
- stratiform chromite in Ural-Alaska Type ring intrusion.

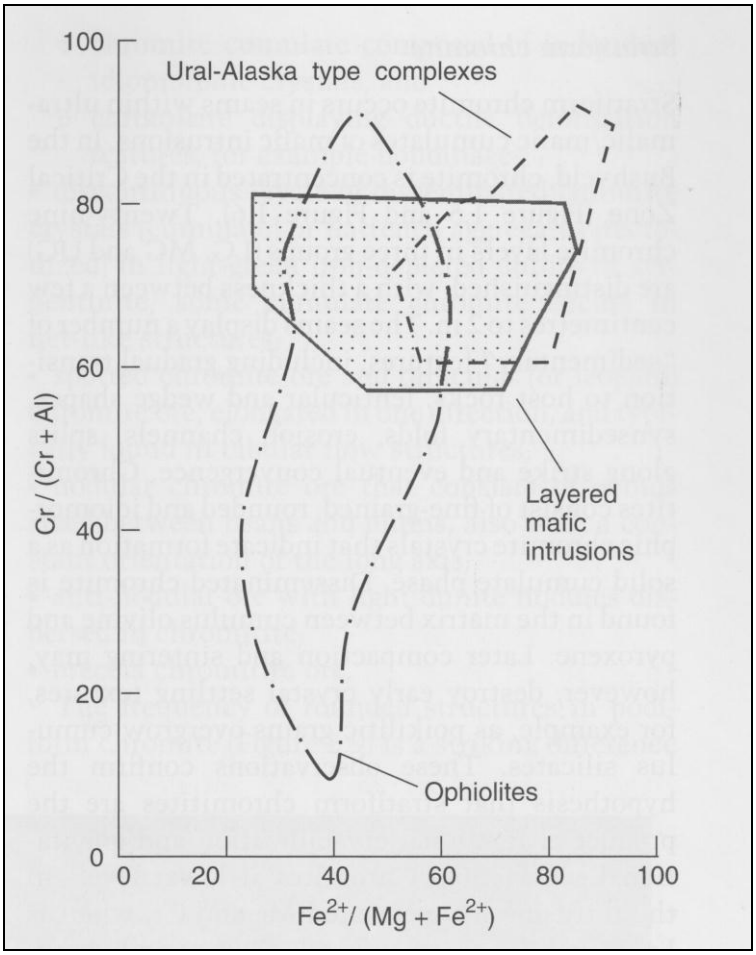

Figure 1. Variation of chromium, magnesium, iron and aluminium in chromites of layered mafic intrusions, Ural-Alaska type ultramafic complexes and ophiolites (adapted from Irvine 1967).

Secondary chromite-containing deposits exist as laterite deposits derived from weathering and leaching of peridotite host rock that contains 1% to 2% of the mineral chromite; they are not commonly ore grade. Large peridotite bodies in tropical climates with favorable chemical topographic environments can undergo chemical weathering that results in residual soils. Subsequent leaching of silicate minerals helps accumulate chromite mineral. These lateritic soils make it easy and inexpensive to concentrate chromite mineral from its matrix. Such deposits are mined in Indonesia and Vietnam. Although production from these deposits is tiny fraction of world production, their potential is enormous.

Placer chromite results from erosion of peridotite host rock. The relatively dense chromite mineral is concentrated as lag deposits on beaches or in streams. These have the least economic importance of the four types of chromite mineral deposits. None are currently being mined.

1.3.3 Stratiform chromite

Stratiform chromite occurs in seams within ultramafic/mafic cumulates of layered intrusions. In the Bushveld, chromite is concentrated in the Critical Zone. Twenty-nine chromitite layers in three groups (LG, MG and UG) are distinguished, with a thickness ranging between a few centimeters and 2 meters. The seams display a number of "sedimentary" features, including gradual transition to host rocks, lenticular and wedge shapes, synsedimentary folds, erosion, channels, splits along strike and eventual convergence.

Chromitites consist of fine-grained, rounded and idiomorphic chromite crystals that indicate formation as a solid cumulate phase. Disseminated chromite is found in the matrix between cumulus olivine and pyroxene. Later

compaction and sintering may, however, destroy early crystal settling textures, for examples as poikilitic grains overgrow cumulus silicates. These observations confirm the hypothesis that stratiform chromitites are a product of fractional crystallization and fractional segregation. Chromites at lower levels in the intrusion have elevated Mg and Cr, whereas Fe, Ti and V increase upwards.

Two main hypotheses have been proposed to explain the cyclic repetition of chromite formation in the Bushveld: the first invokes mixing of resident and fresh magma injected into the chamber (Naldrett et al. 2009), the second invokes assimilation of siliceous roof rocks (Kinnaird et al. 2002). The hybrid melt is oversaturated in respect to chromite, leading to extensive chromite (and PGE) crystallization (Spandler et al. 2005). The second hypothesis relies on physical, not chemical principles. Pressure changes by injection of new melt batches also induce precipitation of chromite. This explanation better accounts for the giant area covered by the seams, simply because pressure must change instantly everywhere in the melt chamber (Cawthorn 2005b).

1.3.4 Podiform chromite

Podiform chromite deposits occur in dunite bodies of the mantle section of ophiolites and more rarely in dunitic and pyroxenitic cumulates of the ophiolitic magma chamber. Ore bodies are irregularly dispersed and relatively small (mostly between 0.1 and 1 Mt). Shape, structure and texture depend on the precise origin. Dunites with chromitite occur in the tectonized mantle harzburgite, displaying ductile deformation and alignment along flow structures. Both dunite and associated chromitite were firstly explained as due to refractory phases of mantle melts rising beneath mid-oceanic rifts (Thayer 1969). The most recent models explain chromite saturation and formation as a process induced by metasomatic reaction of upflowing melt with surrounding harzburgite; assimilation of pyroxenes and pressure decrease drive basaltic and boninitic liquids into the field of chromite (± olivine) precipitation (Arai & Yiurimoto 1994, Zhou & Robinson 1997, Pagé & Barnes 2009). Chromite and dunite bodies are products of liquid unmixing (or fractional crystallization) and gravitational segregation. In the feeder zone of the mid-oceanic magmatic chamber, discordant disseminated and massive ores are formed. Ultramafic cumulates contain concordant lenses and seams of chromitite. Podiform chromite ore can be associated with cross-cutting dykes of chromitite that represent oxide melt injected into host rocks.

Structural types of podiform chromite ore include:

- massive crystalline chromitite, typical for large ore bodies;
- discontinuous layers of disseminated chromite crystals (cumulate) or flattened aggregates (tectonized) in light-green iron-depleted dunite or serpentinite. Some chromite occurs in net-like structures;
- spotted chromite ore and orbicular (or leopard) chromite ore, elongated in one direction, and typically found in tabular flow structures;
- nodular chromite ore that consists of ovoid sized between beans and plums, also with a constant orientation of the long axis;
- anti-nodular ore with light dunite nodules dispersed in chromitites;
- breccia chromite ore.

The frequency of rounded structures in podiform chromite is a striking difference to stratiform chromite, which never displays such features. The cause is probably liquid unmixing of olivine and chromite melt in the former, assisted by aqueous fluids (Matveev & Ballhaus 2002). The directional structures of chromite ores may be due to viscous liquid flow, or to high-temperature ductile deformation in the mantle. Detailed structural investigations provide fascinating insight into mantle dynamics below oceanic spreading centers (Ceuleneer & Niccolas 1985, Ceuleneer et al. 1996). However, the preferred geodynamic setting of podiform chromite ore deposits may be rather suprasubduction fore-arc and back-arc rifts and primitive island arcs than mid-oceanic spreading zone (Zohu & Robinson 1997).

Podiform chromite is chemically different from that of stratiform ore, with higher Mg/Fe and Cr/Fe ratios, and Al_2O_3 contents up to 62%. Alumina and iron concentrations increase with higher position in the ophiolite stratigraphy. This favors formation of refractive ore (e.g. Philippines, Cuba and New Caledonia). The composition of chromites is also linked to the degree of partial melting of the mantle source. High Cr# chromite is believed to originate from higher degrees, whereas low Cr# ore may stem from low degrees of mantle melting (Stowe 1994). Highest chromium and magnesium contents are observed in lowest sections of ophiolites. Compared with stratiform and disseminated ore, podiform chromite ore bodies in the mantle section tend to display higher Cr_2O_3 and lower Al_2O_3.

Stowe (1994) pointed out that chromite deposits vary through geological time. Chromite deposits with features similar to the podiform type occur in Paleo- to Mesoarchean (3.5-2.9 Ga) greenstone belts. Giant stratiform deposits appear as soon as large cratons were consolidated (2.9-2.0 Ga). Podiform chromite sensu strictu emerge with the first modern ophiolites, at ~800 Ma.

1.4 Distribution of major chromite deposits

Figure 2 shows the distribution of major chromite ore deposits around the world. Ophiolite complexes are more abundant than stratiform igneous complexes than 2.06 Ga. Nevertheless about 70% of all chromite ore mined in 2002 came from stratiform deposits (Papp 2005).

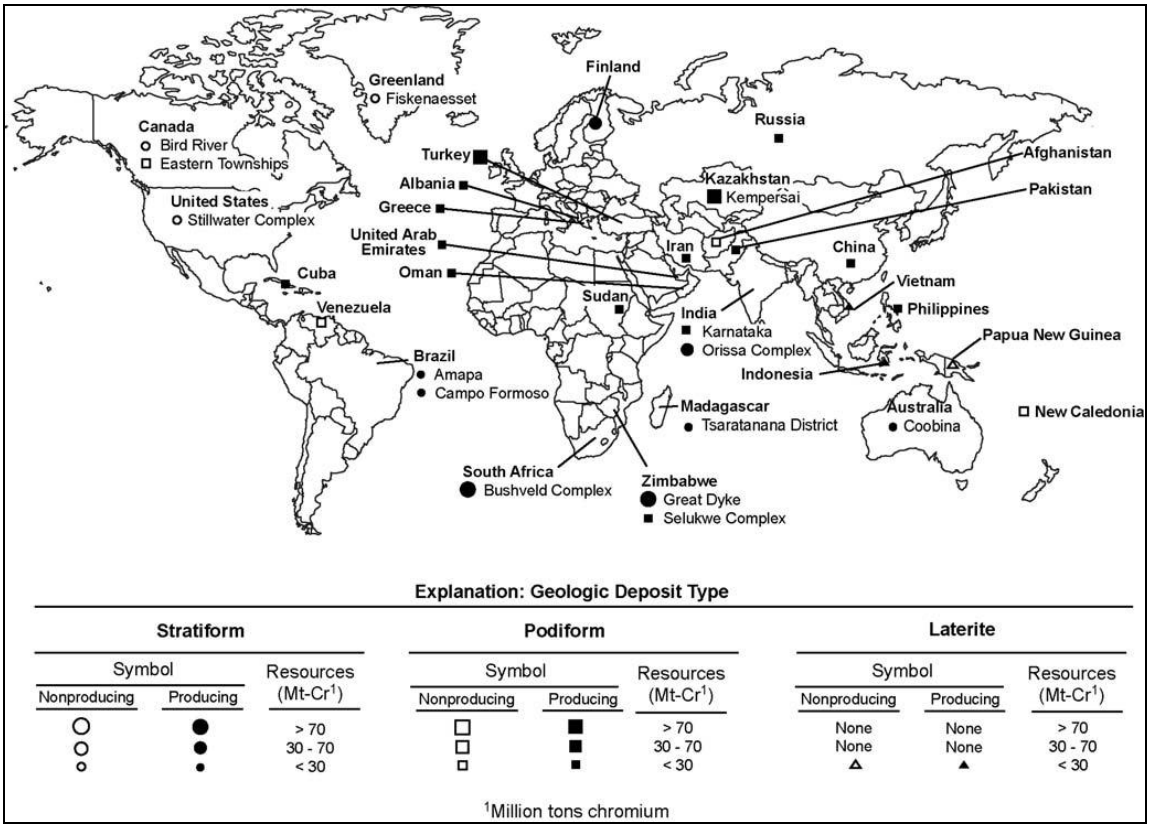

Figure 2. Location, geologic type and size of major chromite ore deposits.

About 95% of the world's chromite ore resources are in the Bushveld Igneous Complex of South Africa and the Great Dyke of Zimbabwe; the majority is in the Bushveld. The largest concentration of podiform chromite ore is in the Kempersai area of Kazakhstan (Papp 2001). Since the dislocation of traditional market that resulted from the dissolution of the Soviet Union in 1991, chromite ore production in the Bushveld from 2000 through 2004 has been two to three times greater than of the Kempersai.

The Bushveld Complex is one of the largest layered intrusions in the world, occupying about 64,340 km² and contains more than 11 billion tons of total resource (Vermaak 1986). One layer, informally called the Steelport Seam, contains 1.4 billion tons of resources. The Steelport Seam can be traced over most of the Bushveld.

The Kempersai area of the Southern Urals in Kazakhstan is home to the world's largest podiform chromite ore deposits, covering about 1,200 km². These deposits occur where parts of the ocean floor were obducted over continental rocks. This area has more than 75 times the reserves and about 4 times more production than the podiform deposits of Turkey, which rank second in podiform chromite production and reserves.

World reserves of chromium are about 213 Mt, and the world reserve base of chromium is about 444 Mt. The worldwide distribution of 1.52 billion tons of chromium in identified chromite ore resources is Africa, 52%; Asia, 38%; Europe, 5%; the Americas, 3%; the Middle East, 2% and Oceania, 0.1%. The U.S. Geological Survey (USGS) reports reserves and reserve base information annually in *Mineral Commodity Summaries*.

1.5 Chromite uses

The International Chromium Development Association (ICDA) reports world production of chromite by end use sector, and categorizes them as chemical, foundry sand, metallurgical, and refractory. In 2009, ICDA reported chromite use as 90% metallurgical, 5% chemical and 5% refractory and foundry sand (Figure 3).

The metallurgical industry processes chromite into ferrochromium or chromium metal, which are used as alloying materials to make a variety of ferrous and nonferrous alloys. The major end use is stainless steel, a ferrous alloy made resistant to oxidation and corrosion by the addition of chromium.

The chemical industry uses chromite to make sodium dichromate, which is a chemical industry product and intermediate product used for making other chromium chemicals. Chromium chemicals find a wide variety of end uses such as leather tanning, pigments, plating for both decorative and engineering application, surface treatment of reactive metals and manufacture of chromium metal, a key ingredient in alloys for aircraft engines and land-bases turbines.

Chromite is useful in the foundry and refractory industries because it retains its physical properties at high temperatures and is chemically inert. Chromite is used as facing sand in the foundry industry, and the refractory industry uses chromite to produce refractory material, including shapes, plastics, and gunning mixes. Refractory materials are used in the production of ferrous and nonferrous alloys, glass and cement.

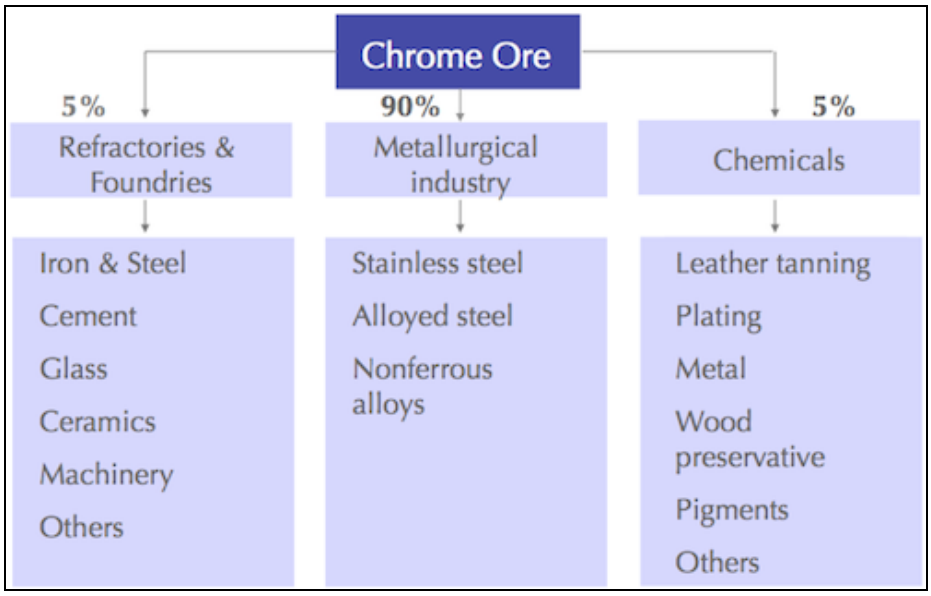

Figure 3. Rate of world chromite production divided in end use sector.

1.6 Metallurgical Industry

In the metallurgical industry, chromite is used to make ferrochromium, which is in turn used to make steel and nonferrous alloys. Ferrochromium is produced from chromite ore in an electric-arc furnace using reluctant and fluxes to remove oxygen.

1.6.1 High-carbon ferrochromium

Most ores smelted with coke in an electric furnace produce metals that are saturated with carbon. For ferrochromium, the saturation point is approximately 9%, but actual carbon content varies with the condition of the ore and the composition of the slag. For example, with a lumpy, refractory ore and a slag containing approximately equal amounts of magnesia, alumina, and silica, a ferrochromium is produced that contains 4 to 6 % carbon and less than 1.5% silicon. This is a result of high temperatures generated by a viscous slag, of a slowly reacting bulky ore, and, possibly, of refining of the molten metal by undissolved ore in the slag. When the rate of the reducing reaction is increased by using fine ore, or when the slag is made less viscous by adding lime to the melt, the carbon level of the ferrochromium approaches saturation.

Adding more silica to the charge produces what is called charge ferrochromium, a carbon-saturated alloy with increased silicon content.

During the smelting of high-carbon or charge ferrochromium, slag and metal are tapped from the furnace into a ladle and separated by decanting or skimming. The recovery of chromium from the ore varies: in a good operation 90% is recovered in the molten metal; of the 10% remaining in the slag, some is in metallic form and can be recovered by mineral processing techniques. The smelting of charge ferrochromium consumes 4,000 kilowatt-hours of electric power per ton of alloy produced, compared with 4,600 kilowatt-hours per ton for high-carbon ferrochromium.

If silica is added to the charge until its weight equals that of the ore, the smelting processes will yield what is known as ferrochrome silicon. Containing 38-42% silicon and less than 0.1% carbon, this alloy is used as a deoxidizer in the production of stainless steel and as an intermediate material in the production of low-carbon ferrochromium. Because of the greater energy required to reduce silica to silicon, the smelting of ferrochrome silicon consumes 7,600 kilowatt-hours per ton of product.

1.6.2 Low-carbon ferrochromium

When chromite and lime are melted in an open electric-arc furnace and then contacted with ferrochrome silicon, a low-carbon (0.05%) ferrochromium can be obtained. In an alternate process, high-carbon ferrochromium is oxidized and then blended with additional high-carbon ferrochromium. The briquetted mixture is placed in a large vacuum furnace, which is heated by graphite resistors to 1,400 °C at a reduced pressure of 30 Pascal.

The carbon is removed from the alloy (going off as carbon monoxide) to a level as low as 0.01%.

1.6.3 Steels

Formerly, much of the alloy had to be of the low-carbon type, but since the advent of the argon-oxygen decarburization process, which allows steelmakers to burn off impurities such as silicon and carbon without also removing too much chromium, the demand has shifted to charge ferrochromium. Refined ferrochromium is now used principally as a trimming agent.

Stainless steels have a high resistance to oxidation and atmospheric corrosion owing mainly to the presence of chromium, which, at levels varying between 10% and 26%, forms a protective oxide film on the surface of the steel. The low-carbon ferritic stainless steels cannot be hardened by heat treatment; ferritic varieties containing 17% to 18% chromium are used in automobile trim and in equipment for handling nitric acid. High-carbon martensitic

stainless steels are used when hardness and abrasion resistance are desired; steels of this type with 13% chromium are made into cutlery. Nickel and manganese can be added to high-chromium (16% to 26%) stainless steels to form the austenitic types, of which the 18% chromium – 8% nickel variety is probably the best known. In addition to their resistance to oxidation and corrosion, austenitic steels maintain their strength at high temperatures better than do the plain chromium steels. Sometimes molybdenum, tungsten, niobium, or titanium is added to improve strength and corrosion resistance or to stabilize the carbides present. Steels of this type containing up to 26% chromium have excellent oxidation resistance at high temperatures; they are used in furnace parts, burner nozzles, and kiln linings.

Up to 2% chromium is added to low-alloy steel to improve hardenability, wear resistance, and high-temperature strength. Such steels, containing chromium in combination with other elements, such as molybdenum, nickel, manganese, and vanadium, are used for springs, roller and ball bearings, dies, rails, and high-strength structures. Steels containing 6-10% chromium have increased corrosion and oxidation resistance and are used in the form of tubes in the oil industry.

1.6.4 Chromium metal

Pure chromium is produced either by the thermal reduction of Cr_2O_3 with aluminum or by the electrolysis of trivalent chromium solutions.

The aluminothermic process begins with the roasting of fine ore, soda, and lime in air at 1,100 °C. This creates a calcine containing sodium chromate, which is leached from the insoluble gangue and then reduced and precipitated as Cr_2O_3. The Cr_2O_3 is blended with finely divided aluminum powder, charged to a refractory-lined container, and ignited. The combustion quickly generates temperatures in excess of 2,000 °C giving a clean separation of chromium from the slag. The purity of the metal, varying from 97% to 99% chromium, depends on the starting materials.

In the electrolytic process, milled high-carbon ferrochromium is leached by a mixture of reduced anolyte (electrolytic solution recycled from the anode side of the smelting cell), a chrome alum mother liquor based on a solution of ammonium sulfate recycled from a later stage in the process, and sulfuric acid. The resulting slurry is cooled, and silica and other undissolved solids are filtered from the solution. The iron forms crude ferrous ammonium sulfate crystals, which also are filtered out. The mother liquor is then clarified in a filter press, and about 80% of the chromium is stripped by precipitation as ammonium chrome alum. The mother liquor is sent back to the leach circuit while the chrome alum crystals are dissolved in hot water and fed into the cathode portion of an electrolytic cell. The cell is divided by a diaphragm in order to prevent the chromic and sulfuric acids formed at the anode from mixing with the catholyte (cathode electrolyte). With the passage of electric current from a lead anode to a thin stainless-steel cathode sheet, chromium is plated onto the cathode and, every 72 hours, is stripped from the sheet, sealed in stainless steel cans, and heated to 420 °C to remove water and hydrogen. This electrolytic chromium contains 0.5% oxygen, which is too high for some applications; combining it with carbon and heating the briquettes to 1,400 °C at 13 Pascal lowers the oxygen content to 0.02%, resulting in a metal more than 99.9% pure.

1.6.5 Nonferrous alloys

Chromium is added to cobalt alloys in amounts up to 25% to obtain corrosion resistance and hardness. Cobalt-chromium-tungsten alloys are used for cutting tools and hard facings.

Nickel-chromium super alloys with up to 60% chromium and sometimes a little iron are used for high-temperature applications. Chromium is also added to aluminum alloys in quantities up to 0.5% to improve their strength and corrosion resistance.

1.7 Chemical Industry

Chromite has been the key raw material in the manufacture of chromium chemicals since the early 19th century, initially to make brightly colored pigments.

Today, production includes biocides, catalysts, corrosion inhibitors, metal plating and finishing chemicals, oil field chemicals, pigments, printing chemicals and tanning compounds. The largest single use of chromium chemicals today is the use of chromium salts in the manufacture of leather from animal skins, a process which began in the middle of the 19th century. Chromium plating is the electro deposition of chromium from a solution of chromic acid; it was started in the early 1900s.

A recent use for chromium is for wood preservation. Chromium-copper-arsenate (CCA) impregnates wood to protect it from weathering, insects, and decay for up to 20 years.

Major chromium chemical plants are in Japan, Kazakhstan, Russia, South Africa, the United Kingdom and United States.

Sodium dichromate and chromic acid accounted for the largest amount of U.S. chromium chemical exports and imports, respectively.

1.7.1 Pigments

Pigments account for about one-third of the primary production of chromium chemicals. Chrome oxide green, which is nearly pure Cr_2O_3, is the most stable green pigment known. It is used for coloring roofing granules, cements, and plasters. It is also employed as a fine powder for polishing. Chromium yellow varies greatly in the shades available and is essentially lead chromate, or crocoite. This pigment makes an excellent paint for both wood and metal. Zinc yellow, a basic zinc chromate, is used as a corrosion-inhibiting primer on aircraft parts fabricated from aluminum or magnesium. Molybdate orange is a combination of lead chromate with molybdenum salts. Chrome green is a mixture of lead chromate with iron blue. This pigment has excellent covering and hiding power and is widely used in paints.

1.7.2 Tannings

About 25% of the chromium chemicals produced goes into chrome tanning of leather. This process uses chrome reagents in the form of basic chromic sulfates that, in turn, are produced from sodium dichromate. This reagent is produced by heating the ore with soda ash and then leaching out soluble chromate, which is then converted to the dichromate by treatment with sulfuric acid.

1.7.3 Surface treatments

More than one-fourth of the production of primary chromium chemicals is employed in metal-surface treatments and corrosion control. Such applications include chromium plating, chromizing, anodizing of aluminum, and treatment of zinc and magnesium. Chromium chemicals are used in dips for iron, steel, brass, and tin and also as inhibitors for brines and for recirculating water systems.

1.7 Refractory Industry

Chromite is used directly in the refractory industry because it resists degradation when exposed to heat. Basic refractories are made of chromite, dolomite, magnesite, or various combinations of magnesite and chromite. Refractories also are categorized as shaped or unshaped. Shaped refractories are manufactured to fit together, like building blocks, to form a desired geometric structure. Unshaped refractories include mortars (materials used to

bind shape refractories together), plastics (materials that are formed into a desired shape), and gunning (material that is sprayed onto a surface).

Major end users for chromite refractories are in the cement, copper, glass, nickel and steel industries. Basic refractories are used in copper and nickel furnace. The glass industry uses chromite refractories in glass tank regenerators; the cement industry uses chromite refractories primarily in transition zones of cement kilns. Basic refractories typically have been used in open hearth and electric arc steelmaking furnaces.

A typical analysis of a chromite ore suitable for refractory purposes is 38% to 48% Cr_2O_3, 12% to 24% Al_2O_3, 14% to 24% Fe_2O_3, 14% to 18% MgO, and less than 2.5% SiO_2. The usefulness of chromite as a refractory is based on its high melting point of 2,180 ° C, moderate thermal expansion, the stability of its crystalline form at elevated temperatures, and its neutral chemical behavior.

Bricks of 100% chromium ore have been largely replaced by bricks composed of mixtures of chromite and added magnesia for greater refractoriness, volume stability, and resistance to spalling. One of the refractories used in the fused-cast condition is composed of 80% alumina and 20% chromite. This product is highly resistant to the corrosive action of a variety of fluxes, slags, and glasses.

1.7 Foundry sand

Foundry sand forms the mold in which molten metal is contained until the metal solidifies in the desired shape. The sand is washed, graded, and dried beforehand. Because silica sand is refractory, common, and inexpensive, it is the most widely used mineral for foundry sand; other sand (e.g. zircon, olivine, or chromite) may be chosen, however, depending on physical or chemical conditions.

The use of chromite foundry sand is a modern development. Chromite foundry sand is used in the ferrous and copper casting industries.

Chromite sand is compatible with steel casting. It is typically used as facing sand in heavy section (greater than 4 ton) casting and enjoys a technical advantage over silica sand in casting austenitic manganese steel (chromite sand does not react with the manganese in steel). Because chromite and zirconia have higher melting temperatures than silica, they are chosen when casting temperatures exceed those acceptable for silica sand.

Chromite sand casting was developed in South Africa where chromite fines are readily available as an inexpensive grade of chromite. After successful results in South Africa in the late 1950s, use expanded into the 1960s in the United Kingdom and closely thereafter in the United States.

Initial use of chromite sand coincided with a shortage of zircon sand; chromite sand had the additional advantage of being an inexpensive substitute. Foundry characteristics that make chromite sand desirable are good thermal stability, good chill properties, not easily wetted, resistant to metal penetration, highly refractory, and chemically nonreactive. Compared with zircon sand the disadvantages of chromite are higher thermal expansion, occasional presence of hydrous mineral impurities, and different bonding characteristics with some binding agents.

1.8 Report analyses for chromium market

The combination of strong demand and sharp rises in the costs of freight, energy chromite and ferrochrome prices reached their highest levels for ten years in early 2005, at 72-74 U$/lb, according to a new report from market analyst Roskill.

This represents a significant recovery from early 2002 when prices of 27-29 U$/lb were at their lowest level for 30 years. The Economics of Chromium (10th Edition, 2005) explains that the recovery in the ferrochrome market was primarily due to the growth in stainless steel production, which is forecast to maintain strong growth through the mid-2000s, led by Asian demand.

After the 2008 financial crisis that put the chromium industry into recession in 2009, 2010 was a year of recovery. World chromite ore, ferrochromium, and stainless steel production decreased from 2008 to 2009; and

then increased from 2009 to 2010 with 2010 production of ferrochromium and stainless steel exceeding that of 2008, leading to the expectation that chromite ore production would continue to increase.

Agnello (2010) reported that foundry-grade chromite, which accounted for 3% of global chromite ore consumption, was used as core and molding sands, initially used in manganese steel casting, and has moved to the manufacture of alloy and carbon steel castings and nonferrous metal castings. Since 1970, about 70% of foundry capacity in developed countries closed, resulting in a shift of casting to Southeast Asia and developing countries. Refractory-grade chromite is used more in shaped-refractory (80%) than in monolithic products. Magnesite-chromite refractories are preferred in nonferrous metallurgy (such as copper, lead, and zinc refining); however, the cement, lime, and glass industries have moved away from using magnesite-chromite bricks because of environmental considerations associated with the disposal of used refractories.

About 850,000 ton of sodium dichromate was produced in 2008 from about 1.25 to 1.3 Mt of chromite ore. The sodium dichromate was converted to chromium oxide (34%), chromic acid (29%), chromium sulfate (23%), and other chemicals (14%). Agnello forecast of chromium sulfate production, which is used in leather manufacturing, to increase between

1% and 1.5%; chromic acid, which is used in metal finishing and to preserve wood, to increase between 3% and 3.5%, and chromium oxides, which are used in alloy, ceramic, and pigment manufacture, to increase between 2% and 3%.

Historically, three events outside of the chromium industry (the dissolution of the Soviet Union, the economic growth of China, and the world financial crisis in 2008–09) have had significant impacts on the chromium industry, making industry analysts and company planners sensitive to the potential for such events.

Chapter 2

Chromite: enrichment processes

2.1 Mineral processing concept

Mineral processing, sometimes called ore dressing, mineral dressing or milling, follows mining and prepares the ore for extraction of the valuable metal in the case of most metallic ores, and produces a commercial end product for commodities such as iron ore and coal. Apart from regulating the size of the ore, it is a process of physically separating the grains of valuable minerals from the gangue minerals, to produce an enriched portion, or concentrate, containing most of the valuable minerals, and a discard, or tailing, containing predominantly the gangue minerals.

The importance of mineral processing is today taken for granted, but it is interesting to reflect that less than a century ago, ore concentration was often a fairly crude operation, involving relatively simple gravity and hand-sorting techniques performed by the mining engineers. The twentieth century saw the development of mineral processing as a serious and important professional discipline in its own right, and without physical separation, the concentration of many ores, and particularly the metalliferous ores, would be hopelessly uneconomic (Wills & Atkinson, 1991).

It has been predicted, however, that the importance of mineral processing of metallic ores may decline as the physical processes utilized are replaced by the hydro and pyro metallurgical routes used by the extractive metallurgist (Gilchrist, 1989), because higher recoveries are obtained by some chemical methods. This may certainly apply when the useful mineral is very finely disseminated in the ore and adequate liberation from the gangue is not possible, in which case a combination of chemical and mineral processing techniques may be advantageous, as is the case with some highly complex ores containing economic amounts of copper, lead, zinc and precious metals (Gray, 1984; Barbery, 1986). Also new technologies such as direct reduction may allow direct smelting of some ores. However, in the majority of cases the energy consumed in direct smelting or leaching of low-grade ores would be so enormous as to make the cost prohibitive. Compared with these processes, mineral processing methods are inexpensive, and their use is readily justified on economic grounds.

If the ore contains worthwhile amounts of more than one valuable mineral, it is usually the object of mineral processing to separate them; similarly if undesirable minerals, which may interfere with subsequent refining processes, are present, it may be necessary to remove these minerals at the separation stage.

There are two fundamental operations in mineral processing: namely the release, or liberation, of the valuable minerals from their waste gangue minerals, and separation of these values from the gangue, this latter process being known as concentration.

Liberation of the valuable minerals from the gangue is accomplished by comminution, which involves crushing, and, if necessary, grinding, to such a particle size that the product is a mixture of relatively clean particles of mineral and gangue. Grinding is often the greatest energy consumer, accounting for up to 50% of a concentrator's energy consumption. As it is this process which achieves liberation of values from gangue, it is also the process which is essential for efficient separation of the minerals, and it is often said to be the key to good mineral processing.

In order to produce clean concentrates with little contamination with gangue minerals, it is necessary to grind the ore finely enough to liberate the associated metals. Fine grinding, however, increases energy costs, and can lead to the production of very fine untreatable "slime" particles which may be lost into the tailings. Grinding therefore becomes a compromise between clean (high-grade) concentrates, operating costs and losses of fine minerals. If the ore is low grade, and the minerals have very small grain size and are disseminated through the rock, then grinding

energy costs and fines losses can be high, unless the nature of the minerals is such that a pronounced difference in some property between the minerals and the gangue is available.

An intimate knowledge of the mineralogical assembly of the ore is essential if efficient processing is to be carried out. Knowledge not only of the nature of the valuable and gangue minerals but also of the ore "texture" is required.

The texture refers to the size, dissemination, association and shape of the minerals within the ore. The processing of minerals should always be considered in the context of the mineralogy of the ore in order to predict grinding and concentration requirements, feasible concentrate grades and potential difficulties of separation (Hausen, 1991; Guerney et al., 2003; Baum et al., 2004).

2.2 Mineral processing methods

The most important physical methods which are used to concentrate ores are:

i. Separation based on optical and other properties. This is often called sorting, which used to be done by hand but is now mostly accomplished by machine.

ii. Separation based on differences in density between the minerals. Gravity concentration, a technology with its roots in antiquity, is based on the differential movement of mineral particles in water due to their different hydraulic properties. The method has recently enjoyed a new lease of life with the development of a range of enhanced gravity concentrating devices. In dense medium separation particles sink or float in a dense liquid or (more usually) an artificial dense suspension; it is widely used in coal beneficiation, iron ore and diamond processing, and in the pre-concentration of metalliferous ores.

iii. Separation utilizing the different surface properties of the minerals. Froth flotation, which is one of the most important methods of concentration, is affected by the attachment of the mineral particles to air bubbles within the agitated pulp. By adjusting the "climate" of the pulp by various reagents, it is possible to make the valuable minerals air-avid (aerophilic) and the gangue minerals water-avid (aerophobic). This results in separation by transfer of the valuable minerals to the air bubbles which form the froth floating on the surface of the pulp.

iv. Separation dependent on magnetic properties. Low intensity magnetic separators can be used to concentrate ferromagnetic minerals such as magnetite (Fe_3O_4), while high-intensity separators are used to separate paramagnetic minerals from their gangue. Magnetic separation is an important process in the beneficiation of iron ores, and finds application in the treatment of paramagnetic non-ferrous minerals. It is used to remove paramagnetic wolframite [(Fe, Mn) WO_4] and hematite (Fe_2O_3) from tin ores, and has found considerable application in the processing of nonmetallic minerals, such as those found in mineral sand deposits.

v. Separation dependent on electrical conductivity properties. High-tension separation can be used to separate conducting minerals from non-conducting minerals. This method is interesting, since theoretically it represents the "universal" concentrating method; almost all minerals show some difference in conductivity and it should be possible to separate almost any two by this process. However, the method has fairly limited application, and its greatest use is in separating some of the minerals found in heavy sands from beach or stream placers. Minerals must be completely dry and the humidity of the surrounding air must be regulated, since most of the electron movement in dielectrics takes place on the surface and a film of moisture can change the behavior completely. The biggest disadvantage of the method is that the capacity of economically sized units is low.

In many cases a combination of two or more of the above techniques is necessary to concentrate an ore economically.

2.3 Chromite ore beneficiation and processing

The purpose of beneficiation is to render the ore concentrate physically (granulometry) and chemically suitable for subsequent treatments. Beneficiation practices depend on the mineral characteristics of the ore deposits, gangue mineral assemblage and the degree of dissemination of constituent minerals.

In general chromite beneficiation flow sheet (Figure 1) has two major sections: comminution (for preparing the material to the subsequent unit operations) and concentration. The feed preparation unit incorporates two stage crushing (primary and secondary crusher) and screening to produce less than 3 mm size fraction. This fraction is further ground to less than 1 mm and then upgraded utilizing conventional gravity techniques like spiral concentrator and shaking table in the concentration section. Though gravity techniques are well established and widely accepted for the concentration of chromite ore, such techniques become inefficient and complex while treating fine size particles (less than 75 μm). Each gravity separation technique delivers its maximum efficiency under specific operating conditions and particle size range.

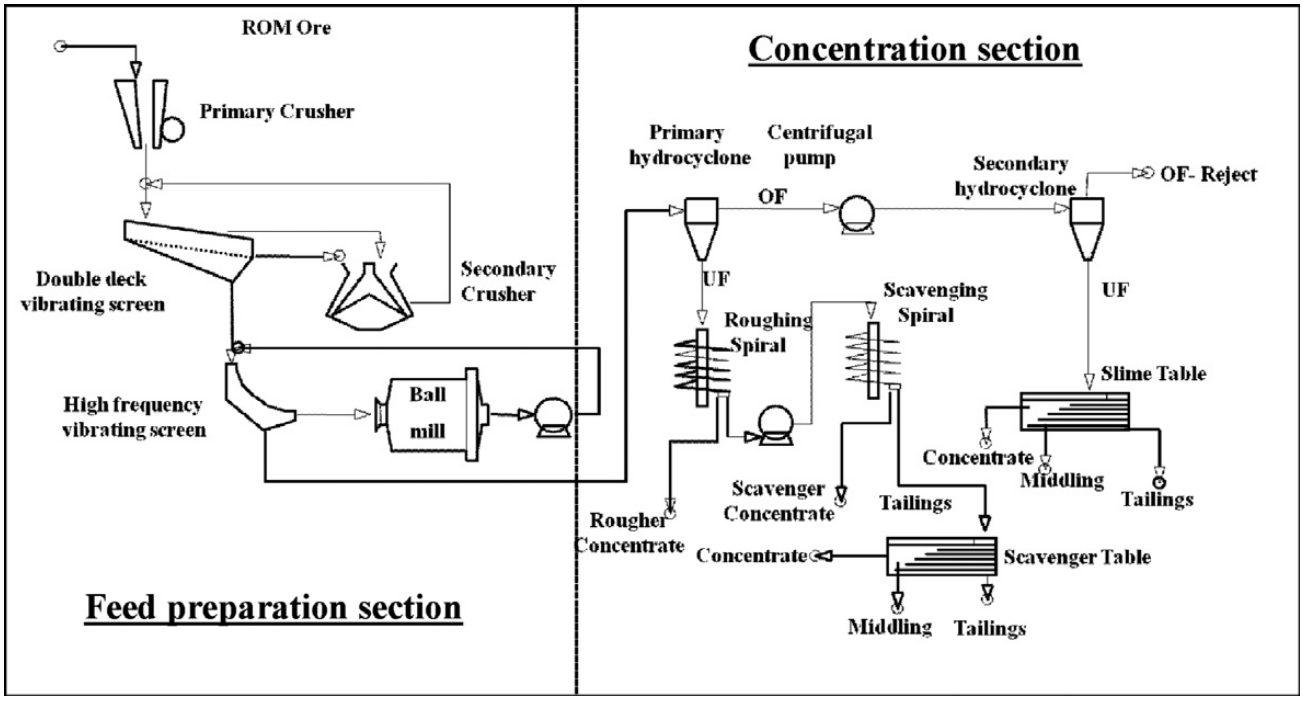

Figure 1. General process flow sheet for chromite ore beneficiation.

2.4 Comminution

Because most minerals are finely disseminated and intimately associated with the gangue, they must be initially "unlocked" or "liberated" before separation can be undertaken. This is achieved by comminution in which the particle size of the ore is progressively reduced until the clean particles of mineral can be separated by such methods as are available.

Comminution in its earliest stages is carried out in order to make the freshly excavated material easier to handle by scrapers, conveyors, and ore carriers, and in the case of quarry products to produce material of controlled particle size.

Comminution in the mineral processing plant takes place as a sequence of crushing and grinding processes. Crushing reduces the particle size of run-of-mine ore to such a level that grinding can be carried out until the mineral and gangue is substantially produced as separate particles.

Crushing is accomplished by compression of the ore against rigid surfaces, or by impact against surfaces in a rigidly constrained motion path. This is contrasted with grinding which is accomplished by abrasion and impact of the ore by the free motion of unconnected media such as rods, balls, or pebbles. Crushing is usually a dry process, and is performed in several stages. Tumbling mills with either steel rods or balls, or sized ore as the grinding media, are used in the last stages of comminution.

Grinding is usually performed "wet" to provide a slurry feed to the concentration process, although dry grinding has limited applications.

2.4.1 Crushers

Crushing is usually performed by primary and secondary crushers.

Primary crushers are heavy-duty machines, used to reduce the run-of-mine ore down to a size suitable for transport and for feeding the secondary crushers (generally to 10-20 cm). There are two main types of primary crushers in metalliferous operations: jaw and gyratory crushers.

The distinctive feature of this class of primary crushers is the two plates which open and shut like animal jaws. The jaws are set at an acute angle to each other, and one jaw is pivoted so that it swings relative to the other fixed jaw. Material fed into the jaws is alternately nipped and released to fall further into the crushing chamber. Eventually it falls from the discharge aperture. The gyratory crusher consists essentially of a long spindle, carrying a hard steel conical grinding element, the head, seated in an eccentric sleeve.

Secondary crushers are much lighter than the heavy-duty, rugged primary machines. Since they take the primary crushed ore as feed, the maximum feed size will normally be less than 15 cm in diameter and, because most of the harmful constituents in the ore, such as tramp metal, wood, clays, and slimes have already been removed, it is much easier to handle. Secondary crushers also operate with dry feeds, and their purpose is to reduce the ore to a size suitable for grinding. The bulk of secondary crushing of metalliferous ores is performed by cone crushers, although crushing rolls and hammer mills are used for some applications.

Vibrating screens are sometimes placed ahead of the secondary crushers to remove undersize material, or scalp the feed, and thereby increase the capacity of the secondary crushing plant. Undersize material tends to pack the voids between the large particles in the crushing chamber, and can choke the crusher, causing damage, because the packed mass of rock is unable to swell in volume as it is broken.

2.4.2 Grinding mills

According to the ways by which motion is imparted to the charge, grinding mills are generally classified into two types: tumbling mills and stirred mills.

Tumbling mills are of three basic types: rod, ball, and autogenous. In tumbling mills the mill shell is rotated and motion is imparted to the charge via the mill shell. The grinding medium may be steel rods, balls, or rock itself. Tumbling mills are typically employed in the mineral industry for coarse-grinding processes, in which particles between 5 and 250 mm are reduced in size to between 40 and 300 μm.

In stirred mills the mill shells with either a horizontal or a vertical orientation is stationary and motion is imparted to the charge by the movement of an internal stirrer. Fine grinding media inside the mill are agitated or rotated by a stirrer, which typically comprises a central shaft to which are attached pins or discs of various designs. Stirred mills find application in fine (15-40 μm) and ultra-fine (<15 μm) grinding.

2.5 Gravity concentration

Gravity concentration methods separate minerals of different specific gravity by their relative movement in response to gravity and one or more other forces, the latter often being the resistance to motion offered by a viscous fluid, such as water or air.

It is essential for effective separation that a marked density difference exists between the mineral and the gangue. The motion of a particle in a fluid is dependent not only on its specific gravity, but also on its size, large particles will be affected more than smaller ones. The efficiency of gravity processes therefore increases with particle size, and the particles should be sufficiently coarse to move in accordance with Newton's law.

Particles which are so small that their movement is dominated mainly by surface friction, respond relatively poorly to commercial high-capacity gravity methods. In practice, close size control of feeds to gravity processes is required in order to reduce the size effect and make the relative motion of the particles specific gravity-dependent.

Many different machines have been designed and built in the past to effect separation of minerals by gravity, and they are comprehensively reviewed by Burt (1985). Many gravity devices have become obsolete, and only equipment that is used in modern enrichment plants will be described in this chapter. Essentially these machines are jigs, spirals and shaking tables. A classification of the more commonly used gravity separators on the basis of feed size range is shown in Figure 2.

It is essential for the efficient operation of all gravity separators that the feed is carefully prepared. Grinding is particularly important in adequate liberation; successive regrinding of

middlings is required in most operations. Primary grinding should be performed where possible in open-circuit rod mills, but if fine grinding is required, closed-circuit ball milling should be used, preferably with screens closing the circuits rather than hydrocyclones in order to reduce selective overgrinding of heavy friable valuable minerals.

Gravity separators are extremely sensitive to the presence of slimes (ultra-fine particles), which increase the viscosity of the slurry and hence reduce the sharpness of separation, and obscure visual cut-points. It is common practice in most gravity concentrators to remove particles less than about 10 μm from the feed, and divert this fraction to the tailings, and this can account for considerable loss of values. De-sliming is often achieved by the use of hydrocyclones, although if hydraulic classifiers are used to prepare the feed it may be preferable to de-slime at this stage, since the high shear forces produced in hydrocyclones tend to cause degradation of friable minerals.

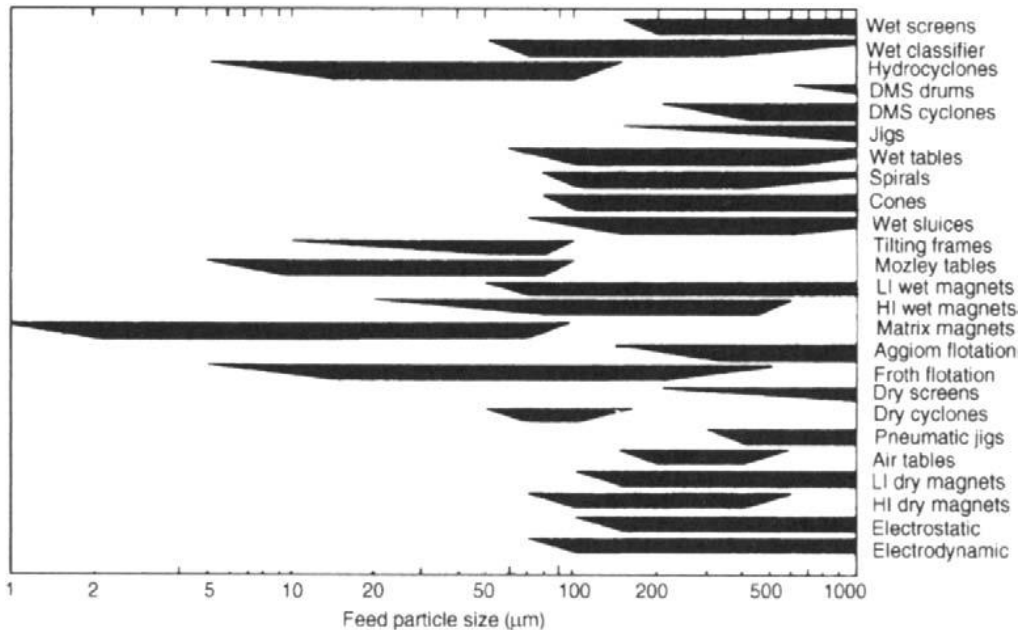

Figure 2. Effective range of application of conventional processing techniques.

2.5.1 Jigs

Jigging is one of the oldest methods of gravity concentration, yet the basic principles are only now beginning to be understood. The jig is normally used to concentrate relatively coarse material and, if the feed is fairly closed sized (e.g. 3-10 mm), it is not difficult to achieve good separation of a fairly narrow specific gravity range in minerals in the feed.

In the jig the separation of minerals of different specific gravity is accomplished in a bed which is rendered fluid by a pulsating current of water so as to produce stratification. The aim is to dilate the bed of material being treated and to control the dilation so that the heavier, smaller particles penetrate the interstices of the bed and the larger high specific gravity particles fall under a condition probably similar to hindered settling (Lyman, 1992).

On the pulsion stroke the bed is normally lifted as a mass, then as the velocity decreases it tends to dilate, the bottom particles falling first until the whole bed is loosened. On the suction stroke it then closes slowly again and this is repeated at every stroke. Fine particles tend to pass through the interstices after the large ones have become immobile. The motion can be obtained either by using a fixed sieve jig, and pulsating the water, or by employing a moving sieve, as in the simple hand-jig.

Essentially the jig is an open tank filled with water, with a horizontal jig screen at the top, and provided with a spigot in the bottom, or hutch compartment, for concentrate removal (Figure 3). The jig bed consists of a layer of coarse, heavy particles, or ragging, placed on the jig screen on to which the slurry is fed. The feed flows across the ragging and the separation takes place in the jig bed so that grains with a high specific gravity penetrate through the ragging and screen to be drawn off as a concentrate, while the light grains are carried away by the cross-flow to be discarded as tailings. The harmonic motion produced by the eccentric drive is supplemented by a large amount of continuously supplied hutch water, which enhances the upward and diminishes the downward velocity of the water.

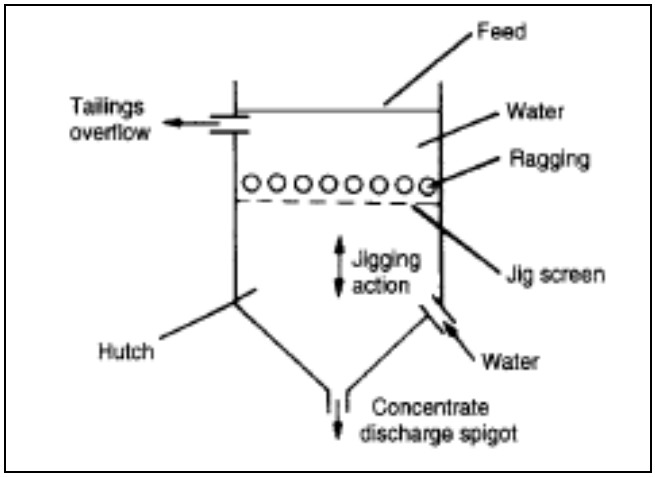

Figure 3. Basic jig construction.

2.5.2 Spirals

Spiral concentrators have, over numerous years found many varied applications in mineral processing, but perhaps their most extensive usage has been in the treatment of heavy mineral sand deposits, such as those carrying chromite, ilmenite, rutile, zircon, and monazite, and in recent years in the recovery of fine coal.

The Humphreys spiral was introduced in 1943, its first commercial application being on chrome-bearing sands (Hubbard et al., 1953). It is composed of a helical conduit of modified semicircular cross-section. Feed pulp of between 15 and 45 % solids by weight and in the size range 3 mm to ~75 μm is introduced at the top of the spiral and, as it flows spirally downwards, the particles stratify due to the combined effect of centrifugal force, the differential settling rates of the particles, and the effect of interstitial trickling through the flowing particle bed.

These mechanisms are complex, being much influenced by the slurry density and particle size. Some workers (Mills, 1978) have reported that the main separation effect is due to hindered settling, with the largest, densest particles reporting preferentially to the concentrate, which forms in a band along the inner edge of the stream (Figure 4). Bonsu (1983), however, reported that the net effect is reverse classification, the smaller, denser particles preferentially entering the concentrate band.

Ports for the removal of the higher specific gravity particles are located at the lowest points in the cross-section. Wash-water, added at the inner edge of the stream, flows outwardly across the concentrate band. The width of concentrate band removed at the ports is controlled by adjustable splitters. The grade of concentrate taken from descending ports, progressively decreases, tailings being discharged from the lower end of the spiral conduit.

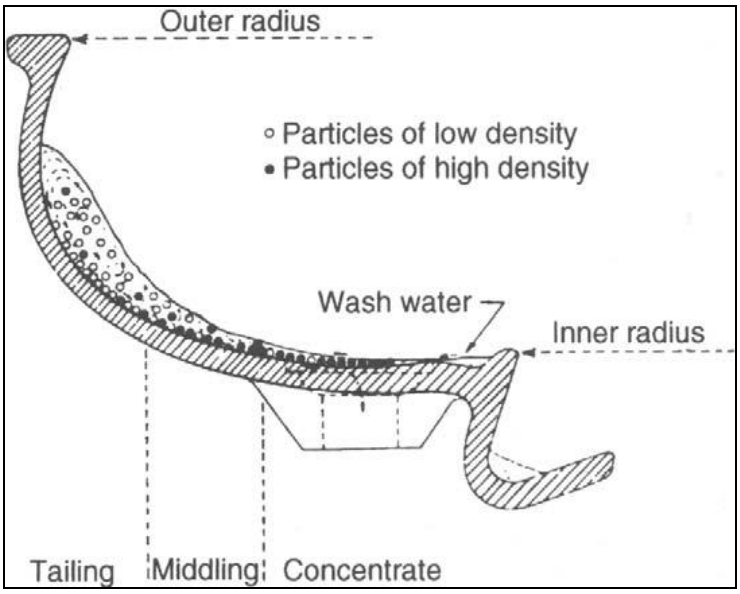

Figure 4. Cross-section of spiral stream.

Until relatively recently, all spirals were very similar, based upon the original Humphreys design, which is now obsolete. However, in recent years, there have been considerable developments in spiral technology, and a wide range of devices are now available. The main areas of development have been in the introduction of spirals with only one concentrate take-off, at the bottom of the spiral, and the use of spirals without added wash water. Wash waterless spirals reportedly offer lower cost, easy operation, and simple maintenance, and have been installed at several gold and tin processing plants.

2.5.2 Shaking tables

Shaking table concentrator (Figure 5) is perhaps the most metallurgical efficient form of gravity concentrator, being used to treat the smaller, more difficult, flow-streams, and to produce finished concentrates from the products of other forms of gravity systems (Wills and Napier-Munn, 2006).

It consists of a slightly inclined deck (A), onto which feed, at about 25% solids by weight, is introduced at the feed box and is distributed along a duct (C); wash water is distributed along the balance of the feed side from launder (D). The table is vibrated longitudinally, by a mechanism (B), using a slow forward stroke and a rapid return, which causes the mineral particles to "crawl" along the deck parallel to the direction of motion.

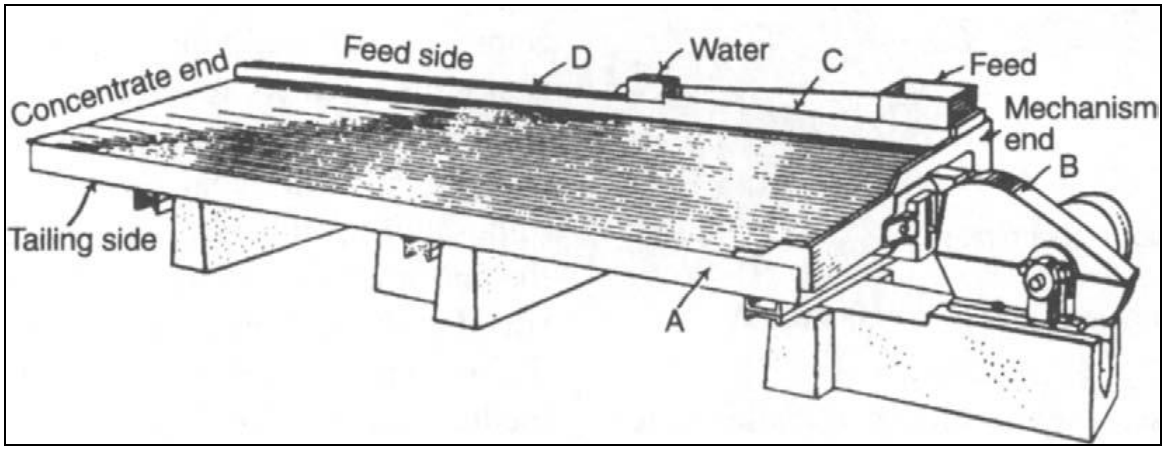

Figure 5. Shaking table.

The minerals are thus subjected to two forces, that due to the table motion and that, at fight angles to it, due to the flowing film of water. The net effect is that the particles move diagonally across the deck from the feed end and, since the effect of the flowing film depends on the size and density of the particles, they will fan out on the table, the smaller, denser particles tiding highest towards the concentrate launder at the far end, while the larger lighter particles are washed into the tailings launder, which runs along the length of the table.

The separation of concentrate from gangue minerals on a shaking table is controlled by a number of operating variables such as wash water, feed pulp density, deck slope, amplitude, and feed rate.

Many other factors, including particle shape and the type of deck, play an important part in table separations. Flat particles with lamellar habit, for example mica, although light, do not roll easily across the deck in the water film; such particles cling to the deck and are carried down to the concentrate discharge. Likewise, spherical dense particles may move easily in the film towards the tailings launder.

Particle size plays a very important role in table separation; as the range of sizes in a table feed increases, the efficiency of separation decreases because the middlings produced are not "true middlings", i.e. particles of associated mineral and gangue, but relatively coarse dense particles and fine light particles.

Since the shaking table effectively separates coarse light from fine dense particles, it is common practice to classify the feed, since classifiers put such particles into the same product, on the basis of their equal settling rates. In order to feed as narrow a size range as possible on to the table, classification is usually performed in hydrosizers or sieves.

Since the introduction of the Wilfley Table in 1896, a wide variety of shaking tables have been marketed. Currently, however, there are only a few major manufacturers of shaking tables, although several other less known types are operating in some locations. The major differences between tables are the shape and suspension of deck, and the type of mechanism which imparts the asymmetric reciprocating motion to the deck.

Typically there are two basic shapes of table deck: rectangular, with riffles parallel to longer side, and diagonal, with riffles oblique to longer side. There are two basic types of mechanism, or head motion. In the more common variant the mechanism casing is rigidly fixed to a sub-frame and asymmetric motion is imparted to the deck by a toggle and pitman mechanical linkage. In the other type the mechanism is rigidly fixed to the deck and the whole shaken, as one, by eccentric weights in the mechanism.

2.6 Efficiency of mineral processing operations

2.6.1 Liberation

One of the major objectives of comminution is the liberation of the valuable minerals from the associated gangue minerals at the coarsest possible particle size. If such an aim is achieved, then not only is energy saved by the reduction of the amount of fines produced, but any subsequent separation stages become easier and cheaper to operate. If high-grade solid products are required, then good liberation is essential; however, for subsequent hydrometallurgical processes, such as leaching, it may only be necessary to expose the required mineral.

In practice, complete liberation is seldom achieved, even if the ore is ground down to the grain size of the desired mineral particles. The particles of "locked" mineral and gangue are known as middlings, and further liberation from this fraction can only be achieved by further comminution.

The "degree of liberation" refers to the percentage of the mineral occurring as free particles in the ore in relation to the total content. This can be high if there are weak boundaries between mineral and gangue particles, which is often the case with ores composed mainly of rock-forming minerals, particularly sedimentary minerals. Usually, however, the adhesion between mineral and gangue is strong and, during comminution, the various constituents are cleft across. This produces much middlings and a low degree of liberation. New approaches to increasing the degree of liberation involve directing the breaking stresses at the mineral crystal boundaries, so that the rock can be broken without breaking the mineral grains (Wills and Atkinson, 1993).

Many researchers have tried to quantify degree of liberation with a view to predicting the behavior of particles in a separation process (Barbery, 1991).

The first attempt at the development of a model for the calculation of liberation was made by Gaudin (1939); King (1982) developed an exact expression for the fraction of particles of a certain size that contained less than a prescribed fraction of any particular mineral. These models, however, suffered from many unrealistic assumptions that must be made with respect to the grain structure of the minerals in the ore, in particular that liberation is preferential, and in 1988 Austin and Luckie concluded that "there is no adequate model of liberation of binary systems suitable for incorporation into a mill model". For this reason liberation models have not found much practical application.

However, some fresh approaches by Gay, allowing multi-mineral systems to be modeled (not just binary systems) free of the assumptions of preferential breakage, have recently demonstrated that there may yet be a useful role for such models (Gay, 2004a,b). The quantification of liberation is now routinely possible using the dedicated scanning electron microscope MLA and QEMSCAN systems and concentrators are increasingly using such systems to monitor the degree of liberation in their processes.

It should also be noted that a high degree of liberation is not necessary in certain processes, and, indeed, may be undesirable. For instance, it is possible to achieve a high recovery of values by gravity and magnetic separation even though the valuable minerals are completely enclosed by gangue, and hence the degree of liberation of the values is zero. As long as a pronounced density or magnetic susceptibility difference is apparent between the locked particles and the free gangue particles, the separation is possible. A high degree of liberation may only be possible by intensive fine grinding, which may reduce the particles to such a fine size that separation becomes very inefficient.

In practice, ores are ground to an optimum grin size, determined by laboratory and pilot scale test work to produce an economic degree of liberation. The concentration process is then designed to produce a concentrate consisting predominantly of valuable mineral, with an accepted degree of locking with the gangue minerals, and a middlings fraction, which may require further grinding to promote optimum release of the minerals. The tailings should be mainly composed of gangue minerals.

2.6.2 Concentration

The object of mineral processing, regardless of the methods used, is to separate the minerals into two or more products with the values in the concentrates, the gangue in the tailings, and the "locked" particles in the middlings.

Such separations are, of course, never perfect, so that much of the middlings produced are, in fact, misplaced particles, i.e. those particles which ideally should have reported to the concentrate or the tailings.

It should be pointed out that the separation process is also limited by the mineralogical nature of the ore (Wills, 2006). For example, in an ore containing native copper it is theoretically possible to produce a concentrate containing 100% Cu, but, if the ore mineral was chalcopyrite ($CuFeS_2$), the best concentrate would contain only 34.5% Cu.

The *recovery*, in the case of the concentration of a metallic ore, is the percentage of the total metal contained in the ore that is recovered from the concentrate; a recovery of 90% means that 90% of the metal in the ore is recovered in the concentrate and 10% is lost in the tailings. The recovery, when dealing with non-metallic ores, refers to the percentage of the total mineral contained in the ore that is recovered into the concentrate, i.e. recovery is usually expressed in terms of the valuable end product.

The *ratio of concentration* is the ratio of the weight of the feed to the weight of the concentrates. It is a measure of the efficiency of the concentration process, and it is closely related to the grade or assay of the concentrate; the value of the ratio of concentration will generally increase with the grade of concentrate.

The *enrichment ratio* is the ratio of the grade of the concentrate to the grade of the feed, and again is related to the efficiency of the process.

Ratio of concentration and recovery are essentially independent of each other, and in order to evaluate a given operation it is necessary to know both.

There is an approximately inverse relationship between the recovery and grade of concentrate in all concentrating processes. If an attempt is made to attain a very high-grade concentrate, the tailings assays are higher and the recovery is low. If high recovery of metal is aimed for, there will be more gangue in the concentrate and the grade of concentrate and ratio of concentration will both decrease.

Since concentrate grade and recovery are metallurgical factors, the *metallurgical efficiency* of any concentration operation can be expressed by a curve showing the recovery attainable for any value of concentrate grade. Figure 6 is a typical recovery grade curve showing the characteristic inverse relationship between recovery and concentrate grade. Mineral processes generally move along a recovery-grade curve, with a trade-off between grade and recovery. The mineral processor's challenge is to move the whole curve to a higher point so that both grade and recovery are maximized. Concentrate grade and recovery, used simultaneously, are the most widely accepted measures of assessing metallurgical (not economic) performance (Wills, 2006).

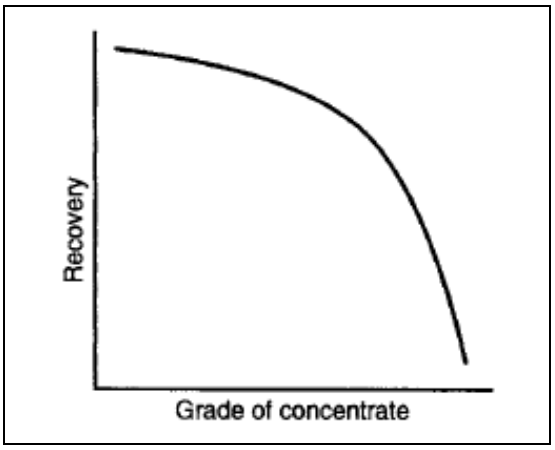

Figure 6. Typical recovery-grade curve.

There have been many attempts to combine recovery and concentrate grade into a single index defining the metallurgical efficiency of the separation. These have been reviewed by Schulz (1970), who proposed the following definition of *Separation Efficiency* (SE):

$$SE = Rm - Rg \quad (1)$$

Where Rm is the % recovery of the valuable mineral and Rg is the % recovery of the gangue into the concentrate.

Previous equation can be used practically in the following form proposed by Wills (1979):

$$SE = \frac{100Cm(c-f)}{(m-f)f} \quad (2)$$

Where C is the fraction of the total feed weight that reports to the concentrate, m is the percentage metal content of the valuable mineral, c is the metal % of the concentrate and f is the metal % of the feed.

Anyway this formula is valid only assuming that all the valuable metal is contained in the same mineral (Wills, 1979). Therefore in the case of chromite ore where the valuable metal is present in both chromite and gangue this formula cannot be used and it should be reviewed.

Chapter 3

Madagascar chromite ore deposits: study and selection

3.1 Introduction

Chromite ore deposits within layered igneous complexes, like those of the Bushveld complex, are the most important mining source for the extraction of chromite. However, even if South Africa is the top chromite producer of the world, new emerging countries have entered the chromite international market, and Madagascar is one of these.

Indeed Madagascar is a minor chromite producing country, ranking 15th between the world chromite ore producers in 2009 (Papp, 2011) with all production coming from the Bemanevika Mine in the Andriamena chromite district of central Madagascar. In the past several other chromite deposits were exploited, often for very short time, and many chromitite occurrences were found, most of which during prospection works in the middle 20th century, when Madagascar was a French colony.

Madagascar has a very complicated geologic history and hosts important chromite mineralization of Precambrian age, which was interested by strong deforming phenomena that obliterated primary textural features of mineralization.

The study of these mineralizations occurs in collaboration with UT Group s.r.l. that works in the national and international marketing field of industrial minerals; with mining company Kraomita Malagasy and with Antananarivo University.

The study of chromite ores, started in 2008 in three different igneous complexes, has focused in the last three years (during my PhD) on their chemical and textural characterization.

The aims of the last years of study are scientific but also applicative, with the purpose to improve and increase the production of the only Madagascar enrichment plant. This is possible through an evaluation of potential new mining sites and through elaborate chemical, textural and mineralogical studies of feeding materials and also of final products during the different working steps of plant.

In this chapter are presented the studies regarding chromitite samples from the five major chromitite occurrence localities of Madagascar: Andriamena, North Befandriana, North Toamasina, Maevatanana and North Belobaka. These last two places have never been studied and exploited.

Within each chromite district samples were taken from the biggest chromitite occurrences, exploiting the opportunity to collect them from the walls of working or abandoned chromite open pit mines, where possible. In those cases the lithologies associated to chromitite have been described. The study of chromitites was aimed to the description of primary mineralogical association, for which all secondary alteration features, where present, were recognized and described. The result is a comparative description of lithological, mineralogical, textural and chemical features of the chromitites.

Some parts of this chapter are extracted directly from a scientific paper entitled "The origin of Madagascar chromitites" (Grieco, Merlini, Pedrotti, Moroni & Randrianja, 2012), which in September has been accepted with revision for publication in the journal *Ore Geology Reviews (Elsevier)*.

3.2 Geology of Madagascar

Precambrian basement forms about two thirds of Madagascar and is in contact with Phanerozoic cover on an almost 2000 km-long line stretching north to south in western Madagascar (Figure 1).

Within the basement the main structure is the Bongolova-Ranotsara shear zone that separates two different crustal blocks (Muller et al., 1997). All Madagascar chromitite districts are placed within the bigger northern block (Figure 1), while no chromitites have ever been found to the south of the shear zone, comprising the three Neoproterozoic domains of Vohibory, Androyen and Anosyen (De Waele et al., 2011).

Collins (2006) divided the basement into four main units, and four metasedimentary covers, comprising the region to the south of the Bongolova-Ranotsara shear zone. A more recent description, based on a phase of 1:100.000 to 1:500.000 mapping of northern and central Madagascar (BGS-USGS-GLW, 2008), can be found in Tucker et al. (2010, 2011) and in De Waele et al. (2011). In this view the Madagascar basement comprises three Archean domains (Tsaratanana, Antananarivo and Antongil-Masoara), three Paleoproterozic sedimentary cover sequences (Itremo, Sahantaha and Maha), a Neo- to Mesoproterozoic terrain (Ikalamavony) and four Neoproterozoic domains and belts (Vohibory-Androyen-Anosyen, Anaboriana-Manampotsy, North Bemarivo and South Bemarivo).

The distribution of Archean and Proterozoic terrains draws a picture where two main Archean crustal blocks (Antananarivo and Tsaratanana to the west, Antongil-Masoara to the east) are separated by the Neoproterozoic Anaboriana-Manampotsy belt (De Waele et al., 2011). The latter, firstly described by Bésairire (1970, 1971) and previously known as the Betsimisaraka belt (e.g. Collins, 2000; Collins and Windley, 2002; Raharimahefa and Kusky, 2006; Schofield et al., 2010), is a strongly debated structure, whose interpretation is pivotal in understanding the geodynamic evolution of Madagascar (e.g. Collins, 2006; Collins and Pisarewksy, 2005; Collins and Windley, 2002; Collins et al., 2003, Kroner et al., 2000; Raharimahefa and Kusky, 2009; Tucker et al., 2010; Tucker et al., 2011). Two main different hypotheses have been proposed. According to the first one, well described in Collins (2006), the belt is a convergent margin boundary active throughout Neoproterozoic time. According to the second one the belt is a Neoproterozoic metasedimentary unit that mostly covers the Archean boundary between Meso- and Neoarchean domains of the Greater Dharwar Craton (Tucker et al., 2011). The two different views imply that central Madagascar is respectively a portion of Azania mini-continent of African origin or a portion of Greater Dharwar craton of India. Chromitites in Madagascar can be found in different tectonic domains belonging to both eastern Antongil-Masoara and western Antananarivo cratons and to the Anaboriana-Manampotsy belt (Figure 1).

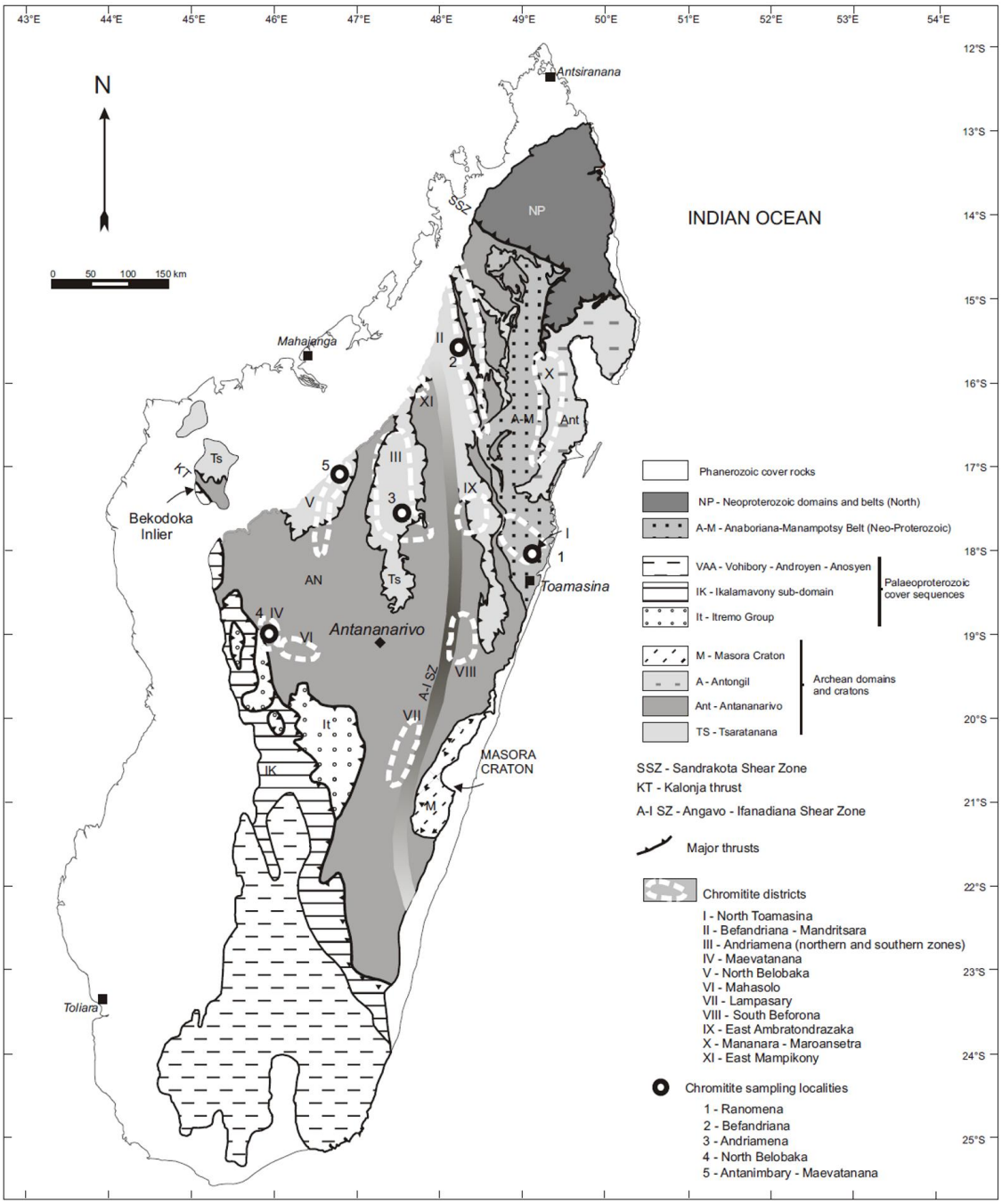

Figure 1. Geological sketch map of Precambrian Madagascar with location of chromitite districts and sampling localities. Modified from BGW-USGS-LGW (2008) and De Waele et al. (2011).

Three out of five chromitite localities studied for the present work lie within the Tsaratanana sheet. They are North Befandriana, Andriamena and Antanimbary. Tsaratanana sheet, belonging to the western craton, is described as a series of structurally overlying, possibly allochthonous, belts of predominantly mafic gneisses within the Antananarivo craton (Collins et al., 2003; BGS-USGSGLW, 2008). Chromitites were found in three of the four belts of the sheet, whereas only the westernmost and smaller Ambohipaky belt is barren. The Antanimbary chromitites belong to the Maevatanana belt, the Andriamena chromitites belong to the Andriamena belt and the Befandriana chromitites belong to the Beforona-Alaotra belt (Figure 1).

The Ranomena chromitites, belonging to the North Toamasina chromite district, crop out within the Anaboriana-Manampotsy belt (Figure 1). The belt is mainly composed of graphite-rich schists but with entrained blocks of mafic and ultramafic rocks (Raharimahefa and Kusky, 2009) that in turn host chromitite occurrences.

The North Belobaka chromitites crop out in a very small area within a region of poor outcropping in the western portion of the Antananarivo domain, very close to the border with Ikalamavony and Itremo Proterozoic domains (Figure 1). The rock association of Antananarivo domain consists of Archean orthogneisses and paragneisses that were metamorphosed and partially melted under granulite- and upper amphibolite facies conditions in Neoarchean times (BGS-USGSGLW. 2008; De Waele, 2011). Large volumes of magma were intruded throughout the Antananarivo Craton – Tsaratanana Complex as a result of Neoproterozoic to Cambrian orogenesis (De Waele et al., 2011).

3.3 Local geology, texture and mineral chemistry

Some information on local geology of chromitite hosting mafic/ultramafic rocks and texture of chromitite bodies can be found mainly in old prospecting works of French Authors, for the area covered, in the BGS-USGS-GLW report and, for Befandriana and North Belobaka respectively, in a private company internal report (UT, 2009) and in an unpublished PhD thesis (Ravelonandro, 2011). This information is, in the following description, integrated by observations carried out during sampling field surveys. A summary of lithological and mineralogical observations is shown in Tables 1 and 2.

Table 1. Host rock lithologies.

Site	Host rock
Andriamena	Serpentinized Mg-rich peridotite. Thickness: about 120 m. Presence of interlayered septa of pyroxenite, serpentinite and talc rocks. 800-770 Ma
Befandriana	Pegmatoidal pyroxenite and interlayered horizon of dunite or harzburgite. Peridotite at Anengitra
Ranomena	Lenticular body of altered pyroxenite/harzburgite
Antanimbary	Metagabbro with an orthoamphibolite sheath
Belobaka	Mafic-ultramafic bodies characterized by an amphibole gneiss with amphibolites

Table 2. Mineralogical paragenesis of chromitites matrix.

Phases	Andriamena	Befandriana	Ranomena	Antanimbary	Belobaka
Silicates	Ol, En, Tr, Ed, Phl, Tlc, Ap	Ol, En, Tr, Chl	Ol, En, Tr, Phl, Tlc, Srp, Qtz, Chl	Chl, Ed, En, Ab, Bt, Tlc, Ttn	Ol, En, Fe-En, Hbl, Chl, Tlc, Srp
Oxides	Rt, Ilm	Ilm	Mag, Rt, Ilm	Ilm, Rt	Mag, Ilm, Rt,
Sulphides	Pn, Po	Pn	Ccp, Pn, Po	Po	-
PGM	Rare	Extremely rare	Abundant	Not Detected	Not Detected

Mineral chemistry of spinels and silicate gangue was determined with a JEOL 8200 electron microprobe at the University of Milan. For the analyses the system was operated using an accelerating voltage of 15 kV, a sample current on brass of 15 nA and a counting time of 20 s on the peaks and 10 s on background. A series of natural minerals (kaersutite for Si, Mg, Na, Ti, K, Fe, Al; chromite for Cr and rhodonite for Mn) were used as standards for spinels and silicates. Representative analyses of spinels and orthopyroxenes are shown in Tables 3 and 4 (Appendix A).

3.3.1 Andriamena

The Andriamena district accounts for more than 70% of past Madagascar chromite production, with three active mines in the last decade: Ankazotaolana, Bemanevika and Telomita. After the closure of Ankazotaola mine in 2007, production was shifted to Bemanevika mine with a minor contribution from Telomita. All three mines are worked in open pit. The original total reserves were estimated at 4.310.000 tons for Ankazotaolana, 4.393.000 tons for Bemanevika (SIGM, 1984) and 730.000 tons for Telomita (Cazzaniga, 2009).

The Ankazotaolana chromitite lenses are hosted in an ultramafic body with an overall thickness of about 40 m. Individual lenses vary in thickness between 10 and 20 m and are separated by narrow septa of pyroxenite, bastite, serpentinite and talcose rocks. Chromitite is hosted within serpentinized Mg-rich peridotite which may explain the relatively high Cr/Fe ratio of the chromite (BGS-USGS-GLW, 2008). The mafic-ultramafic body that hosts chromitites comprises also gabbro-norite and minor anorthosite and pyroxenite.

Chromitite samples were collected from two massive lenses of unknown length and more than 2 m thick outcropping at the bottom of Ankazotaolana open pit, from one minor outcrop about 200 m from Ankazotaolana open pit and from a massive chromitite lens on the northern wall of Bemanevika open pit. High angle pegmatite dykes, rare at Ankazotaolana, much more abundant and thick at Bemanevika, crosscut the ultramafic rocks.

Chromitite is massive and chromite crystals are euhedral well preserved and never zoned. They never show ferritchromite rims and alteration of the silicate matrix into serpentine and talc is limited. Gangue phases are dominated by olivine with minor orthopyroxene. Tremolitic amphibole is abundant in some samples. Other minor gangue phases are pyrrhotite, pentlandite, ilmenite and rutile.

At Andriamena chromite chemistry is quite similar between Ankazotaolana and Bemanevika mines but, at least at Ankazotaolana, where more samples were collected, show a quite wide range of compositions. Here XCr (Cr/(Cr+Al)) ranges between 0.50 and 0.70 and XFe (Fe/(Fe+Mg)) between 0.35 and 0.65. Cr_2O_3 content ranges between 46.5 and 53.2 wt %, FeO shows a wide range of values being between 12 and 23 wt%, Al_2O_3 content is generally between 16.5 and 18.5 wt%, TiO_2 is quite low, being always less than 0.20 wt%. At Bermanevika Cr_2O_3 content is in the highest range of Ankazotalana chromite, between 52.5 and 53.5 wt% FeO is around 13 wt%, Al_2O_3 between 16 and 17 wt%. TiO_2 is again below 0.20 wt%.

3.3.2 North Befandriana

The North Befandriana chromitite area is located to the north of the Sona River, between Befandriana and Bas Androna. The area consists of small chromite mines and occurrences. Chromite is associated with amphibolite and pyroxenite lenses within NNW striking belts of sillimanitegarnet- graphite schists, quartzite and marble. Zavindravoy and Anengitra are the largest deposits in the area (BGS-USGS-GLW, 2008). Two minor, never exploited, chromitite zones are Ankotondambo and Andrafiabe (UT, 2009).

All chromitite samples were collected from Zavindravoy chromite deposit that was exploited by Kraomita Malagasy mining Company in the 1970's. The production was resumed in 1995 and, finally, ended in 1999 due to the opening of Ankazotaolana mine. At Zavindravoy chromitite was mined in four different places, from north to south Dymitriak, BC, Delgrange and Cortes, both from chromitite lenses and from levels of chromitite blocks within laterite (UT, 2009).

According to BGS-USGS-GLW (2008) the edge of the smaller open pit at Zavindrovay consists of a lateritized, very coarse, crystalline pyroxenite with 2 mm-sized clots of evenly disseminated chromite. Remnant pyroxene and chromite create a net texture visible in less lateritized outcrops in the western part of the pit. Needles of actinolite in the pegmatoidal pyroxenite, and pseudomorphic after plagioclase, are present in clusters up to 5 cm in diameter. Outcrop in the north wall of the pit is completely lateritized. Relict textures suggest that most of north wall probably consists of pegmatoidal pyroxenite and possibly an interlayered horizon of dunite or harzburgite.

The larger of the two pits (Dymitriak), located 0.5 km NNE of the first pit (BC), is characterized by a lateritized host rock composed of coarse-grained equigranular pyroxenite and by a pegmatoidal pyroxenite. In the western corner of the pit the contact between ultramafite and granite migmatite gneiss is exposed. The pit is also characterized by abundant cross-cutting quartz potassic feldspar-biotite-phlogopite veins and small pegmatite bodies. As in the first pit, no outcrop of massive chromitite is exposed anywhere. However loose boulders of massive chromite litter the floor (BGS-USGS-GLW, 2008). A cross-section through the Dymitriak open pit, dating back to the time of exploitation and based on about 40 m deep drillings, shows the presence of serpentinite outcropping at the bottom of the open pit and now hidden and below the lake that nowadays fills the open pit and not outcropping peridotite. Chromitite lenses are bent at decametric scale and hosted within serpentinite and peridotite.

At Anengitra, about 5 km southwest of Zavindravoy, chromite was mainly mined from chromitite-rich levels in laterite close to a 500x200 m outcropping serpentinized peridotitic body (UT, 2009). BGS-USGS-GLW (2008) describes a deeply weathered and lateritized host consisting of several different rock types: gabbro pegmatite, pyroxenite, chromitite and plagioclase lherzolite.

Chromitite was sampled from Dymitriak and BC open pits at Zavindravoy, from outcrops with densely disseminated texture as well as from scattered blocks of massive chromitite.

Analyzed chromitites are massive and show large euhedral crystals with well-preserved rims. Silicate matrix, preserved in small areas or in fractures occurring in the crystals, is mainly composed of fresh olivine, with minor serpentine and tremolitic amphibole. Other gangue phases are ilmenite, pentlandite and rare magnetite.

Chromites are chemically characterized by an XMg between 0.5 and 0.65 and an XCr between 0.70 and 0.80. Moreover they are characterized by a high Cr_2O_3 content that sometimes can reach 65 wt % and is never below 53 wt%. TiO_2 is never more than 0.3 wt% and Al_2O_3 ranges between 10 and 14.50 wt%.

3.3.3 North Toamasina

The North Toamasina chromite district comprises several chromitite bodies spread in an area of about 800 km^2 most of which are only deduced from alluvial chromitite findings. The only extensive chromitite outcrop can be seen at Ranomena open pit mine, where chromitite occurs as lenses within a lenticular body of altered pyroxenite/harzburgite (Grieco et al., 2012).Ten lenses, up to 5 m in thickness and of variable length, have been firstly recognized by Bésairie (1966). The deposit was exploited by UGINE from 1960 to 1967.

Most of Ranomena chromitites are massive, contain 60 to 85 modal % chromite and exhibit a cumulus texture where the cumulus phase is always chromite with intercumulus silicates. Chromite grains up to 1 mm in size are euhedral and are enclosed in anhedral silicates consisting of primary orthopyroxene and secondary tremolitic amphibole, serpentine, chlorite and talc. Magnetite is the most common accessory mineral, followed by ilmenite, rutile, zircon, chalcopyrite, bornite, pentlandite and heazlewoodite.

Chromite crystals are generally euhedral and sometimes zoned, with a primary chromite core and a ferrit-chromite rim. Ferrit-chromite alteration is restricted to a few samples where Cr-chlorite is also present and usually affects only a small portion of chromite grains. Inclusions of primary silicates and accessory phases are common. Porosity within chromite grains can be as high as 20% and is a diagnostic feature in altered ferritchromite grains. Most of the samples show brittle fracturing of chromite grains, with fractures often filled by later magnetite.

A peculiar feature of Ranomena chromitites is their abundance in platinum group minerals that show a rich mineralogical assemblage, comprising sulphides, alloys and arsenides (Grieco et al., 2012).

Generally chromites are quite low in Cr_2O_3, never exceeding 50 wt%, FeO is high, ranging between 17.5 and 22.5 wt%, and calculated Fe_2O_3 is never below 5 wt%. MgO is low; systematically below 12 wt% and as low as 8 wt%. Al_2O_3 content is strongly variable, with lowest and highest limits at 11 and 21 wt%, respectively. TiO_2 content is comprised between 0.15 and 0.7 wt%.

3.3.4 Antanimbary

The Antanimbary chromitites outcrop within the Maevatanana belt where a large number of lenticular bodies of mafic/ultramafic rocks occur, including talc schists, serpentinites, orthoamphibolites, actinotremolites and metagabbros (BGS-USGS-GLW, 2008). Chromitites, outcropping in seven lenses, were sampled close to the village of Antanimbary. They are hosted within an orthoamphibolite sheath that is in turn surrounded by massive metagabbro.

Chromitiferous layering is concordant with the dominant fabric of the metagabbro and the lenses range from 10 to 200 m in length and 1.5-20 m in thickness.

Chromitites are massive with more than 70 and up to 90 modal % chromite and have a cumulus texture where the cumulus phase is always chromite with intercumulus silicates.

The ore is massive and with quite high tonnage but has never been exploited due to the low Cr_2O_3 content and very low Cr/Fe ratio.

Chromite grains are completely altered into ferritchromite. Grains range from 0.1 to 0.5 mm in size, are euhedral, with fractured cores and porous rims, and enclosed in an anhedral silicate gangue. Gangue is mainly composed of clinochlore to sheridanite chlorite with minor tremolitic to actinolitic amphibole and very rare talc. Primary gangue phases, mainly as inclusions, are orthopyroxene, albite and biotite. Ti phases are very common and comprise rutile, ilmenite and titanite (Figure 2). Secondary magnetite is rare as scattered small grains in the gangue.

Chromite crystals (isolated or in aggregates) preserve the original shape even if they are completely altered to ferritchromite. A slight core-to-rim zoning occurs, with porous ferritchromite cores surrounded by a more porous corona showing a stronger alteration. Grains never preserve composition of primary chromite. Generally ferritchromites are very low in Cr_2O_3, never exceeding 43 wt%. FeO is high, ranging between 29 and 33 wt%, calculated Fe_2O_3 is never below 6.60 wt% and reaches very high values, up to 28 wt%, in more altered ferritchromite grains, that can better be described as Cr-magnetites. MgO is extremely low, systematically below 2.2 wt%. Al_2O_3 content is strongly variable, with the lowest and highest limits at 3.3 and 22.0 wt%. TiO_2 is highly variable, but in general high, ranging between 0.3 and 1.3 wt%.

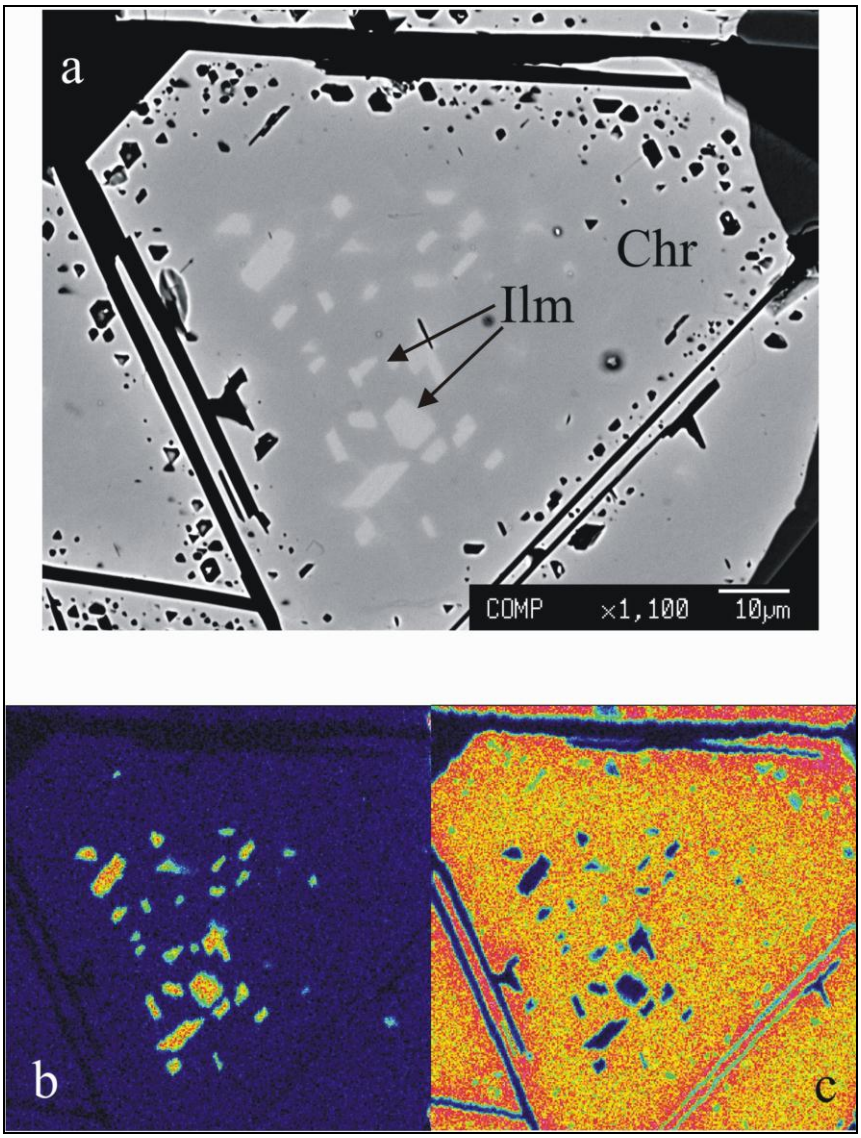

Figure 2. Back Scattered Electron image (a), and Ti (b) and Cr (c) atomic maps of a chromite grain with ilmenite inclusions from Antanimbary chromitites.

3.3.5 North Belobaka

Chromite ores in the Belobaka area were found 2.5 km SE of Anosibe village (6 km north of Belobaka). They are hosted in an area of approximately 10x2 km with a high concentration of alluvial chromitite occurrences. Outcropping rocks are mainly biotite- and amphibole-bearing migmatites, with an intrusive body of mafic-ultramafic rocks that comprise diorite, gabbro, pyroxenite and orthoamphibolite. Chromitite host rock is a mafic-ultramafic body characterized by an amphibole gneiss with amphibolites (Marchal, 1959). Samples were collected from four outcrops of small centimetric chromitite layers aligned along 250-300 m. Chromite grains are mainly euhedral and rarely show initial ferrit-chromite alteration. Silicate gangue is composed of widespread primary orthopyroxene and secondary talc, serpentine, chlorite and tremolitic amphibole. Ti phases (rutile and ilmenite) are common, as well as magnetite.

The composition of chromite is extremely homogeneous within each outcrop, but differs slightly between different outcrops. Main differences concern Cr_2O_3 and Al_2O_3 that do not vary for each outcrop more than 2 wt% but that show a total range of 41-47 wt% for Cr_2O_3 and 10-17 wt% for Al_2O_3 due to differences between different outcrops. Other elements do not show systematic differences between outcrops and their ranges are 25-28 wt% for FeO, 7-10 wt% for Fe_2O_3 and 5.5- 6.5 wt% for MgO. Finally, TiO_2 is high as it ranges between 0.5 and 0.7 wt%.

3.4 Discussion

The Madagascar chromitites, like chromitites all over the world, are always strictly associated to mafic and ultramafic rocks but outcrop in different geotectonic domains of the Madagascar Precambrian shield. The five main bodies studied in this work are located in three different units: Tsaratanana sheet, Antananarivo block and Anaboriana-Manampotsy belt (Figure 1). Minor chromitite localities and chromitite clues have been found in the same units, with the exception of those of the Mananara-Manoantsetra district, that are hosted in the Antongil block of the Antongil-Masoara craton.

The ultramafic association (Table 1) is dominated by secondary metamorphic rocks like serpentinite, talcose rocks, and orthoamphibolites. The main primary lithologies preserved are pyroxenite and peridotite, although usually partially to almost completely serpentinized.

Serpentinization usually does not allow any further discrimination within peridotite. Relationships between chromitite and ultramafic rocks are often not clear due to paucity of outcrops, weathering (often as deep as to produce a decametric thick laterite cover), intensive chromitite exploitation or the formation of lakes within the abandoned open pits that hide outcrops.

The only place where the relationship is clear, mainly thanks to the ongoing exploitation, is in the Andriamena district, where chromitites are included in serpentinized peridotites and in gabbro at Ankazotaolana and in serpentinized peridotites with minor pyroxenites at Bemanevika. At Zafindravoy, North Befandriana district, disseminated chromitites are included in pegmatitic orthopyroxenites, while relationships with nearby peridotites are, at present not clear. At Anengitra the outcrops are close to a small body of serpentinized peridotites.

Chromitite-ultramafite association is even less clear in the other localities, where hos rocks are deeply metamorphosed and altered: at Antanimbary host rock is orthoamphibolite, at Ranomena host rock is serpentinized and strongly weathered even if Bésairie (1966), who might have had access to the mine during exploitation, describes it as harzburgite/pyroxenite. Finally at North Belobaka the host rock is again orthoamphibolite, which is part of a mafic-ultramafic intrusion comprising also diorite, gabbro and pyroxenite.

With the exception of the work by Grieco et al. (2012) about the North Toamasina chromitites, genetic interpretation of the Madagascar chromitites and their association with geodynamic domains has been so far based only on geological, petrographic and structural data. The location of North Toamasina chromite district within an important and controversial shear zone focused most attention on these chromitites. Chromitite-hosting ultramafic bodies were interpreted as remnants of oceanic lithosphere (Collins, 2006) or preserved parts of an ophiolitic melange (De Waele et al., 2009). This ophiolitic genesis and oceanic geodynamic environment were more an inference from the interpretation of the Betsimisaraka belt as an oceanic suture than a hypothesis based on actual geological, structural, mineralogical and geochemical data. A stratiform type origin for the North Toamasina chromitites has been firstly suggested by BGS-USGS-GLW (2008) and then supported by Grieco et al. (2012). The Authors claim that, on the basis of mineralogy, mineral chemistry of olivine and chromite and Platinum Group Element distribution and mineralogy, the North Toamasina chromitites can better be interpreted as belonging to a layered intrusion in an extensional continental environment.

The Andriamena and North Befandriana chromitites have been associated to a Bushveld-type layered intrusion environment, mainly on the basis of the lithological association of mafic ultramafic rocks and their spatial relationships (BGS-USGS-GLW, 2008). While this interpretation is strongly supported for the Andriamena chromitites, the same Authors are more open to a possible ophiolite origin for the Befandriana chromitites due to their much lower tonnage, their association with pyroxenite and the absence or scarcity of mafic rocks.

The absence of detailed studies, probably due to the low economic potential of the ore bodies, may explain the lack of any genetic interpretation for the Antanimbary and North Belobaka chromitites.

The gangue mineralogy, summarized in Table 2, is not very helpful for discriminating between the different chromitites studied. Apart of widespread secondary minerals, the most common primary phases are orthopyroxene and olivine among silicates, ilmenite, rutile and magnetite among oxides and pyrrhotite and pentlandite among

sulphides. Quantitative relationships between primary gangue phases usually are not preserved as they are mostly found as relics in a serpentinized matrix or as inclusions in chromite crystals. Anyway the least serpentinized samples at Ranomena contain a gangue that is mostly composed of orthopyroxene, while olivine is very rare. On the other hand, olivine, by far, prevails on orthopyroxene in the matrix of weakly serpentinized chromitites from North Befandriana. Antanimbary is a peculiar case where a pervasive ferritchromitization produced a gangue silicate assemblage dominated by secondary iron-rich Cr-chlorite with minor actinolitic amphibole. Primary phases (orthopyroxene, albite and biotite) were found only as relics. These data show that Antanimbary has a distinctive mineralogical signature that has never been found in ophiolite chromitites and strongly argue for a layered intrusion origin of these chromitites. In the other localities the ubiquitous presence of orthopyroxene in the gangue is not discriminating even if mantle-hosted chromitites have a dunitic gangue with very rare orthopyroxene. On one hand preferential serpentinization of primary silicates could have altered olivine to orthopyroxene proportion in the gangue and, on the other hand, chromitites from the cumulate sequence of ophiolites can have an orthopyroxene-rich gangue (e.g. Malitch et al., 2003). Only at Ranomena the abundance of orthopyroxene is a clear clue that excludes the derivation of chromitites from an ophiolitic mantle.

Mineral chemistry of primary phases can be a useful tool to unravel the genetic processes that led to the formation of chromitite bodies. Spinel composition has widely been used as a petrogenetic indicator, especially in ultramafic rocks where it is the phase that best preserves primary composition, so that now a very large database of spinel compositions is available (e.g. Roeder, 1994; Barnes and Roeder, 2001). The most important changes in spinel composition within ultramafic rocks comprise post-magmatic re-equilibration with matrix silicates, metamorphic growth of secondary magnetite during serpentinization and formation of ferritchromite rims or halos. Post-magmatic re-equilibration in massive chromitites, like most of the samples studied, affects mainly silicate compositions whereas spinel compositions are only slightly affected by this process due to the high spinel/silicate mass ratio (Mondal & Mathez, 2007). Magnetite growth does not obliterate primary spinel composition as magnetite grows at the expenses of silicates because serpentine cannot host the iron derived from primary silicates. On the other hand formation of ferritchromite occurs at the expenses of primary spinel and leads to formation of Cr-bearing chlorite, whose Cr content derives completely from spinel (Merlini et al., 2009 and references therein). Luckily primary spinel cores, especially in massive chromitites, are not affected by ferritchromitization and, even when primary spinels are completely transformed into ferritchromite like at Antanimbary, ferritchromite compositions draw an alteration path that provides useful information on primary spinel composition.

The Madagascar chromites cover a wide range of compositions in the XMg [(Mg/(Mg+FeII)] vs XCr [Cr/(Cr+Al+FeIII)] chart (Figure 3) widely used for the genetic interpretation of chromites (Barnes & Roeder, 2001 and references therein). North Toamasina, North Belobaka and Antanimbary chromites all show a clear trend of XCr increase and XMg slight decrease that is associated to the partial ferritchromitization of these rocks. The continuous trend indicates that transformation into ferritchromite is gradual and hence we decided not to plot chromite and ferritchromite separately as any chemical discrimination would be arbitrary. Primary compositions are those showing the lowest XCr values. Both North Toamasina and North Belobaka chromites plot in the field of layered intrusions, with more evolved compositions for North Belobaka. North Befandriana chromites are very homogeneous, do not show any trace of ferritchromite and plot in the area of overlapping between layered intrusion and ophiolite fields. On the contrary, Andriamena chromites show a wide range of compositions that are puzzling. As a matter of fact, most of the analyses plot also in the field of overlapping but some data plot in the field of ophiolite- and some others in the field of layered intrusion-related chromites. The highest XMg chromites are those with a peridotitic host rock, while intermediate and low XMg values are from chromitites hosted within gabbro. Finally the Antanimbary chromites are the most puzzling. Their XMg is extremely low, lower than the lowest values attributed to the most differentiated chromites within layered intrusions.

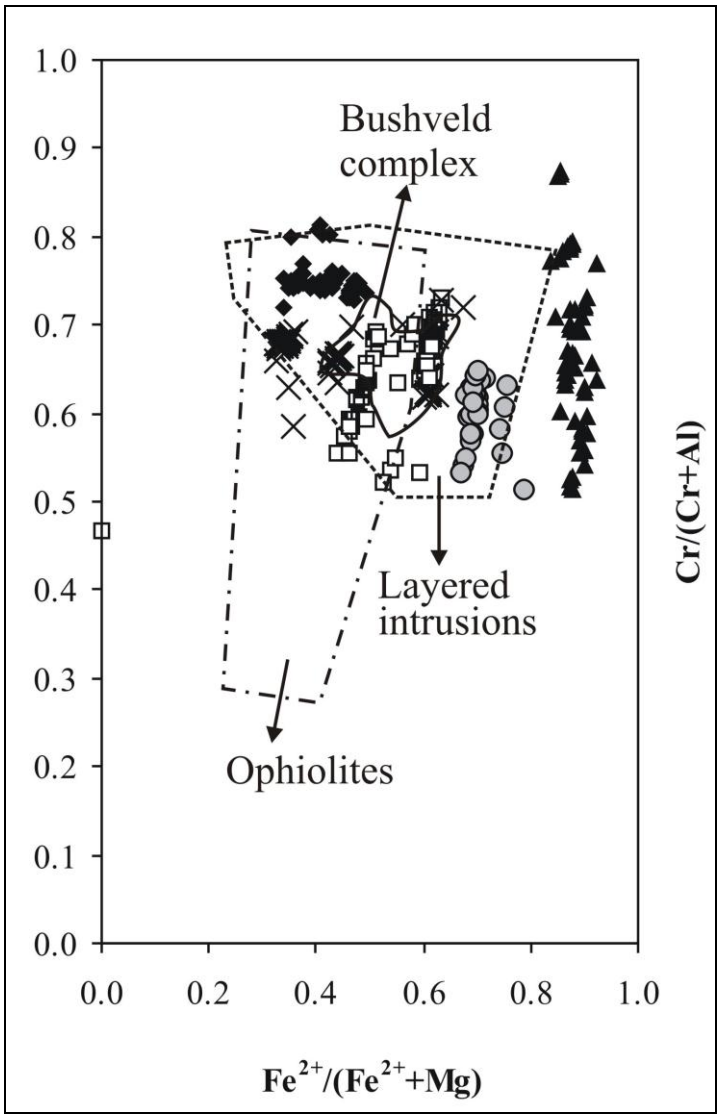

Figure 3. Chromite XFe vs XCr chart. Symbols: cross: Andriamena, diamonds: Befandriana, squares: North Toamasina, circles: North Belobaka, triangles: Antanimbary. Continuous contour line: Bushveld complex, dashed contour lines: ophiolites and layered intrusions. Compositional fields from Leblanc & Nicolas (1992).

A second plot used to discriminate chromite origin proposed by Ferrario & Garuti (1988) and afterwards widely used, is the Cr_2O_3 vs TiO_2 plot (Figure 4). In this plot the Madagascar chromites group into two different fields. On one hand Andriamena and Befandriana chromites are very low in TiO_2 and plot in the field of ophiolite chromites, with an overall trend of increasing TiO_2 with Cr_2O_3 increase. North Toamasina, North Belobaka and Antanimbary chromites are instead TiO_2- rich and plot in the field of layered intrusions, with a large overlapping between the three localities. North Toamasina and North Belobaka chromites show compositions similar to those of Lower and Middle Group chromitites from Bushveld even if with slightly lower TiO_2 contents. Antanimbary chromites instead are much lower in Cr_2O_3 than those from any Bushveld chromitites, suggesting a different and possibly higher stratigraphic position within the layered intrusion.

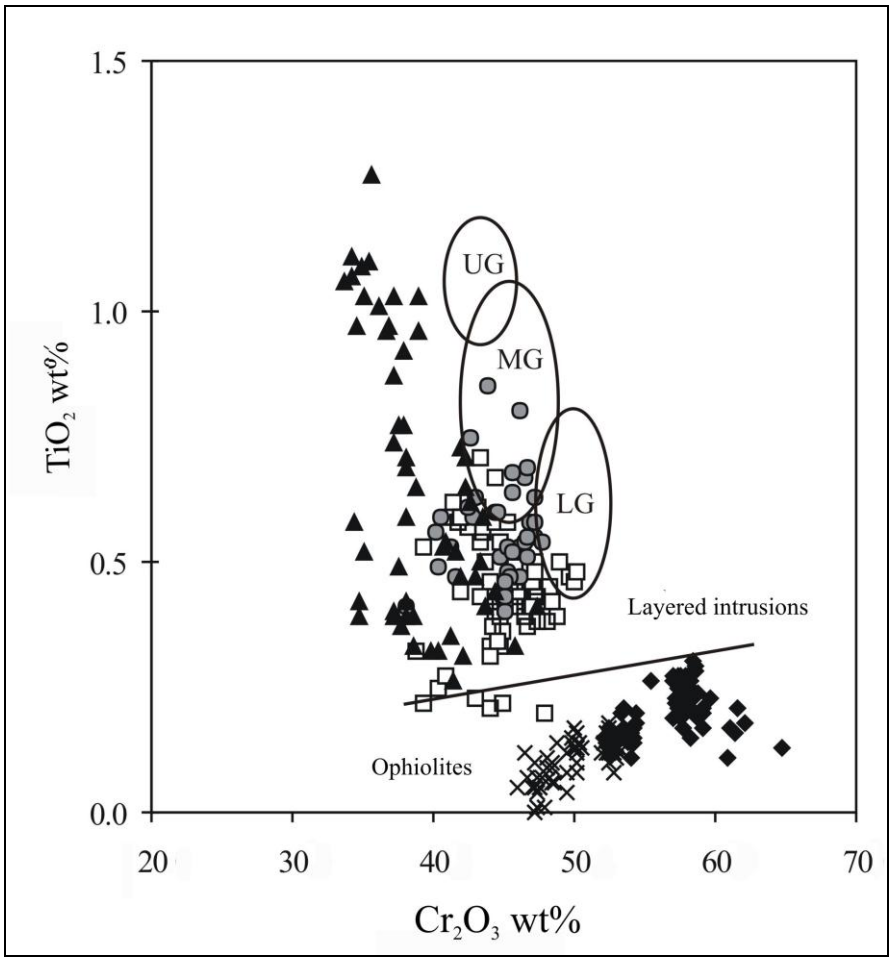

Figure 4. Chromite Cr_2O_3 vs TiO_2 chart. Symbols: crosses: Andriamena, diamonds: Befandriana, squares: North Toamasina, circles: North Belobaka, triangles: Antanimbary. LG = Lower Group, MG = Middle Group, UG = Upper Group chromitites from Bushveld complex. Compositional fields from Ferrario and Garuti (1988) and from Naldrett et al. (2009).

Ophiolite chromites show a wide range of Cr_2O_3 content due to a large Cr-Al substitution so that the two metals are usually inversely well correlated, while such correlation is not evident in layered intrusion chromites where larger amounts of FeIII can substitute for Cr and Al. When plotted in a Cr_2O_3 vs Al_2O_3 chart once again North Befandriana chromite compositions fit in the field of ophiolites, North Toamasina, Antanimbary and North Belobaka chromites fit in the field of layered intrusions and Andriamena chromite distribution overlaps the two fields (Figure 5).

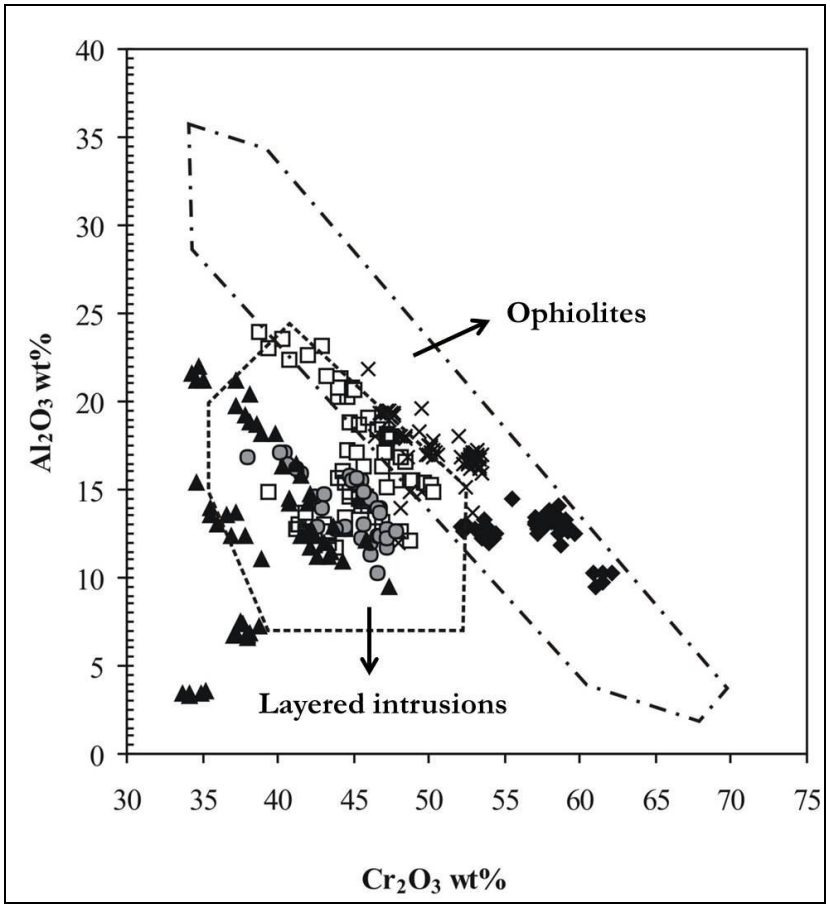

Figure 4. Chromite Cr_2O_3 vs Al_2O_3 chart. Symbols: crosses: Andriamena, diamonds: Befandriana, squares: North Toamasina, circles: North Belobaka, triangles: Antanimbary. Compositional fields from Bonavia et al. (1993).

The new chemical and mineralogical data together with lithological and petrographic observations argue for a different origin of the chromitite bodies. All data fit a layered intrusion origin for North Toamasina and North Belobaka chromitites, the most discriminating being the lithological association of mafic and ultramafic rocks and the mineral chemistry of chromite. The geochemical signature of Platinum Group Elements can be added to these factors for North Toamasina (Grieco et al., 2012).

Data on the Andriamena chromites are not as discriminating as those on the North Toamasina and North Belobaka ones because of the presence of high XMg chromites in chromitites associated to a peridotitic host rock. Anyway, the close association of chromitites and gabbro-norite, the presence of a trend of decreasing XMg at constant XCr, typical of layered intrusions, and the area covered by data plots in the Cr_2O_3 vs Al_2O_3 chart argue for a layered intrusion origin of these chromitites. Lower XMg chromites and close association with plagioclase-bearing rocks can be found in the chromitites hosted within the cumulate sequence at the base of the crustal sequence of ophiolite successions (e.g. Grieco et al., 2007; Malitch et al., 2003) but in these cases chromite usually shows different composition in each layer also with low XCr values that are not found at Andriamena. Moreover the big size (millions of tons) of chromitite ores at Ankazotaolana and Bemanevika is in contrast with the typical small size of chromitite ores in the cumulate sequence of ophiolites. In this picture the very low TiO_2 content of chromite remains controversial.

Among all the Madagascar chromite ores, the North Befandriana chromites are those with the clearest clues of an ophiolitic origin. Even though they are associated to the Andriamena chromitites in a layered intrusion origin (BGS-USGS-LGW, 2008) the same Authors acknowledge that, the absence of clear association with mafic rocks move them closer to the ophiolite chromite typology. Chromite mineral chemistry provides a strong argument for an ophiolitic origin. If, on one side, the high XMg, more typical of ophiolite chromites, is balanced by the absence

of high Mg-low Cr compositions the low TiO_2 content, the high Cr_2O_3 content, up to 62 wt%, that is typical only of ophiolite chromitites, and the area covered in the Cr_2O_3 vs Al_2O_3 chart argue for this type of origin. Another possible hint for an ophiolite origin is the association of disseminated chromitite with pegmatitic orthopyroxenite, as such rocks are typical of ultramafic layers in the basal cumulate sequence of ophiolites and also often present in the ophiolite mantle as orthopyroxenite dykes.

Antanimbary are the most striking of all Madagascar chromitites. Their very low XMg rules out any possible ophiolitic origin for these rocks. But XMg values are too small even for the layered intrusion chromites that usually never decrease below 0.1 XMg. The least altered chromites get close to Cr-magnetite compositions, with up to 60 wt% FeO_{tot} and almost devoid of MgO and Al_2O_3. Mineralogy and orthopyroxene mineral chemistry can provide important data on their origin. Peculiarities in mineralogy comprise the presence of plagioclase among gangue minerals, the abundance of titanium phases (rutile, ilmenite and titanite) and the absence of olivine and serpentine. The mineral chemistry of chromites resembles that of North Belobaka and North Toamasina but at Antanimbary TiO_2 content of chromite reaches much higher values that are testified also by the frequent unmixing of titanium phases within chromite (Figure 2). Another important character is the extreme enrichment in iron that is positively correlated with TiO_2 increase. Such enrichment is not only found in chromites but also in primary orthopyroxene, whose composition reflects that of orthopyroxene from the Bushveld Upper Zone (Vantongeren et al., 2010) (Figure 6). Finally different lenses show different and evolving chromite compositions that argue for different position of chromitite lenses within a magmatic sequence, even if in absence of a stratigraphy. A possible explanation for Antanimbary chromitites is that they represent the equivalent of the Ti-magnetite layers of the Bushveld Upper Zone. This interpretation is strengthened by the absence of ultramafic rocks at Antanimbary. Bushveld Ti-magnetites contain low amounts of Cr_2O_3 that, anyway, increase up to 2 wt% at the bottom of each layer (McCarthy and Cawthorn, 1983; Cawthorn et al., 1983) and have TiO_2 content similar to that of Antanimbary chromites (Figure 6). It is possible that at Antanimbary chromites or Cr-magnetites are related to a final differentiation stage of the melt similar to what occurred in the Bushveld but, differently from Bushveld, the absence of clinopyroxene (never found at Antanimbary), prevented Cr scavenging from the melt that occurred in the Bushveld main zone due to clinopyroxene crystallization.

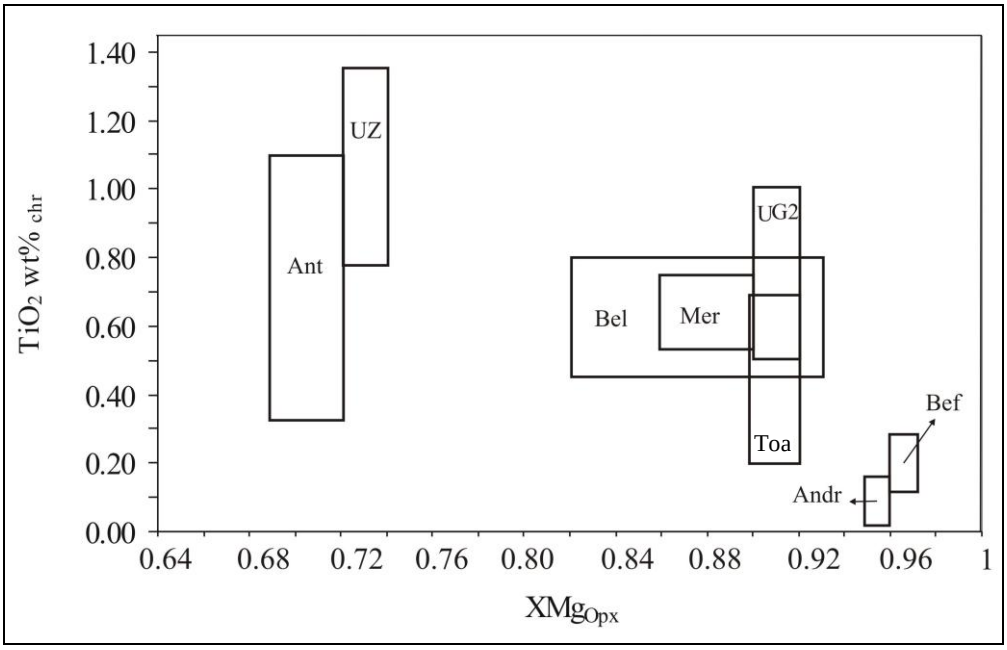

Figure 5. Orthopyroxene XMg vs TiO_2 content of chromite. Rectangle sides represent compositional variability of selected parameter. Andr = Andriamena, Bef = North Befandriana, Ant = Antanimbary, Bel = North Belobaka, Toa = North Toamasina. Data for Bushveld from Mathez & Mey (2005), Mondal & Mathez (2007), Vantongeren et al., 2010.

3.5 Conclusions

In spite of the Archean age of geotectonic domains where most of Madagascar chromitites outcrop their most relevant common feature is the relatively young, Neoproterozoic to Cambrian, age of emplacement of the mafic-ultramafic intrusions they are hosted in. Differences are anyway much more marked than similarities, comprising lithological association, texture, tonnage of the ores, mineralogy of spinels and gangue phases, mineral chemistry of both spinels and silicates and type and development of alteration. Anyway they do not reflect different geotectonic settings but likely a primary feature related to the position of the chromitite bodies within the stratigraphic sequence of zoned layered intrusions. Actually, all but North Befandriana chromitites fit into a layered intrusion genetic model. Further differences are due to the specific metamorphic and alteration history that which any of the intrusions underwent.

The full set of data suggests a deep stratigraphic position within a basal cyclic ultramafic series of layered intrusion for Andriamena chromitites, a higher position for North Toamasina and North Belobaka chromitites, where chromite composition is more evolved and the magmatic sequence already comprises mafic rocks. Finally Antanimbary chromitites can be associated to the upper portion of a layered intrusion with strongly differentiated compositions.

North Befandriana chromitites are most likely of ophiolitic type. The close association with pegmatitic pyroxenites and the pyroxene gangue of massive chromitites favors a location of the studied chromititc bodies above the petrologic Moho within the basal ultramafic cumulates of the ophiolitic sequence.

Alteration mainly affected the silicate gangue that shows always the presence of secondary phases that in some places almost completely obliterate the primary assemblage. The only secondary process that, in some places, strongly affected chromite composition was ferritchromitization, that anyway occurred giving rise to specific and easily recognizable geochemical patterns, absent at North Befandriana and Andriamena, partially developed at North Toamasina and North Belobaka and fully developed at Antanimbary.

North Befandriana is a high quality deposit that could be exploited without any beneficiation of the ore, Andriamena needs beneficiation to reach market standard, Antanimbary and North Belobaka is low quality for metallurgical or chemical use but could be a good prospect for refractory market. Finally North Toamasina chromite ore is not suitable for any market even after beneficiation.

Chapter 4

Evaluation of geological parameters affecting chromite enrichment processes

Planning of beneficiation plants for chromite sands based on gravity separation of chromite from gangue minerals is a complicated topic. As a matter of fact, the results in term of grade and recovery of the final product are strongly affected by a great amount of geological parameters, either mineralogical, chemical or textural. Some aspects of these parameters and their influence on the quality of the final product were studied in chromite ores in Greece where gravity enrichment of chromite sands either occurs, occurred or is planned.

Chromite alteration in metamorphic conditions can lead to redistribution of Cr_2O_3 from chromite to silicates. Such redistribution was studied in the Vavdos chromite deposit (Greece) where more than 3 wt% Cr_2O_3 can be found in silicates. The effect of the redistribution is to lower the efficiency of gravity plants as Cr_2O_3 contained in silicate phases will be preferentially discharged into the tailing during enrichment.

The results of this study led to the publication of a scientific paper entitled "Metamorphic redistribution of Cr within chromitites and its influence on chromite ore enrichment" (Grieco, Pedrotti and Moroni, 2011), which was published in the journal *Minerals Engineering (Elsevier)*. This paper is presented below.

4.1 Introduction

Chromite ore beneficiation is mostly achieved by physical methods (mainly tabling, jigging and magnetic separation) in order to separate chromite from gangue minerals (Nafziger, 1982). In the last two decades Multi-Gravity Separator has been added to gravity separation techniques used for chromite (Traore et al., 1994). Planning of chromite sand beneficiation plants based on physical separation of chromite from gangue minerals is a complicated topic. As a matter of fact, the results in terms of grade and recovery of the final product are strongly affected by a great amount of geological parameters, either mineralogical, chemical or textural.

Mineralogical and chemical parameters used to set up enrichment plants for chromite sands and/or to predict final product quality are based essentially on texture, whole-rock analyses, mineralogy and average mineral chemistry of chromite (e. g. Dahlin et al., 1983, Traore et al., 1995; Guney et al., 2001; Agakayak et al., 2007; Pascoe et al., 2007).

Mineralogy is used to predict behavior of gangue minerals during beneficiation, according to their specific weight and habitus but mineral chemistry of gangue minerals is never taken into account, because of the generally accepted assumption that all the Cr_2O_3 is hosted within chromite.

Such assumption is valid for unmetamorphosed chromite ores but is not valid for chromite ores that were metamorphosed in presence of aqueous fluids and that show a partial metasomatic redistribution of chromium within gangue minerals.

The most common metasomatic alteration of chromitites is related to the formation of a ferritchromite + Cr-chlorite assemblage, partially replacing primary chromite + olivine or secondary chromite + serpentine assemblages (Kimball, 1990; Barnes, 2000; Mellini et al., 2005). Such kind of alteration is widespread and reported in chromitites, either mined or not, from all over the world and of different genetic types and ages (e.g. Christofides et al., 1994; Mohanty et al., 1996; Garuti et al., 2007; Khalil, 2007; Prendergast, 2008; Gonzalez-Jimenez et al., 2009) and even in studies of chromite ore beneficiation (Dahlin et al., 1983).

Merlini et al. (2009) developed a model for chromitite alteration where such process occurs in presence of circulating aqueous fluids without any external income of metallic elements. As a result the whole-rock chemistry is

not affected by this process, anyway several elements are redistributed between old and newly formed phases. New phases are Cr-chlorite, growing on serpentine, and ferritchromite, that substitutes chromite. The modal ratio between newly formed and old phases is ruled by the initial modal chromite content within chromitite. Moreover Grieco et al. (in press) suggested that such alteration may occur also in unserpentinized chromitites, where Cr-chlorite grows on olivine instead of serpentine.

Cr-chlorite is an important Cr-bearing phase where Cr_2O_3 content can strongly vary, being usually between 0.5 and 8 wt% (e.g. Mohanty et al, 1996; Arai et al., 2006; Khalil, 2007; Hamada et al, 2008). It is worth to note that, according to Merlini et al. (2009), alteration of any chromitite with more than 34.16 modal % chromite will produce an assemblage devoid of serpentine, where the only silicate phase is Cr-chlorite. It can be deduced that deeply altered chromitites potentially contain significant amounts of Cr_2O_3 within Cr-chlorite which, due to its low density, its low magnetic suscettivity and its lamellar crystal habitus, is preferentially discharged into the tail in any physical enrichment plant.

On the other hand ferritchromite is usually slightly to highly enriched in Cr_2O_3 compared to chromite but is also strongly enriched in Fe, thus lowering the Cr/Fe ratio in the final product. In most altered chromitites ferritchromite composition can shift into chromian-magnetite and even magnetite field, thereby resulting in a complete loss of Cr_2O_3 content (Mellini et al, 2005). Due to the typical rim-to-core substitution pattern of ferritchromite on chromite, the usual core analyses of chromite grains, done to assess average chromite composition, are misleading when in presence of such alteration phenomena.

The purpose of the present work is to study and to quantify the effect on chromite sand concentrate grade and recovery of Cr metasomatic redistribution within chromite ore.

4.2 Materials and methods

The effect of chromite metasomatic alteration on enrichment efficiency and final product quality was studied on an altered chromitite ore from Vavdos Mine, Halkidiki peninsula, Greece. The Vavdos Mine is located inside the Vavdos ultramafic massif, one of several, NW-SE aligned ultramafic bodies belonging to the Halkidiki ophiolite in the Circum-Rhodope orogenic belt (Boccaletti et al., 1974). Chromitite ore, composed of several metric to plurimetric chromitite lenses, is hosted inside completely serpentinized dunites (Figure 1).

Alteration is widespread and newly formed Cr-chlorite and ferritchromite are ubiquitous, while serpentine is usually a relict phase (Christofides et al., 1994).

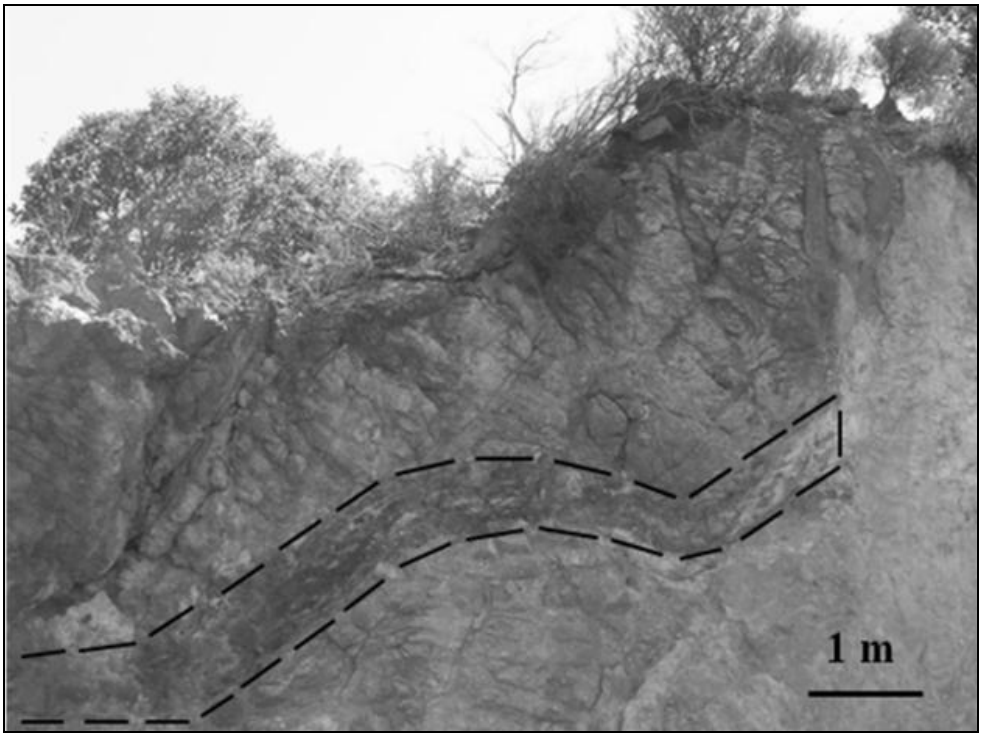

Figure 1. Chromitite lens VV-A within completely serpentinized peridotites at Vavdos Mine.

Eleven samples were collected from three different chromitite lenses labeled as VV-A, VV-B and VV-C. Microscopy revealed the ubiquitous presence of Cr-chlorite and ferritchromite in all lenses (Figure 2 and 3) and minor Cr-magnetite in VV-C. Deeper alteration of VV-C is testified also by complete absence of serpentine, that is a minor relict phase in VV-A and in VV-B.

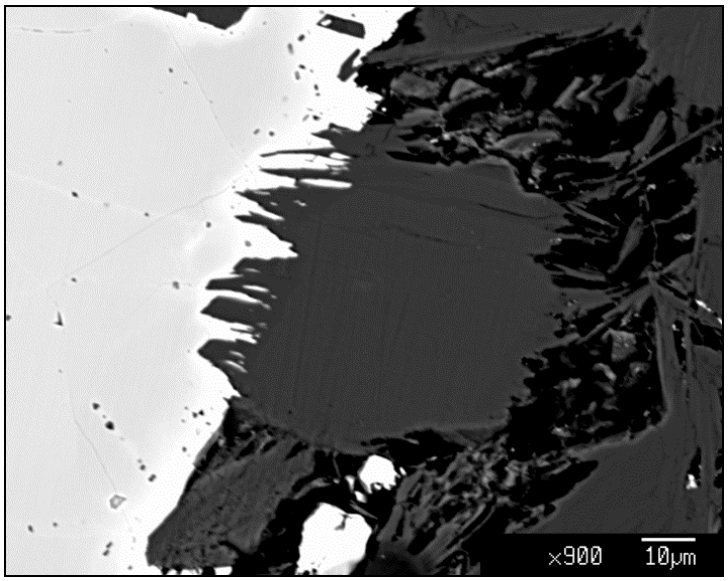

Figure 2. Intergrowth of Cr-chlorite (grey) and ferritchromite (white) replacing the chromite rim (light grey).

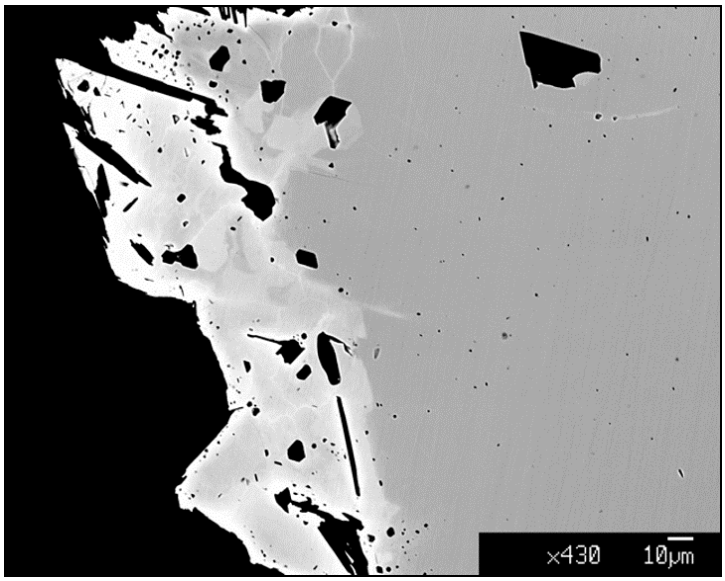

Figure 3. Chromite grain (grey) with a rim to core replacement of ferritchromite (light grey to white).

Whole rock major elements content was analyzed with X-Ray-Fluorescence, and Electron Microprobe (EMP) microanalyses of all phases were carried out with a JXA – 8100 / 8200 JEOL probe both at Dipartimento di Scienze della Terra, University of Milan.

The assessment of the distribution of Cr_2O_3 in the ore requires the knowledge of the relative amount of phases. The modal content of each phase for the three lenses was determined by means of image analysis performed on scanned images of thin sections and on back-scattered electron images acquired by the scanning electron microscope equipment of the microprobe. Images were processed and modal analysis was done using Image Pro Plus© software. First of all different ranges of grey intensities were associated to different phases by comparison with microscopy observations. Subsequently black and white images were transformed into color images where each color was associated to a single phase. Finally the modal percentage of each phase was calculated by area counting for each color. At this stage chromo-magnetite was disregarded due to its negligible modal amount. The modal contents of all phases for each lens were calculated as an average of all samples from that lens.

Enrichment tests were performed using a laboratory shaking table working chromite sand from Vavdos chromitite lenses. 10 kg of chromite ore from each of the three lenses were crushed to -2 mm and sieved. The fraction +0.1 mm was tabled for separation of concentrate and tail three times. After each test all sand fractions were weighed and analyzed by XRF Fluorescence. Modal content of ore and gangue were then assessed by image analysis with the same technique described above. The same sand was used in the three test and the only parameter of the table that changed was the concentrate to tail ratio by shifting the position of the blade between the two fractions.

4.3 Results and discussion

X-Ray Fluorescence (XRF) whole rock analyses of all samples together with average data for the three lenses are shown in Table 1. Cr_2O_3 content is between 31 and 46 wt% with similar average values for the three lenses. These contents may reflect small scale variability of modal chromite more than larger scale changes within the deposit.

Table 1. Representative XRF analyses of chromite samples from Vavdos Mine.

Compound wt%	Samples of lens VV-A				Samples of lens VV-C				Samples of lens VV-B		
	VV1	**VV2**	**VV3**	**VV4**	**VV5**	**VV6**	**VV7**	**VV8**	**VV10**	**VV11**	**VV12**
SiO_2	15.16	10.36	10.07	13.30	14.67	10.98	18.78	8.24	17.13	17.91	12.52
Cr_2O_3	32.31	41.62	41.00	40.84	34.75	42.01	31.26	45.77	31.77	34.66	41.61
Al_2O_3	6.41	8.73	8.86	9.06	9.80	9.53	6.01	10.43	6.94	7.02	9.43
Fe_2O_3	15.02	17.02	16.73	16.45	16.87	16.45	16.23	16.59	15.35	12.58	13.16
MgO	19.52	15.96	15.52	18.97	19.43	18.94	21.79	17.01	21.43	22.32	18.82
CaO	1.10	0.09	0.09	0.11	0.09	0.08	0.09	0.11	0.96	0.90	0.09
Na_2O	0.01	0.01	0.01	0.01	0.01	0.01	0.01	0.03	0.01	0.01	0.01
K_2O	0.01	0.01	0.01	0.01	0.01	0.01	0.01	0.01	0.01	0.01	0.01
TiO_2	0.10	0.12	0.11	0.15	0.22	0.16	0.11	0.18	0.13	0.12	0.15
P_2O_5	0.01	0.01	0.01	0.01	0.01	0.01	0.01	0.01	0.01	0.01	0.01
MnO	0,17	0.14	0.13	0.17	0.28	0.16	0.20	0.19	0.15	0.12	0.14
LOI	6.0	2.9	2.4	2.8	3.6	2.8	4.8	1.8	5.4	5.9	3.3
Total	**95.90**	**97.02**	**94.98**	**101.92**	**99.84**	**101.23**	**99.39**	**100.39**	**99.40**	**101.75**	**99.33**
Cr/Fe ratio	2.10	2.39	2.40	2.43	2.02	2.50	1.88	2.70	2.02	2.70	3.09

Average values of Cr_2O_3, FeOtot and Cr/Fe for all phases are shown in Table 2. The differences in spinel composition between chromite, ferritchromite and chromo-magnetite are apparent in Figure 4 and follow the usual alteration trend of chromite. Cr_2O_3 content of Cr-chlorite is always between 3 and 6 wt% and is very uniform for the three lenses with average values comprised between 4.69 and 4.89 wt%. Worth to note is the low but not negligible Cr_2O_3 content of serpentine which is 1.32 and 2.07 wt% in average in the two lenses where it was detected.

Table 2. Average values of Cr_2O_3, FeOtot, and Cr/Fe for all phases and for each chromitite lens at Vavdos Mine.

Lens	Mineralogical phase	Cr_2O_3 (wt%)	FeO tot (wt%)	Ratio Cr/Fe
VV-A	Chromite	55.24	22.27	2.398
	Ferritchromite	65.36	26.40	2.381
	Cr-chlorite	4.76	1.57	2.932
	Serpentine	2.07	1.37	1.439
VV-B	Chromite	55.53	21.45	2.501
	Ferritchromite	64.65	25.32	2.471
	Cr-chlorite	4.89	1.39	3.479
	Serpentine	1.32	0.94	1.309
VV-C	Chromite	55.53	21.04	2.549
	Ferritchromite	66.10	22.40	2.831
	Chromo-magnetite	49.18	47.33	1.025
	Cr-chlorite	4.69	1.13	4.081

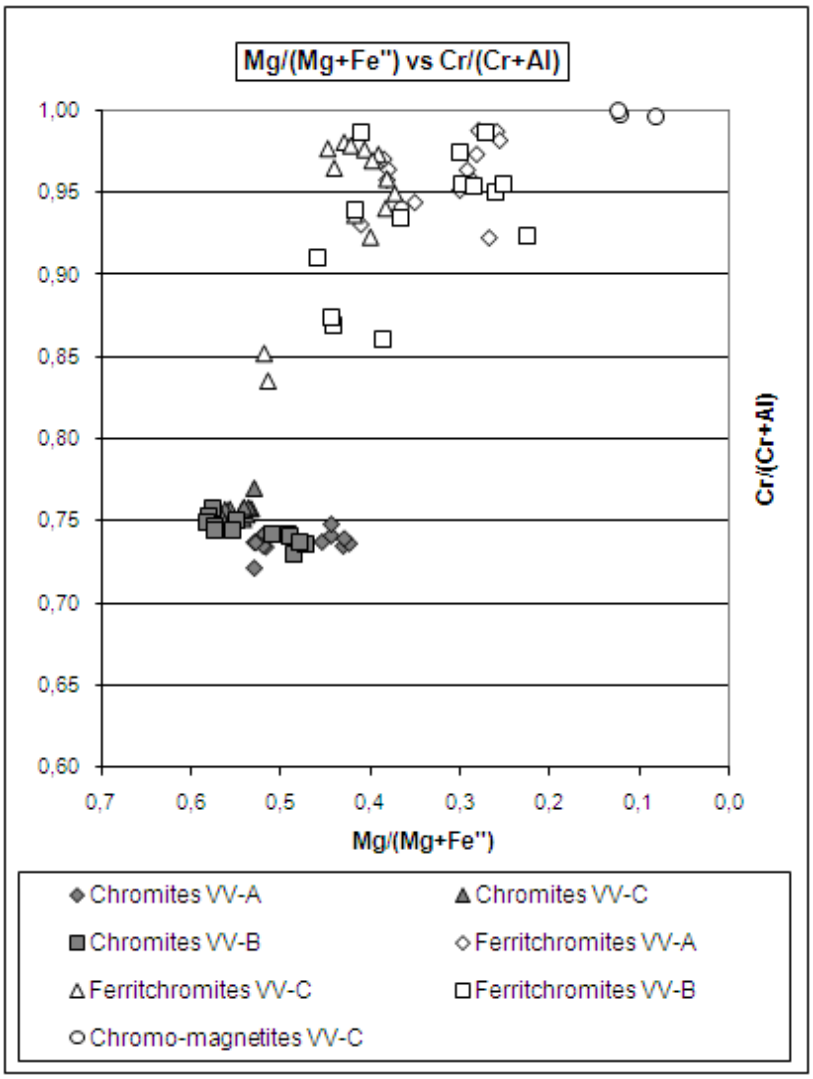

Figure 4. Plot of spinel composition showing differences between chromite, ferritchromite and chromo-magnetite at Vavdos Mine.

4.3.1 Cr_2O_3 distribution in the ore

Results of modal analysis are shown in Table 3. As modal data reflect volume abundance of phases, the next step is to transform them into mass abundances using average density values for each of the phases, chosen on the basis of their mineral chemistry (Table 3).

Table 3. Average modal contents, used densities and average weight % contents for all phases in the three chromitite lenses, and Cr_2O_3 distribution (wt%) between phases for each chromitite lens.

Lens	VV-A	VV-B	VV-C
Modal content of chromite (%)	49.13	40.65	57.25
Modal content of ferritchromite (%)	10.01	4.16	5.80
Modal content of chlorite (%)	36.27	44.16	36.96
Modal content of serpentine (%)	4.29	11.04	0.00
Density of chromite (g/cm³)	4.35	4.35	4.35
Density of ferritchromite (g/cm³)	4.55	4.55	4.55
Density of chlorite (g/cm³)	2.75	2.75	2.75
Density of serpentine (g/cm³)	2.60	2.60	2.60
Weight % content of chromite (wt %)	57.55	50.85	66.01
Weight % content of ferritchromite (wt %)	12.23	5.56	7.00
Weight % content of chlorite (wt %)	26.93	35.26	26.99
Weight % content of chromite (wt %)	3.30	8.33	0.00
Cr_2O_3 distribution in chromite (wt%)	77.29	83.88	86.15
Cr_2O_3 distribution in ferritchromite (wt%)	19.43	10.67	10.88
Cr_2O_3 distribution in chlorite (wt%)	3.11	5.12	2.97
Cr_2O_3 distribution in serpentine (wt%)	0.17	0.33	0.00

Mass abundances of each phase are calculated according to equation (1):

$$Wj = \frac{Mj * \rho j}{\sum_{i=1}^{n} (Mi * \rho i)} \quad (1)$$

where j is the considered phase, ρ is density, n is the number of phases and W_j is the mass abundance of phase j.

Normative Cr_2O_3 whole rock content can be then calculated according to formula (2):

$$Cr_{WR} = \sum_{i=0}^{n} (Cr_i * W_i) \quad (2)$$

where Cr_i and W_i are the Cr_2O_3 content and the mass abundance of phase i and Cr_{WR} is the normative Cr_2O_3 whole rock content.

Average Cr_2O_3 content of all samples determined by X-Ray Fluorescence (XRF) was used to check calibration of image analyses as it should match average normative Cr_2O_3 content. Grey intensity ranges for each phase were hence adjusted to reach the best fitting between normative and XRF Cr_2O_3 average contents.

The wt% amount of total Cr_2O_3 present in each phase can then calculated with (3):

$$W_{Cr2O3j} = \frac{Cr_j * W_j}{Cr_{WR}} \quad (3)$$

The distribution of Cr_2O_3 in all phases was calculated for each lens using equation (3) (Table 3). Between 2 and 3 wt% of total Cr_2O_3 is remobilized within Cr-chlorite and less than 0.2 wt% within serpentine. Most of this Cr_2O_3 will be lost during physical separation as it will be preferentially separated into the tail together with the host phase (serpentine or Cr-chlorite). The amount of Cr_2O_3 lost in this way is proportional to the rate of silicate/chromite separation during processing. As a result the amount of Cr_2O_3 loss will increase with plant efficiency.

4.3.2 Cr_2O_3 distribution in the concentrate sand

As the Cr_2O_3 content of the concentrate chromite sand depends on the ore mineralogy and texture but also on the enrichment plant efficiency, a Separation Efficiency, as defined by Schulz (1970), was introduced:

$$SE = Rm - Rg \quad (4)$$

where Rm is the % recovery of the valuable mineral and Rg is the % recovery of the gangue into the concentrate.

Previous equation can be used practically in the following form (Wills, 1979):

$$SE = \frac{100Cm(c-f)}{(m-f)f} \quad (5)$$

where C is the fraction of the total feed weight that reports to the concentrate, m is the % Cr_2O_3 content of the valuable mineral, c is the Cr_2O_3 wt% of the concentrate and f is the Cr_2O_3 wt% of the feed. Anyway this formula is valid only assuming that all the valuable metal is contained in the same mineral (Wills, 1979).

If we consider a chromite ore where the valuable metal is present in both chromite and gangue with concentrations m_1 and m_2 respectively, with $m_1 > m_2$ then:

$$Rm = 100C\frac{CHRc}{CHRf} \quad (6)$$

where CHRc is the wt% of chromite in the concentrate and CHRf is the wt% of chromite in the feed. But:

$$f = m_1 * CHRf + m_2(1 - CHRf) \quad (7)$$

and:

$$CHRf = \frac{f - m_2}{m_1 - m_2} \quad (8)$$

in the same way:

$$CHRc = \frac{c - m_2}{m_1 - m_2} \quad (9)$$

and hence:

$$Rm = 100C\frac{c - m_2}{f - m_2} \quad (10)$$

Analogous calculations on Rg lead to the equation:

$$Rg = 100C\frac{m_1 - c}{m_1 - f}$$

Finally equation (5) can be rewritten for ores that contain the valuable metal also in the gangue, with an average concentration m2 between all the gangue phases, as:

$$SE = 100C\frac{(c-f)(m_1 - m_2)}{(f - m_2)(m_1 - f)} \quad (11)$$

4.3.3 Enrichment test

Effect of Cr redistribution on Vavdos chromite ore enrichment was tested by tabling 30 kg of ore from the three lenses sampled crushed and sieved to +0.1-2 mm grain size. For such chromite sand m1 is the average Cr_2O_3 concentration in chromite and ferritchromite weighed for their wt% in the feed and m_2 is the average concentration

in Cr-chlorite and serpentine weighed for their wt% in the feed. Parameters of the sand are reported in Table 4 and were applied to equation (11) to get equation (12):

$$SE = 100C\frac{(52.31c - 2013.94)}{619.52} \quad (12)$$

Now it is possible to compare (12) with the equation for the same ore if it did not undergo metasomatic reaction (case A), that is also with another ore with the same f and chromite content in the rock but with no Cr_2O_3 in the gangue. In this case we have the same value of f, no Cr_2O_3 in the gangue and m is given by the ratio between f and the wt% of chromite and ferritchromite in the rock. This case is analogous also to the case when, in altered chromite ore, f is measured by XRF and m is calculated starting from f and modal analysis of chromite. Using equation (5) and collected data we get equation (13):

$$SE = \frac{5890C(c - 38.50)}{785.40} \quad (13)$$

It is also possible to compare equation (12) with equation that is found if Cr_2O_3 is assumed to be only in chromite and ferritchromite and their Cr_2O_3 content is measured by EMPA (case B). In this case $m = m_1$ and, using equation (5), we get:

$$SE = \frac{5662C(c - 38.50)}{697.62} \quad (14)$$

In both cases the result gives a mistake in the evaluation of SE.

Table 4. Values of parameters of chromite sand used for the enrichment tests.

Parameters	f	m	m_1	m_2
Equations (12) and (17)	38.50	/	56.62	4.33
Equations (13) and (18)	38.50	58.90	/	/
Equations (14) and (19)	38.50	56.62	/	/

More interesting is to reverse the problem and to find the amount of C for an enrichment plant of a known efficiency SE for each value of c. For this purpose we can write from (5) the following equation:

$$C = \frac{SE * f(m - f)}{100m(c - f)} \quad (15)$$

and from (11)

$$C = \frac{SE(f - m_2)(m_1 - f)}{100(m_1 - m_2)(c - f)} \quad (16)$$

And again, using collected data, we get from (16):

$$C = \frac{619.52SE}{5231c - 201394} \quad (17)$$

and from (15) for case A:

$$C = \frac{785.40SE}{5890c - 226765} \quad (18)$$

and for case B:

$$C = \frac{697.62SE}{5662c - 217987} \quad (19)$$

Equations (17), (18) and (19) are drawn for different values of SE in a c vs C chart (Figure 5 and 6). When compared to equation (17) both equations (18) and (19) result, to a different extent, in an overestimation of C for a given c, or of c for a given C, and hence in an overestimation of the recovery for a given quality of the concentrate or of the quality of the concentrate for a given recovery.

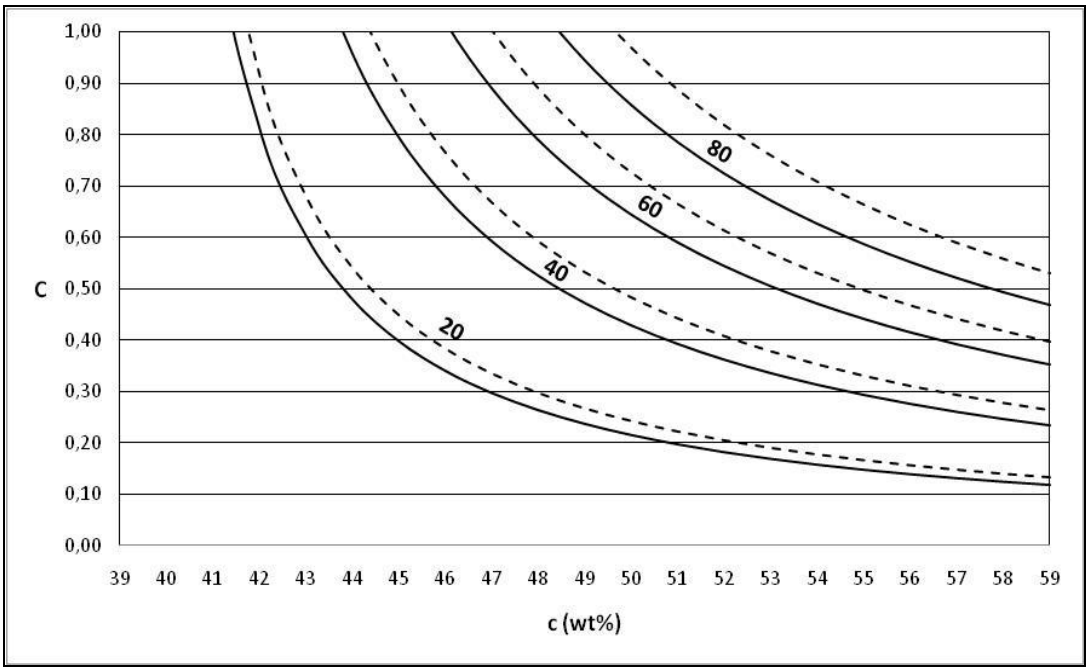

Figure 5. c (wt.%) vs. C for different values of SE (20, 40, 60 and 80) using Eq. (17) (continuous line) or Eq. (18) (dashed line).

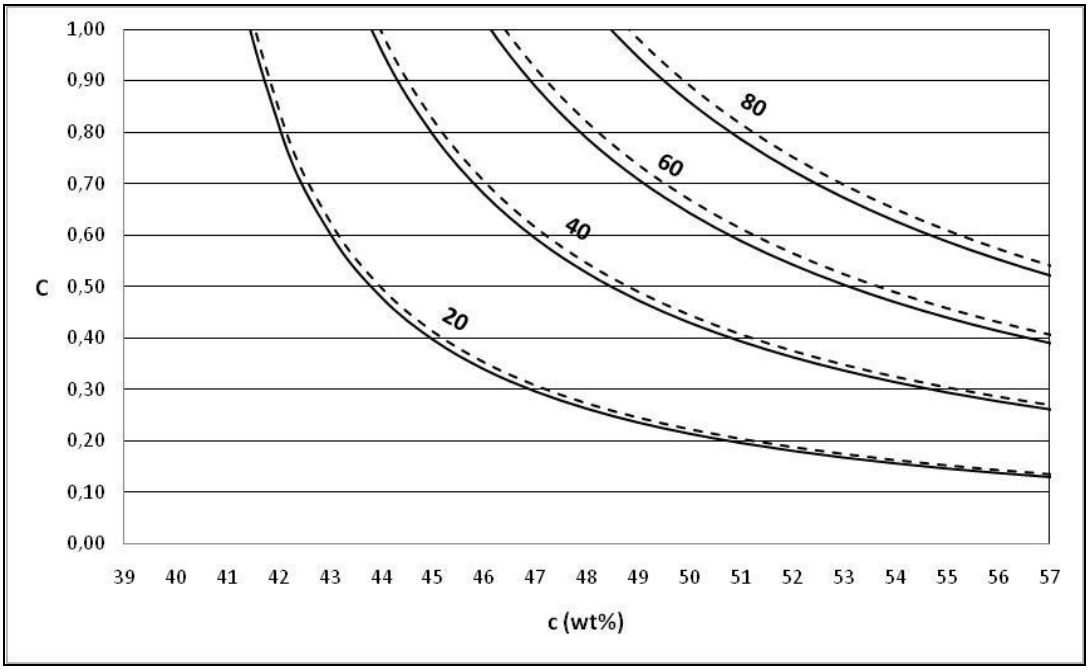

Figure 6. c (wt.%) vs. C for different values of SE (20, 40, 60 and 80) using Eq. (17) (continuous line) or Eq. (19) (dashed line).

Enrichment tests were used to check validity of the equation (17) compared to equations (18) and (19). Moreover equation (16) is based on the assumption that different gangue minerals (i.e. Cr-chlorite and serpentine) with different Cr_2O_3 content behave in the same way during separation. Though the similar specific weight and habitus of Cr-chlorite and serpentine argue for a similar behavior of the two minerals during processing the enrichment tests can also be used to check this assumption.

For each test SE was determined by modal analysis of feed and concentrate using equation (4), c was determined by XRF on the concentrate, and C_0 was calculated as the weight ratio between concentrate and feed. C_0 was then compared with C values from equations (17), (18) and (19).

Results in Table 5 show that equation (17) fits very well experimental results, with C values that never differ more than 0.006 from the measured C_0. Equations (18) and (19), on the other hand, give C values that differ from C up to 0.090 and 0.038 respectively. Comparison of c_0 and c finally provides a measure of the differential separation of the minerals. The low differences between the two values, with a maximum of 0.09 wt% for test 2 confirm that differential separation of Cr-bearing silicates does not occur or anyway does not affect enrichment to a significative extent.

Table 5. Parameters of the enrichment tests. c_0 is calculated from m_1, m_2 and chromite and silicate wt%, c is from XRF analysis of concentrate, C_0 is the measured concentrate to feed ratio and C(17), C(18), C(19) are calculated from equations (17), (18) and (19).

PARAMETERS	TEST 1	TEST 2	TEST 3
Feed modal chromite (%)	54.11	54.11	54.11
Feed modal silicate (%)	45.89	45.89	45.89
Feed wt% chromite	65.36	65.36	65.36
Feed wt% silicate	34.64	34.64	34.64
Concentrate modal chromite (%)	85.18	71.46	60.31
Concentrate modal silicate (%)	14.82	28.54	39.69
Concentrate wt% chromite	90.20	80.03	70.87
Concentrate wt% silicate	9.80	19.97	29.13
SE = Rm - Rg	32.9	29.2	14.6
c_0 (wt%)	51.50	46.18	41.38
c (wt%)	51.44	46.27	41.37
C_0	0.300	0.450	0.600
C (17)	0.301	0.444	0.603
C (18)	0.339	0.500	0.690
C (19)	0.313	0.462	0.638

4.4 Conclusions

Generally accepted assumption that chromite ores do host Cr only in chromite is misleading as metamorphosed chromite ores host significative amounts of Cr in gangue phases and especially in Cr-chlorite. This study, of a completely metasomatized chromite ore, shows that about 3 wt% of total Cr_2O_3 in the rock is hosted in Cr-chlorite, while only about 0.2 wt% of total Cr_2O_3 is hosted within serpentine.

As Cr-chlorite can host even higher Cr_2O_3 than at Vavdos, and as the deepest alteration of chromite due to metasomatism occurs for ores containing about 34 % chromite, the amount of Cr_2O_3 redistributed within the gangue can be even higher than at Vavdos, especially in low grade disseminated ores, where probably about 5-6% of Cr_2O_3 can be hosted in the gangue, a value that could rise to 7-8 wt% for high Cr_2O_3 Cr-chlorite.

The effect of this wrong assumption is a mistake in the calculation of plant efficiency, that will be overestimated, or, if plant efficiency is known, a mistake in the prediction of the C and c values for the plant, that will be again overestimated.

Mistakes due to redistribution of Cr_2O_3 during metamorphism can be easily avoided through mineralogical analysis that can detect the presence of Cr-chlorite in the ore. Cr-chlorite-bearing ores require further investigation, concerning Cr_2O_3 content in Cr-chlorite and Cr-chlorite amount in the ore.

Chapter 5

Study and improvement of a chromite enrichment plant

Textural and mineralogical characters of ore together with technical parameters of enrichment plants strongly affect efficiency of chromite sands concentration by shaking tables. Such parameters were studied at Brieville gravity enrichment plant that works chromite ore from different mines within Andriamena district (Madagascar).

5.1 Introduction

Chromite is an important mineral used in the metallurgy, chemistry and refractory industries. Chromite ores contain a variety of gangue minerals such as serpentine, pyroxene, amphibole and olivine. Therefore, some kind of ore beneficiation is required in order to separate chromite from gangue minerals (Nafziger, 1982). The most commonly used beneficiation methods for chromite ores are the gravity methods, such as the shaking table, jig, spiral and Reichert cone methods (Gence, 1999).

Planning of beneficiation plants for chromite sands based on gravity separation of chromite from gangue minerals is a complicated topic. As a matter of fact, the results in term of grade and recovery of the final product are strongly affected by a great amount of geological parameters, either mineralogical, chemical or textural. Cr_2O_3 content of the concentrate also depends on the enrichment plant efficiency that was defined as Separation Efficiency (SE) by Schulz (1970).

Mineralogy is used to predict behavior of gangue minerals during beneficiation, according to their specific weight and habitus. Chemical parameters of the ores are usually studied through X-Ray Fluorescence (XRF) whole rock analyses and are normally performed to determine major elements. Instead mineral chemistry studies of chromite are rarely carried out, due to high analysis cost, but it is fundamental to know the amounts of elements (especially Cr, Fe and Mg) within chromite because product can acquire different properties. On the other hand mineral chemistry of gangue phases is also necessary to identify for example Cr amount into silicates that can cause loss of Cr during enrichment processes (Grieco et al., 2011). The main textural parameter that affects gravity enrichment processes is the particle size distribution (PSD) of mineral grains within the rock (Chatterjee, 1998; Burt, 1999). Preliminary crushing and/or grinding of ore have the main function of liberating ore minerals from gangue minerals so that gravity enrichment can occur according to the density contrast between the phases.

Some aspects of these parameters and their influence on the quality of the final product were studied in chromite ores of Andriamena district (Madagascar) and Separation Efficiency (SE) of Brieville plant was calculated.

5.2 Geographical and geological setting of Madagascar

Andriamena district is located in north-central Madagascar, about 160 km from Antananarivo capital city and 75 km to the west of Alaotra Lake. The region is a plateau with an average altitude of 800 meters, where the Precambrian basement is covered only by up to 20 m thick lateritic soil that undergoes fast erosion due to recent deforestation.

Precambrian terranes take up two thirds of Madagascar (eastern) while remaining western third is characterized by Phanerozoic covers (Figure 1). Precambrian rocks of Madagascar can be divided into two sectors, an Archaean basement of middle to high metamorphic grade rocks (mainly gneiss, migmatite, granulite, schist and amphibolite) and Proterozoic metasediments (Windley et al. 1994).

The largest Precambrian terrane, to the north of the Bongolova-Ranotsara line, was divided into five main tectonic units (Collins, 2000; Collins et al., 2000; Collins and Windley, 2002), while, more recently, Collins (2006) recognizes four units and four metasedimentary regions, that separate these units and extend also to the southern terrain. Following Collins (2006) the units are (Figure 1): the Meso to Neoarchaean Antongil Block, outcropping in eastern Madagascar; the Tsaratanana sheet, that is Neoarchaean in age and forms three fingers in central Madagascar, the central of which hosts the chromitite occurrences of the Andriamena District; the Neoarchaean to Paleoproterozoic Antananarivo Block, that is the largest one and occupies most of central Madagascar; the Bemarivo Belt, to the far north, that is Neoproterozoic and is thrusted towards south. The four Metasedimentary regions are Neoproterozoic, two of them (Vohibory and Androyen) form the southern terrain, one (Molo) is to the west of Antananarivo block and covered by Phanerozoic sediments and the last one (Betsimisaraka) divides the Antongil and Antananarivo Blocks.

Tsaratanana sheet is a tectonic unit formed by three main belts (Maevatanana, Andriamena and Beforona) of similar lithology, geochronology and structural position. Features of the Andriamena belt, that hosts the biggest chromite ores of Madagascar in the Andriamena district, are here described in more detail. The unit mainly consists of interlayered mafic and tonalitic gneisses (biotite-hornblende and biotite gneisses), metapelitic migmatites (garnet-sillimanite bearing rocks) and quartzites associated with numerous large, deformed, mafic to ultramafic bodies (Goncalves et al., 2003). These mafic bodies include dunites, peridotites and pyroxenites, associated with chromite mineralization, and gabbros equilibrated under P–T conditions of about 4-5 kbar, 500–800 °C and with preserved igneous textures (Cocherie et al., 1991; Guérrot et al., 1993).

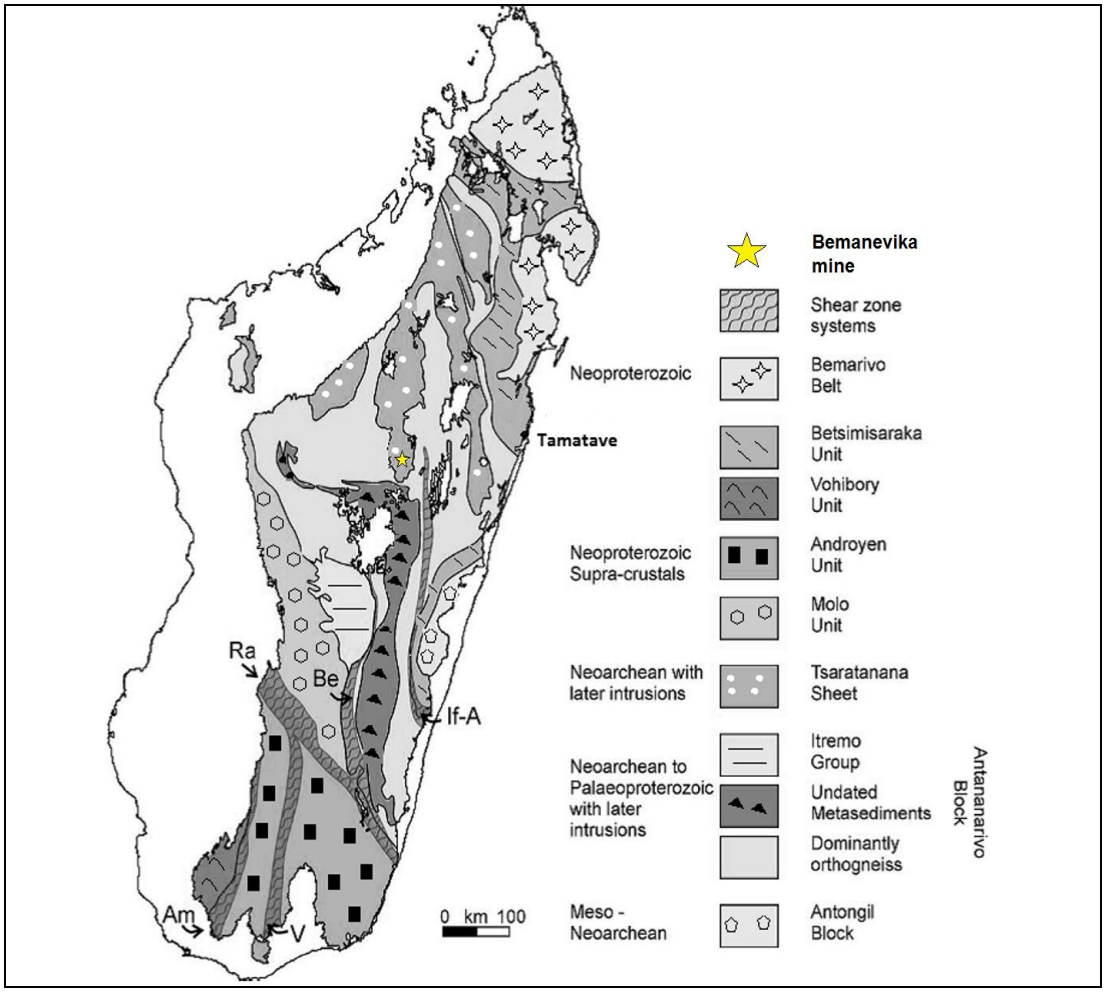

Figure 1. Geological sketch map of Madagascar with location of Bemanevika chromitite mine within the Tsaratanana Sheet. See text for explanation. Modified from Collins (2006).

5.2.1 Bemanevika chromite deposit

Andriamena is the most important chromite district in Madagascar, with two major bodies of several millions of tons each (Ankazotaolana and Bemanevika), several minor lenses and hundreds of chromite clues. Nowadays it hosts the only active chromite mines in Madagascar. Production began in 1968 at Bemanevika mine but was soon shifted to Ankazotaolana that remained the main mine till 2007, then, due to exhaustion of Ankazotaolana mine, production was shifted again to Bemanevika that, at the moment of sampling, provided all the feed to Brieville enrichment plant.

Bemanevika chromite deposit (Figure 2) was studied by French geologists since 1955 (Giraud, 1960) and was exploited from 1968 to 1974 with an extraction of 950.000 t of chromite ore. Several landslides forced the closure of deposit after this period, but it was reopened in 2006. Bemanevika chromite deposit is located in the southern zone of Andriamena District (Figure 3) , where host rocks change their direction moving from a NNE – SSW to a NE – SW orientation. At Bemanevika chromitites are hosted within a large ultrabasic complex, contained within noritic ortogneiss and crossed by pegmatites.

The ultrabasic complex shows coarse-grained, relatively fresh, pyroxenites on the top, characterized by a surface talc alteration. Chromite ore is hosted in the middle of the complex. It is a body of 600 x 200 m, made up of several parallel lenses, with thickness up to 30 m, concordant with, and separated by, host rocks, that are described as pyroxenites and harzburgites (Bésairie, 1966). A fine-grained peridotite, of harzburgite type, occurs, as visible outcrops, on the bottom of the ultrabasic complex.

Most recent studies concerning Bemanevika deposit have estimated reserves of about 2.68 Mt of chromite ore for a product with Cr_2O_3 content around 35.7 wt% and ratio Cr/Fe around 2.29 (SOGEREM, 1981).

Figure 2. Panoramic view of Bemanevika open pit chromite mine.

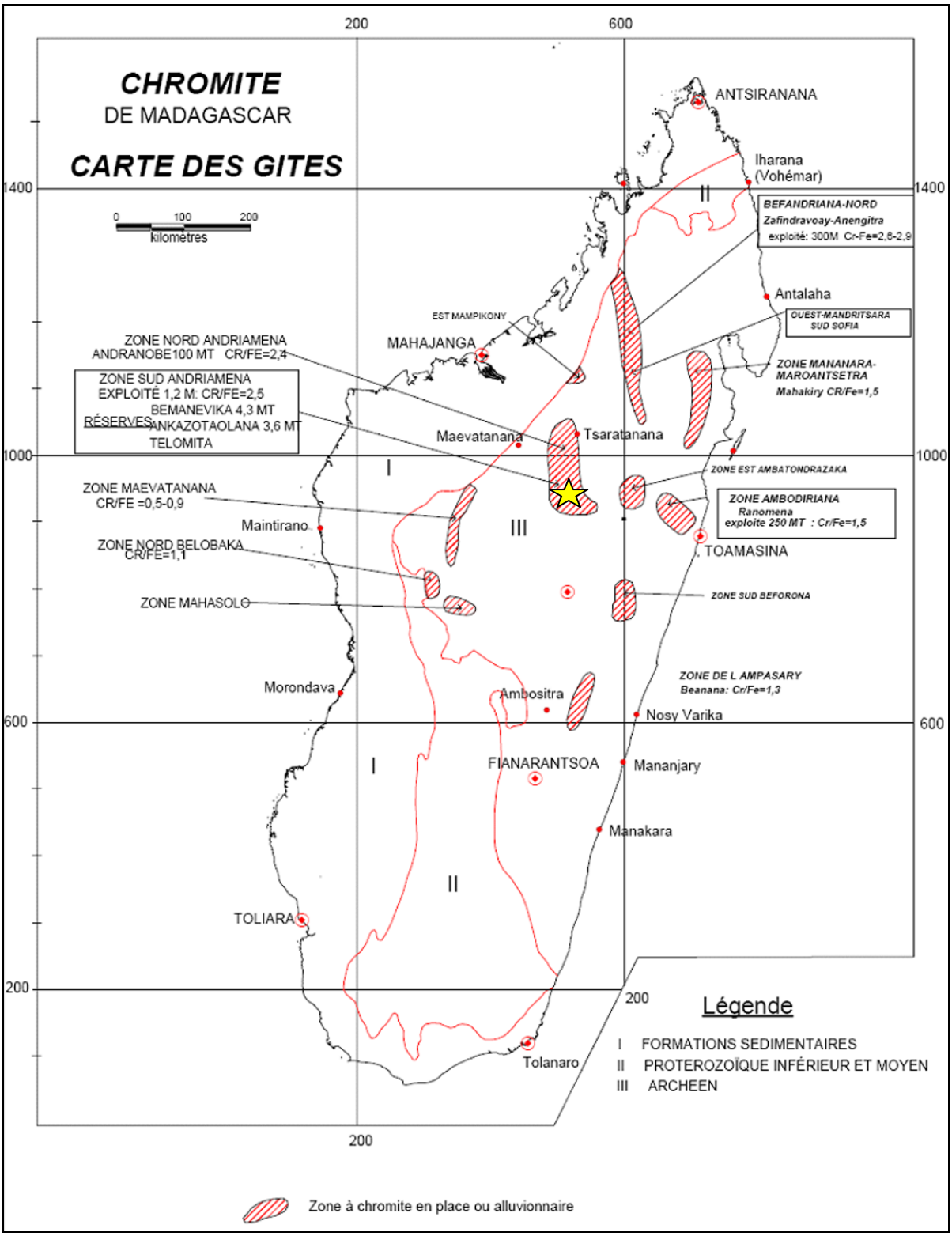

Figure 3. Map of main Madagascar chromite ore deposits (Service géologique de Madagascar). Yellow star indicates the location of Bemanevika chromite deposit.

5.3 Brieville enrichment plant

The Bemanevika mine is exploited by Kraomita Malagasy, a state owned mining company, that produces chromite lumpy (grain size +40 mm) and sand (grain size -1.5 mm) at the Brieville enrichment plant (Figure 4), located in an optimum logistic position, being only eight kilometers from working open pit.

Figure 4. Panoramic view of Brieville enrichment plant.

Enrichment plant is basically composed of three units a crusher working 85 ton/h of feed, a heavy medium separation (HMS) plant for chromite lumpy production working 40 - 50 ton/h of feed and a gravity separation plant, made up of shaking tables and spirals, for chromite sand production that works 50 ton/h of feed.

Materials having grain size below 40 mm after first crushing go to gravity separation plant, where chromite sand enrichment is achieved by crushing and tabling processes (flow sheet of plant in Figure 5).

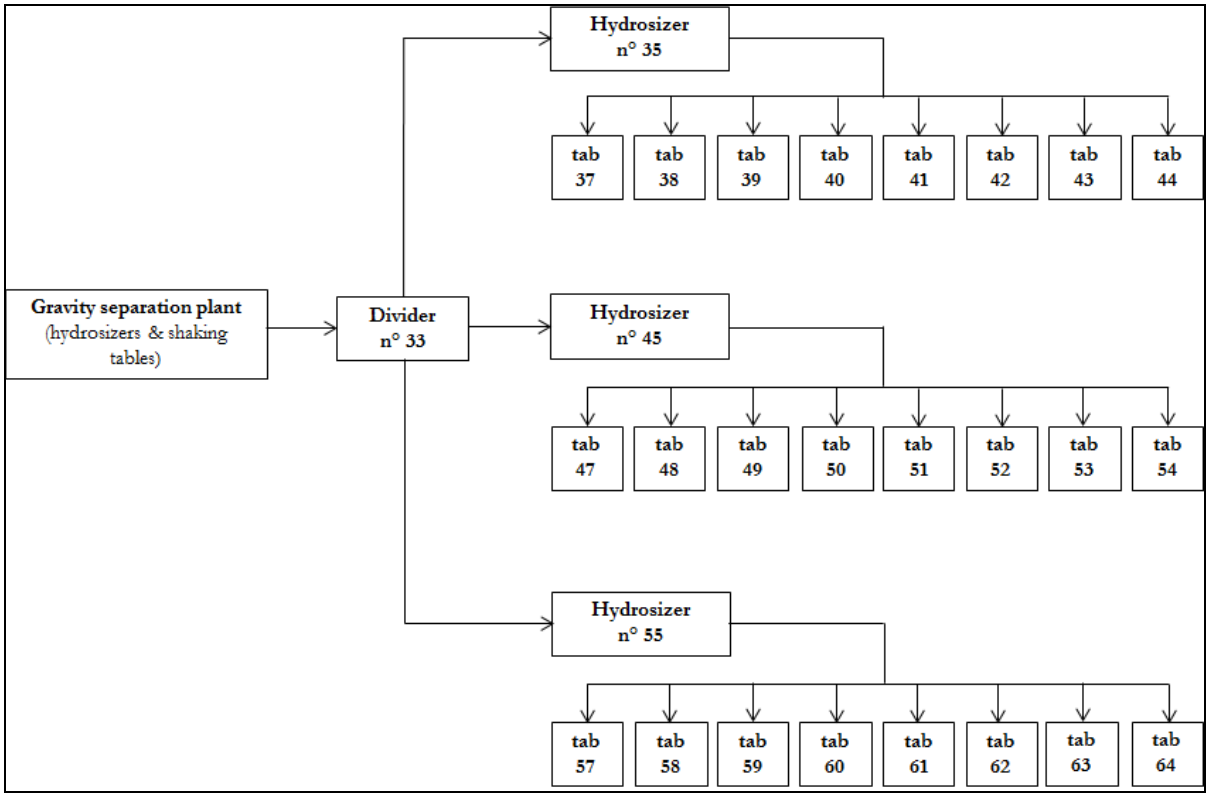

Figure 5. Flow sheet of Brieville enrichment plant.

The crushing plant comprises tumbling ball mills and vibrating screens (Figure 6 & 7) that further reduce feed to -1.5 mm. This material is then sent to the gravity separation plant through a divider, that fairly sends feed to three hydrosizers (Figure 8), consisting of tanks that classify feed depending on its density and grain size. In this way hydrosizers send feed to three different series of shaking tables (Figure 9), comprising eight tables each that work sand coming out from eight different pipes of the hydrosizers.


Figures 6 & 7. Tumbling ball mill (on the left) and vibrating screen (on the right) at Brieville enrichment plant.


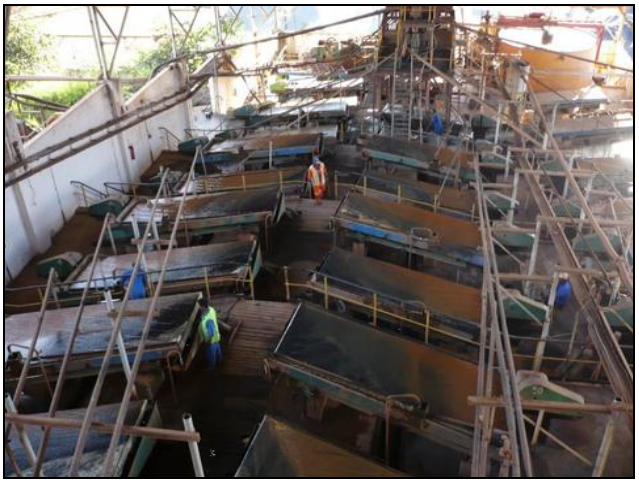

Figures 8 & 9. Hydrosizers (on the left) and series of shaking tables (on the right) at Brieville enrichment plant.

Each table produces three types of materials: concentrate, mix and waste (Figure 10). The concentrate is piped directly to final product stock and can be commercialized, the waste is disused while the mix is given back to gravity plant for re-enrichment processes that use spirals and another series of shaking tables.

Primary concentrate and a second concentrate from re-tabling of mix are stocked as the final product (Figure 11).

All analyses were performed on the series coming out from hydrosizer n° 55, comprising tables from 57 (receiving the coarsest sand) to 64 (receiving the finest sand).

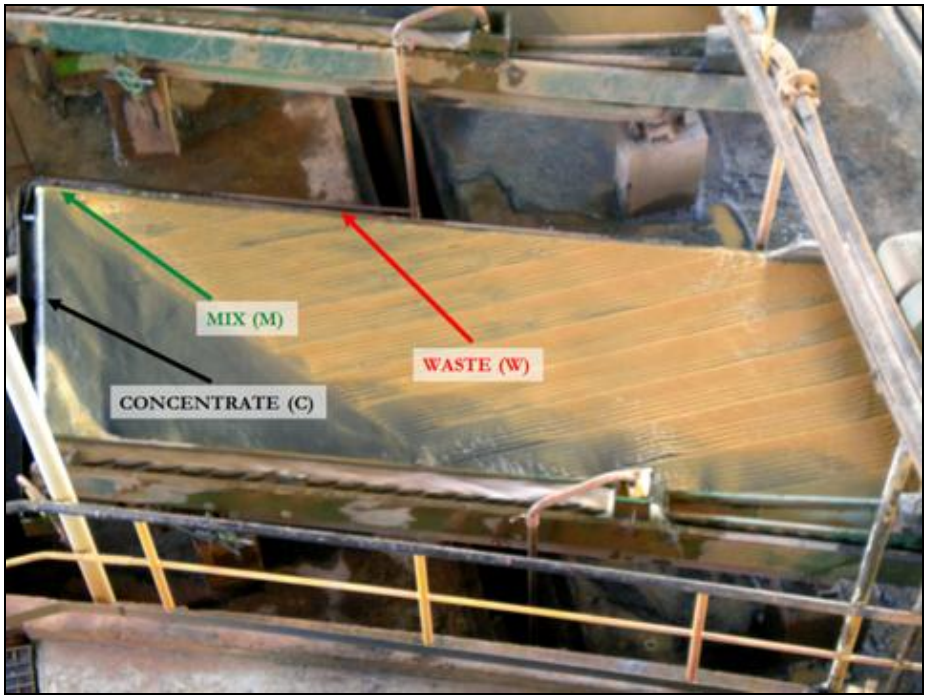

Figure 10. Working shaking table at Brieville enrichment plant. Table produces three types of material: concentrate (C), mix (M) and waste (W).

Figure 11. Stock of final product at Brieville enrichment plant.

5.3.1 Features and working of shaking tables

Shaking table concentrator is perhaps the most metallurgical efficient form of gravity concentrator, being used to treat the smaller, more difficult, flow-streams, and to produce finished concentrates from the products of other forms of gravity systems (Wills and Napier-Munn, 2006).

It consists of a slightly inclined deck, onto which feed, at about 25% solids by weight, is introduced at the feed box and is distributed along a duct; wash water is distributed along the balance of the feed side from launder. The table is vibrated longitudinally, by a mechanism, using a slow forward stroke and a rapid return, which causes the mineral particles to "crawl" along the deck parallel to the direction of motion.

The minerals are thus subjected to two forces that due to the table motion, at fight angles to it, and that due to the flowing film of water. The net effect is that the particles move diagonally across the deck from the feed end and, since the effect of the flowing film depends on the size and density of the particles, they will fan out on the

table, the smaller, denser particles tiding highest towards the concentrate launder at the far end, while the larger lighter particles are washed into the tailings launder, which runs along the length of the table.

The separation of concentrate from gangue minerals on a shaking table is controlled by a number of operating variables such as wash water, feed pulp density, deck slope, amplitude, and feed rate.

Many other factors, including particle shape and the type of deck, play an important part in table separations. Flat particles with lamellar habit, for example mica, although light, do not roll easily across the deck in the water film; such particles cling to the deck and are carried down to the concentrate discharge. Likewise, spherical dense particles may move easily in the film towards the tailings launder.

Particle size plays a very important role in table separation; as the range of sizes in a table feed increases, the efficiency of separation decreases because the middlings produced are not "true middlings", i.e. particles of associated mineral and gangue, but relatively coarse dense particles and fine light particles.

Since the shaking table effectively separates coarse light from fine dense particles, it is common practice to classify the feed, since classifiers put such particles into the same product, on the basis of their equal settling rates. In order to feed as narrow a size range as possible on to the table, classification is usually performed in hydrosizers or sieves.

Since the introduction of the Wilfley Table in 1896, a wide variety of shaking tables has been marketed. The major differences between tables are the shape and suspension of deck, and the type of mechanism which imparts the asymmetric reciprocating motion to the deck.

Typically there are two basic shapes of table deck: rectangular, with riffles parallel to longer side, and diagonal, with riffles oblique to longer side. At Brieville plant tables have diagonal shape (about 2.5 m x 1 m in size) and riffles are oblique to longer side (Figure 10).

There are two basic types of mechanism, or head motion. In the more common variant the mechanism casing is rigidly fixed to a sub-frame and asymmetric motion is imparted to the deck by a toggle and pitman mechanical linkage. In the other type, and also at Brieville plant, the mechanism is rigidly fixed to the deck and the whole shaken, as one, by eccentric weights in the mechanism.

Brieville tables are fed with a 30% solid by weight water mixture and the rate flow of material varies from 0.10 kg/s to 0.15 kg/s.

5.4 Materials and methods

Enrichment efficiency of Brieville plant and final product quality were studied on chromitite ores from Bemanevika deposit, Andriamena district, Madagascar.

At Brieville marketed final product is composed of about 85 wt% primary concentrate, achieved by tabling process and about 15 wt% of second concentrate achieved by re-working mix with spirals and tables. Therefore sampling of plant was especially focused on one of three shaking table series, because each series works the same feed coming from divider (called n°33 in Figure 5).

All types of materials obtained from tabling process, concentrate, mix and waste, were collected from each of the eight tables (the series comprising tables from n° 57 to n°64) together with overall feed, which tables receive from hydrosizer n°55 (Figure 5).

The rate flow material of each table was also measured directly from pipes.

Grain size analyses were performed on representative amounts of selected samples using ASTM E 437 series sieves in laboratory.

Qualitative X-ray powder diffractometer analyses were performed at Dipartimento di Scienze della Terra, University of Milan, on the overall feed (33 F) in order to determine its mineralogy and on four different grain sizes of overall feed, in order to detect eventual selective behavior of minerals during crushing. Final product (FP) and its four different grain sizes XRD patterns were also acquired.

Whole rock major elements content of each table product (feed, concentrate, mix and waste) together with the final product was analyzed with X-ray Fluorescence at Dipartimento di Scienze della Terra, University of Milan.

The degree of liberation of chromite from silicate gangue was evaluated on selected samples by grain counting under transmitted light microscope, where middlings were defined as grains containing 10 to 90% chromite. Each datum refers to 500 grains counted on a thin polished section and relative number of grains is transformed into wt% by using average density of phases.

5.5 Results

5.5.1 Grain size analysis

The wet samples from Madagascar were dried at 105 °C in an oven for about one hour in order to perform grain size analyses. Samples chosen to perform grain size analysis were overall feed (33 F), final product (FP) and each material (feed F, concentrate C, mix M and waste W) of tables 57, 61 and 64, i.e. shaking tables working respectively the coarsest, medium and the finest product coming from hydrosizer n°55 (Figure 5).

Subsequently a statistically representative quantity of each sample has been used, i.e. 200 grams weighed by electronic scale. Consecutively these samples were sieved by a vertical stack of sieves with openings decreasing, according to ASTM: the series is made up of 9 sieves with meshes ranging from 1 mm to 0.053 mm, hence the sands were separated in 10 grain sizes.

Separation of grains in a shaking table occurs due to contrasts in specific weight, grain size and, to a minor extent, grain shape. Specific weight contrast between grains for a given grain size distribution of sand depends on density and degree of liberation of phases (Wills and Napier-Munn, 2006).

The greatest use for hydraulic classifiers, as hydrosizer, in the mineral industry is for sorting the feed to certain gravity concentration processes so that the size effect can be suppressed and the density effect enhanced (Wills and Napier-Munn, 2006).

The above-mentioned role of hydrosizer is respected at Brieville plant. As a matter of fact the comparisons of feeds, concentrates, mixes and wastes of each table highlight a grain size decreasing from table 57 to table 64 (Figure 12, 13, 14 & 15). Moreover both the overall feed (33 F) and the final product (FP) have a grain size that is about the average respectively of feeds and concentrates (Figures 12 & 13).

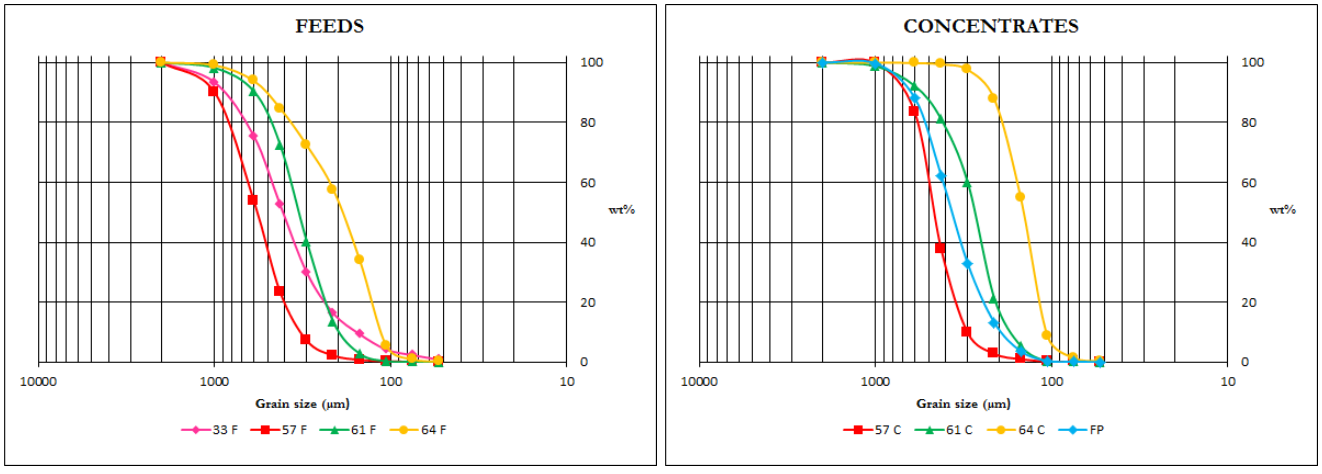

Figures 12 & 13. Grain size patterns comparisons between feeds and concentrates of each table.
33 F = overall feed, FP = final product.

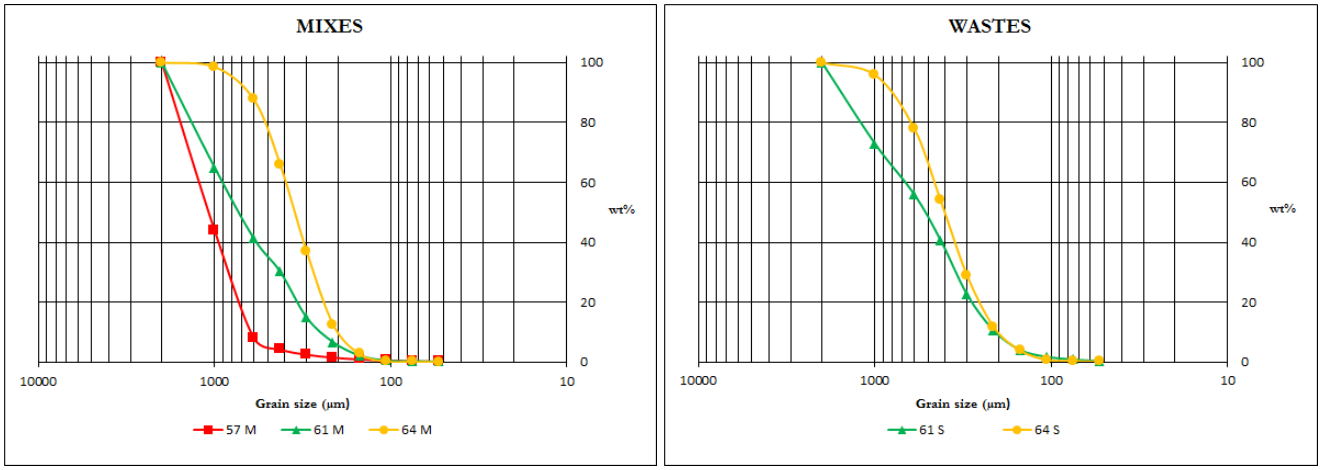

Figures 14 & 15. Grain size patterns comparisons between mixes and wastes of each table.

Instead the different grain size distribution of feed, concentrate, mix and waste shows that gravity separation is strongly affected by low sorting of feed, resulting in grain size separation together with density separation.

In fact mix and waste product of each table have generally a grain size coarser than feed, which is in turn coarser than concentrate (Figures 16, 17 & 18).

The meaning of these results is that the greater is the grain size difference between feed, concentrate, mix and waste, the lower is the separation efficiency of the table as it works not only according to specific weight contrast but also according to size contrast of grains.

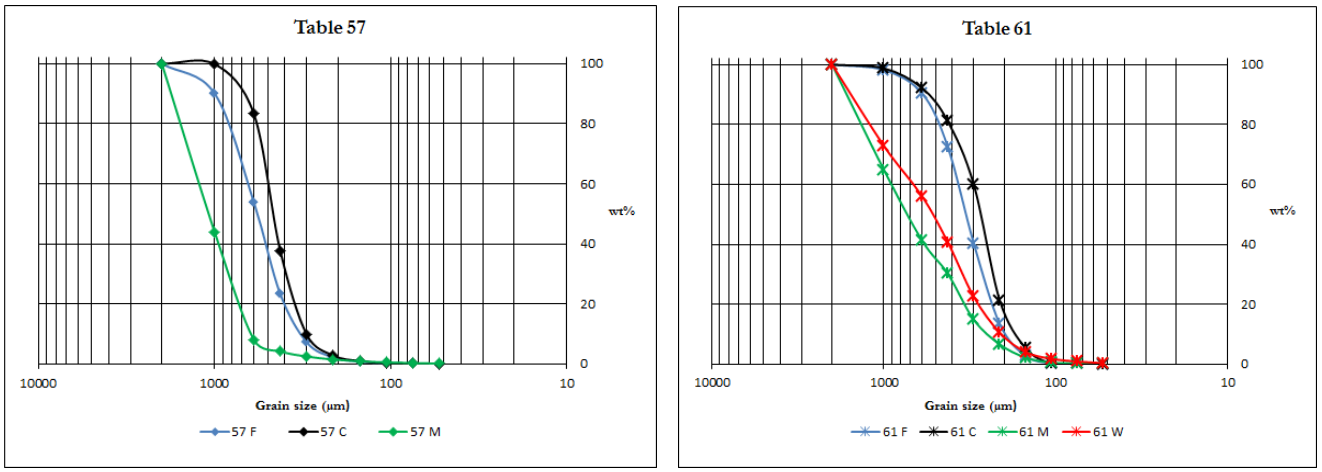

Figures 16 & 17. Grain size patterns of each product of table 57 and 61.
F = feed, C = concentrate, M = mix and W = waste.

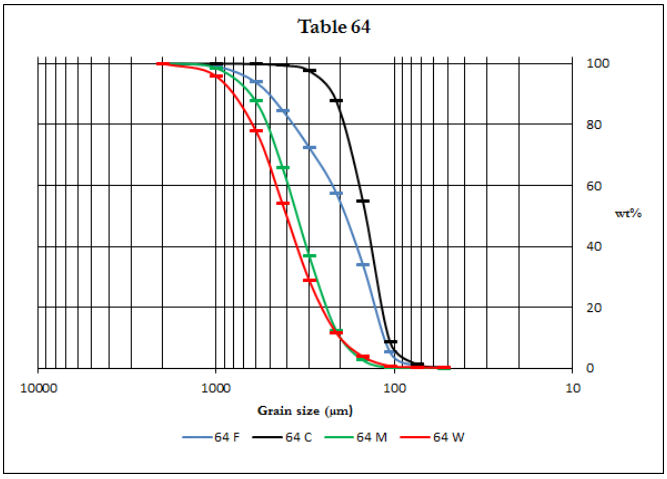

Figure 18. Grain size patterns of each product of table 64. F = feed, C = concentrate, M = mix and W = waste.

Sorting of a sand, i.e. the spread of the sizes around the average (Blott and Pye, 2001), is a very important sand feature because it shows the uniformity degree of grain sizes present in a sample (Wills and Napier-Munn, 2006). Then it is possible to classify sands as well sorted when there is a uniformity of grain sizes and as poor sorted when there is not uniformity.

Sorting of samples was calculated using GRADISTAT software and in this work sand sorting (σ_G) was evaluated with geometric method of Falk and Ward (1957) by with the following statistical formula:

$$\sigma_G = \exp\left(\frac{\ln P_{16} - \ln P_{84}}{4} + \frac{\ln P_5 - \ln P_{95}}{6.6}\right)$$

where P_x is grain diameter in metric units, at the cumulative percentile value of x.

Sorting classification by Falk and Ward (1957) is shown in Table 1.

Table 1. Sorting classification by Falk and Ward (1957).

Sorting (σ_G)	
Very well sorted	< 1.27
Well sorted	1.27 – 1.41
Moderately well sorted	1.41 – 1.62
Moderately sorted	1.62 – 2.00
Poorly sorted	2.00 – 4.00
Very poorly sorted	4.00 – 16.00
Extremely poorly sorted	> 16.00

Results show that the overall feed (33 F) is moderately sorted while feeds of each table (57 F, 61 F and 64 F) are moderately well sorted (Table 2). Therefore hydrosizer apparently improves sorting from overall feed to each table feed, but a proper working of the device should produce a much better sorting, i.e. feed of each table should be very well or well sorted.

In order to verify if hydrosizer n°55 well splits the overall feed, sorting of each shaking table feed was calculated. On the overall feed it was also made a sorting test that consisted in sieved the sample into three different grain size using two sieves with meshes 1 mm and 0.5 mm.

Better sorting results can be reached using sieves in place of hydrosizer, as a matter of fact feeds obtained by sieving are well sorted for coarser grain size (+0.5 mm) and moderately sorted for finer grain size (-0.5 mm) (Table 2). Even using only three grain size classes rather than ten classes, like in Brieville plant, the overall sorting is better using sieves.

Finally sieved materials are better sorted than materials processed by hydrosizer (Figure 19) and hence hydrosizer should be replaced by a series of sieves in order to improve shaking tables working at Brieville plant.

Table 2. Geometric sorting of analyzed feeds. 33 F = overall feed

Table	Geometric Sorting (μm)	Description
33 F	1.952	Moderately Sorted
33F +1 mm	1.285	Well sorted
33F -1 +0.5 mm	1.314	Well sorted
33F -0.5 mm	1.670	Moderately sorted
57 F	1.589	Moderately Well Sorted
61 F	1.592	Moderately Well Sorted
64 F	1.601	Moderately Well Sorted

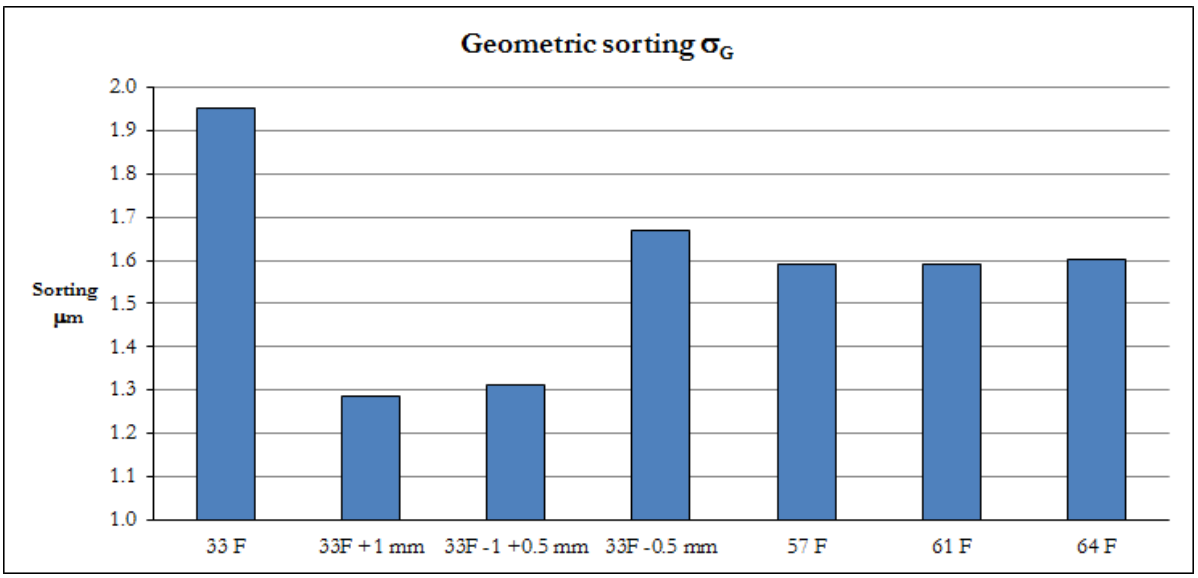

Figure 19. Sorting comparison between overall feed (33 F), sieved feeds (33F +1mm, 33F -1 +0.5 mm, 33F -0.5mm) and feeds of each table (57 F, 61 F and 64 F).

5.5.2 X-ray powder diffractometer analysis

Qualitative X-ray powder diffractometer analyses were performed, in order to understand the mineralogical phases distribution into different grain sizes. Mineralogical studies were carried out on four different grain sizes of overall feed and final product to detect eventual selective behavior of minerals during crushing and enrichment.

Gangue mineralogy of both feed and final product is rich, comprising ortho- and clinopyroxene, tremolitic to edenitic amphibole, serpentine, chlorite and talc.

X-ray powder diffractometer (XRD) patterns show that chromite grains in the overall feed concentrate within -600 +300 μm grain size where, as a matter of fact, there is the highest peak intensity of chromite and the lowest of all silicates. Moreover pyroxenes concentrate within the coarsest grain size while amphiboles, chlorites and serpentines within the finest and talc concentrates within the mean grain size (Figures 20, 21, 22 and 23).

Mineralogical phase distribution concerning the final product is analogous to the overall feed.

X-ray powder diffractometer analyses testify that generally chromite and pyroxenes grains concentrate within coarser grain sizes while the grains of amphibole, chlorite and talc, tend to accumulate within finer grain sizes. This distribution can reflects either the original larger grain size of chromite and pyroxene crystals or the higher hardness of these phases during crushing and grinding.

Comparison between feed and final product at different grain sizes shows that also during enrichment by gravity separation, as occurs at Brieville plant, the mineral behavior depends on density. Moreover comparisons between feed and final product prove that grain shape also affect mineralogical phases distribution within different grain size, in fact minerals with tabular and/or lamellar shape, i.e. chlorite, talc and amphibole, accumulate especially within the lowest grain sizes.

It is important to verify the presence of mineralogical phases with lamellar dress, as chlorite, because this should cause shaking table disease, since dress geometry does not allow the movement of the crystals along the axis. Consequently grains tend to stay attached to the table until to get into concentrate tank.

Collected XRD data show that lamellar phases are much more abundant in the finest grain sizes, but they are well separated as they are much less abundant in the concentrate than in the feed. On the other hand the most hard to separate gangue phase is pyroxene that is by far the most abundant gangue phase in the concentrate. This can be due to a little extent to the concentration of pyroxene into the coarse grain size that favors its presence in the middlings. But mostly pyroxene is hard to separate due to its relatively high specific weight.

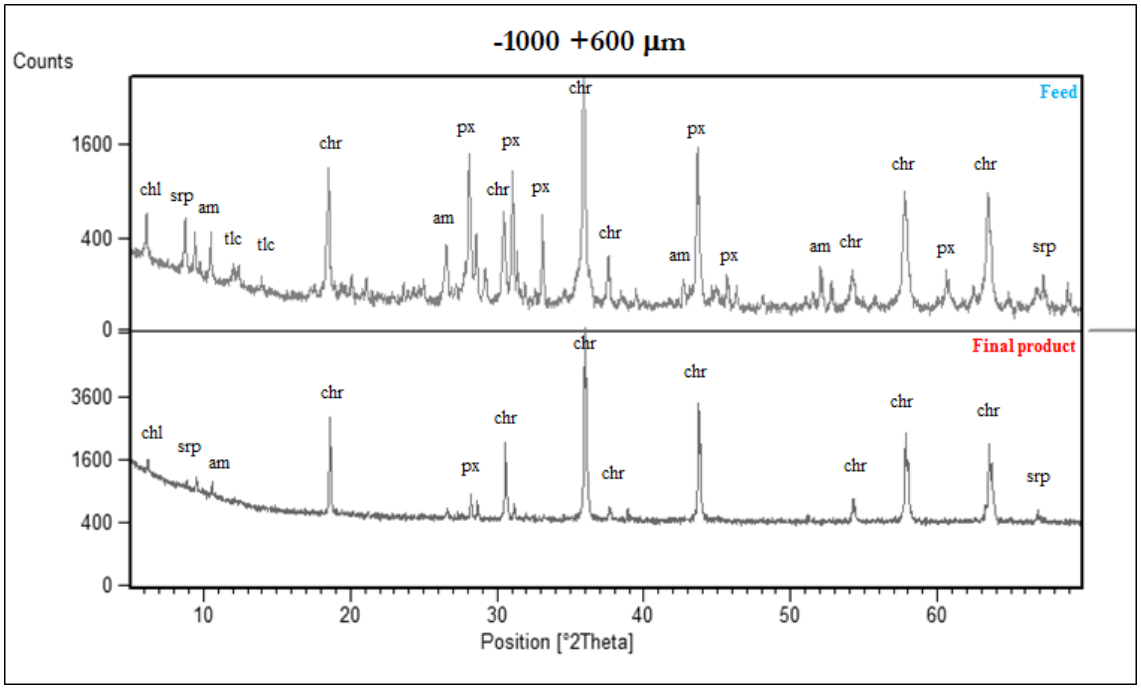

Figure 20. X-ray diffraction patterns of overall feed and final product to -1000 +600 µm grain size.

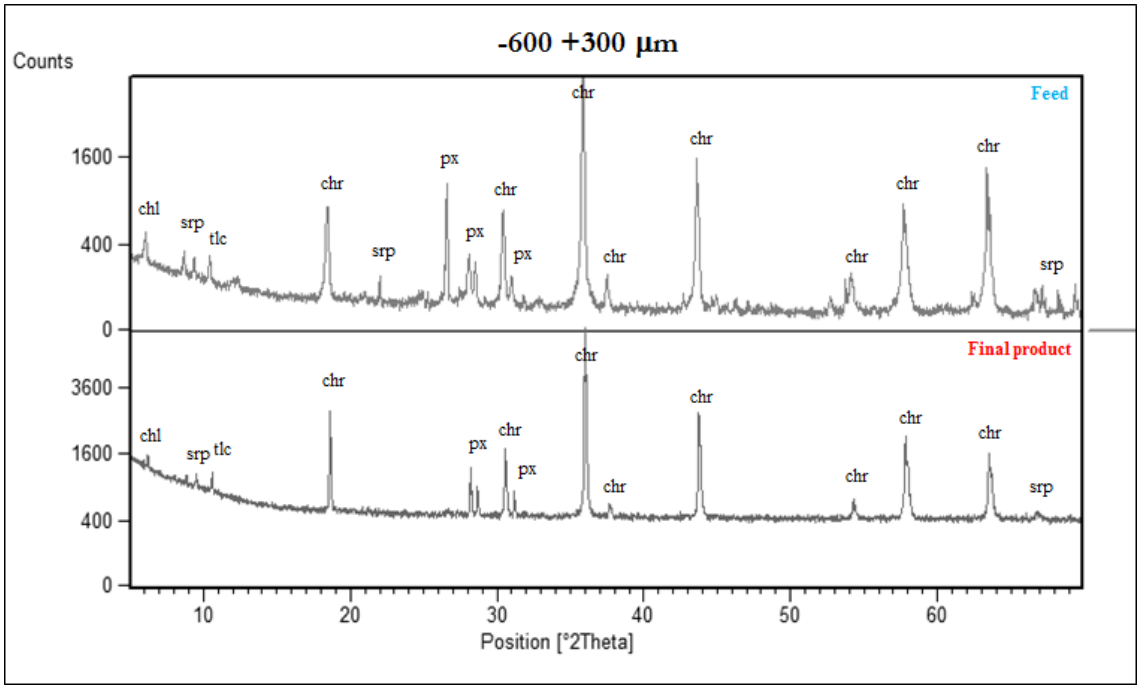

Figure 21. X-ray diffraction patterns of overall feed and final product to -600 +300 µm grain size.

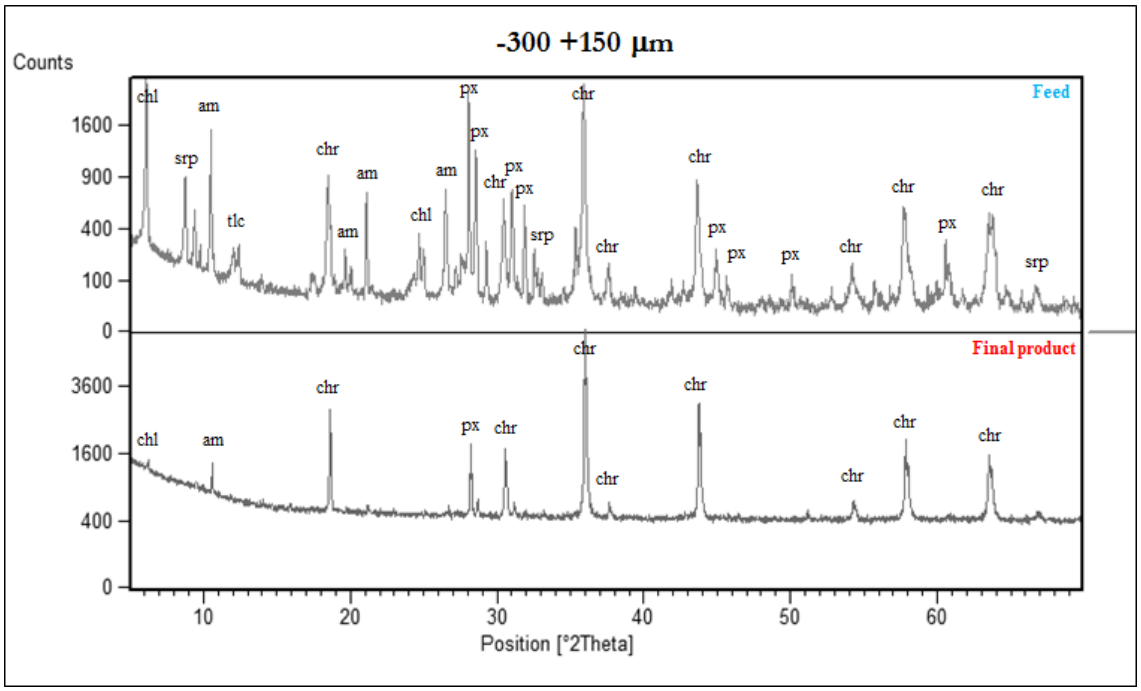

Figure 22. X-ray diffraction patterns of overall feed and final product to -300 +150 µm grain size.

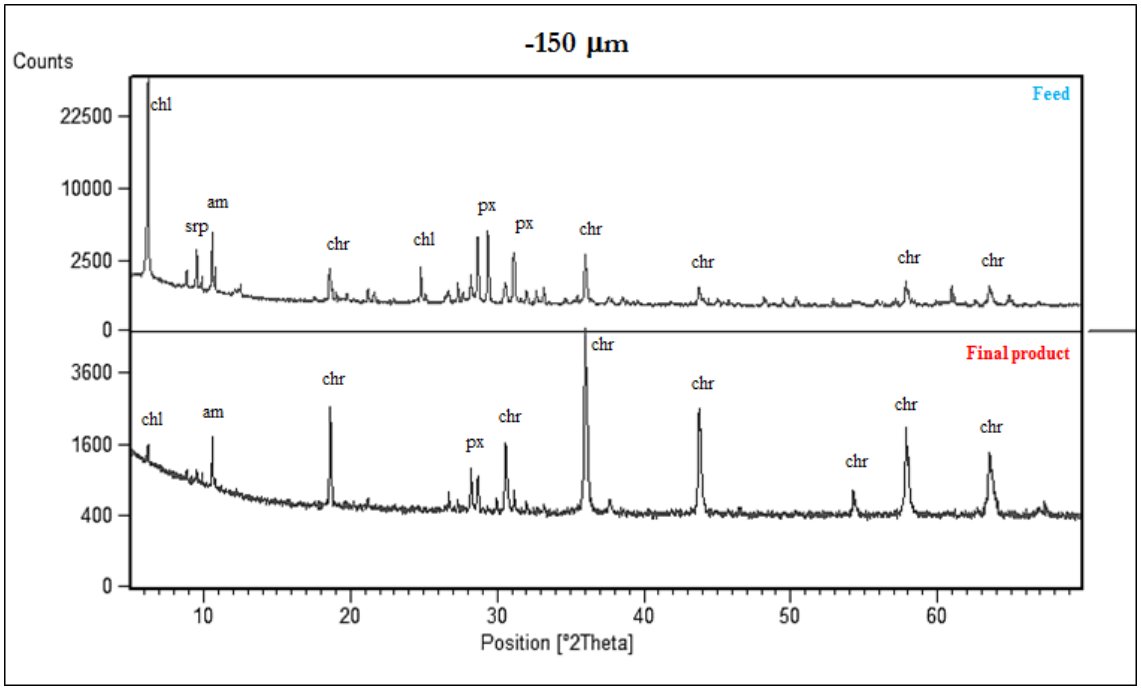

Figure 23. X-ray diffraction patterns of overall feed and final product to -150 µm grain size

5.5.3 X-ray fluorescence analysis

X-ray Fluorescence (XRF) whole-rock analyses were carried out on overall feed, each product of shaking tables and final product at Dipartimento di Scienze della Terra, University of Milan, Italy. Results on analyzed elements (Fe_2O_3, MnO, Cr_2O_3, TiO_2, CaO, K_2O, SiO_2, Al_2O_3, MgO, Na_2O), as oxides, are shown in Table 3.

Cr_2O_3 contents of overall feed and final product are respectively 39.51 and 48.44 wt% with an enrichment of 8.93 wt% Cr2O3 at Brieville plant. This is enough to provide a concentrate useful for the steel market.

Comparison of Cr_2O_3 and SiO_2 wt% contents of each shaking table is shown in Figure 7, and highlights inverse linear trend between the two parameters, because Cr_2O_3 content is directly proportional to chromite content that is inversely proportional to silicate content.

Concentrates of each table, final product and feeds of first tables in the series, i.e. tables 57, 58, 59 and 60, are the materials of Brieville plant that satisfy parameters for chromite special steels use, that are $Cr_2O_3 > 46$ wt% and $SiO_2 < 6$ wt% (red and blue continuous lines in Figure 24).

Table 3. XRF analyses of samples from Brieville enrichment plant.

	Sample	Fe_2O_3	MnO	Cr_2O_3	TiO_2	CaO	K_2O	SiO_2	Al_2O_3	MgO	Na_2O	Total
Overall feed	**33 F**	17.77	0.18	39.51	0.22	1.70	0.07	10.70	10.87	13.10	0.02	94.12
Table 57	**57 F**	20.79	0.20	45.90	0.15	0.79	0.02	5.78	11.10	11.72	0.01	96.45
	57 C	21.94	0.20	51.04	0.15	0.36	0.01	3.37	12.14	10.90	0.01	100.12
	57 M	15.39	0.17	30.80	0.15	2.34	0.04	17.94	8.87	16.67	0.02	92.39
Table 58	**58 F**	21.57	0.20	47.02	0.15	0.86	0.02	5.49	12.07	11.74	0.02	99.14
	58 C	21.67	0.20	50.72	0.14	0.41	0.01	3.55	11.65	10.91	0.01	99.28
	58 M	21.50	0.19	44.47	0.16	1.18	0.03	6.83	12.36	12.31	0.02	99.05
	58 W	16.82	0.13	31.08	0.15	3.20	0.01	20.52	7.64	16.11	0.02	95.68
Table 59	**59 F**	21.63	0.19	47.31	0.15	0.73	0.02	4.28	12.17	11.73	0.02	98.22
	59 C	21.80	0.20	50.89	0.14	0.44	0.01	3.58	11.64	10.90	0.01	99.62
	59 M	18.91	0.19	41.45	0.15	1.48	0.02	9.25	10.59	13.15	0.02	95.21
	59 W	13.63	0.15	24.91	0.15	2.77	0.06	23.48	8.21	18.81	0.02	92.19
Table 60	**60 F**	21.49	0.20	46.86	0.16	0.91	0.02	5.77	12.06	11.90	0.02	99.39
	60 C	21.30	0.20	50.30	0.15	0.47	0.01	3.66	11.59	11.06	0.01	98.75
	60 M	21.84	0.20	40.71	0.18	1.70	0.04	9.55	12.90	13.39	0.03	100.53
	60 W	11.67	0.19	16.13	0.17	2.89	0.03	34.14	8.77	19.89	0.02	93.90
Table 61	**61 F**	19.66	0.18	42.65	0.16	1.40	0.03	8.69	11.24	13.00	0.02	97.04
	61 C	22.82	0.20	52.44	0.16	0.21	0.01	2.42	12.95	10.61	0.01	101.83
	61 M	13.72	0.15	27.01	0.15	2.97	0.00	21.94	8.30	18.13	0.02	92.40
	61 W	6.38	0.09	3.99	0.27	4.70	0.00	40.44	9.77	22.52	0.06	88.22
Table 62	**62 F**	17.88	0.18	38.15	0.17	1.84	0.05	12.01	10.42	14.14	0.03	94.86
	62 C	22.20	0.21	51.13	0.16	0.52	0.01	3.44	11.95	11.02	0.01	100.65
	62 M	13.06	0.15	26.61	0.17	3.93	0.00	22.81	8.88	17.89	0.03	93.53
Table 63	**63 F**	14.78	0.16	29.59	0.22	2.97	0.08	19.36	9.92	16.78	0.03	93.89
	63 C	22.42	0.20	52.26	0.20	0.34	0.01	2.99	12.59	10.71	0.02	101.74
	63 M	8.25	0.12	8.27	0.23	5.56	0.15	37.48	8.29	23.75	0.05	92.15
Table 64	**64 F**	13.54	0.15	26.95	0.22	2.78	0.10	21.25	9.53	17.57	0.03	92.12
	64 C	20.46	0.19	47.21	0.28	1.11	0.01	5.35	12.02	11.65	0.02	98.30
	64 M	7.80	0.13	6.64	0.22	5.14	0.17	42.70	7.25	24.24	0.04	94.31
	64 W	6.93	0.12	4.14	0.38	4.29	0.26	40.84	9.25	22.78	0.04	89.02
Final product	**FP**	20.36	0.20	48.44	0.17	0.68	0.02	4.63	11.23	11.38	0.01	97.11

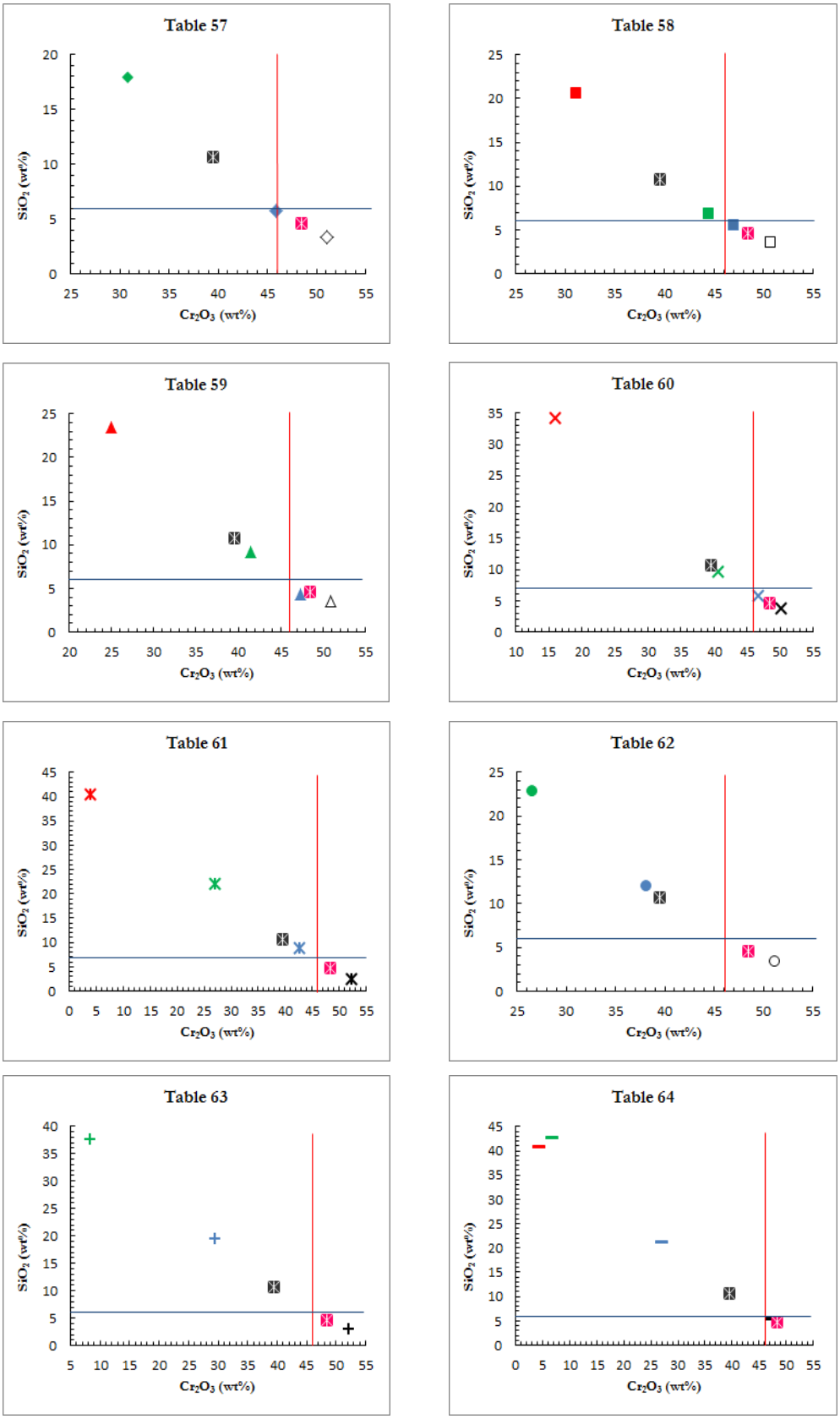

Figure 24. Whole rock Cr_2O_3 vs SiO_2 wt% content of each table. Blue symbol = feed, empty/black symbol = concentrate, green symbol = mix, red symbol = waste, black filled square = overall feed & pink filled square = final product. Red and blue continuous lines indicate respectively Cr_2O_3 and SiO_2 content limits fixed at 46 wt% and 6 wt%, for chromite use in the special steel market.

Concentrates from all the tables are similar with Cr_2O_3 between 50 and 52 wt% with the only exception of table 64 with a concentrate below 50 wt%. In more the detail the best concentrates are those from tables 61 and 63 that slightly exceed 52 wt% Cr_2O_3. Anyway this observation can lead to misleading interpretation of tables efficiency. As hydrosizer preselect feed sand not only by grain size but also by specific weight the result of using hydrosizers instead of sieves is that the feeds sent to the tables strongly differ in Cr_2O_3 content. In fact the first five tables (57, 58, 59, 60 and 61) receive a feed better than the overall feed (33 F) while the last three tables (62, 63 and 64) receive a feed worse than the overall feed (Figure 25). The Cr_2O_3 content of feeds ranges from 26.95 Cr_2O_3 wt% of table 64 to 47.31 Cr_2O_3 wt% of table 59 with a difference as high as 20.36 wt%.

As a whole the feeds of the tables show a general trend of decreasing Cr_2O_3 content moving from table 57 to table 64 because within the hydrosizer chromite more dense grains tend to settle down, together with bigger grains, earlier, and hence to be collected by pipes that bring feed to the first tables (Figure 25).

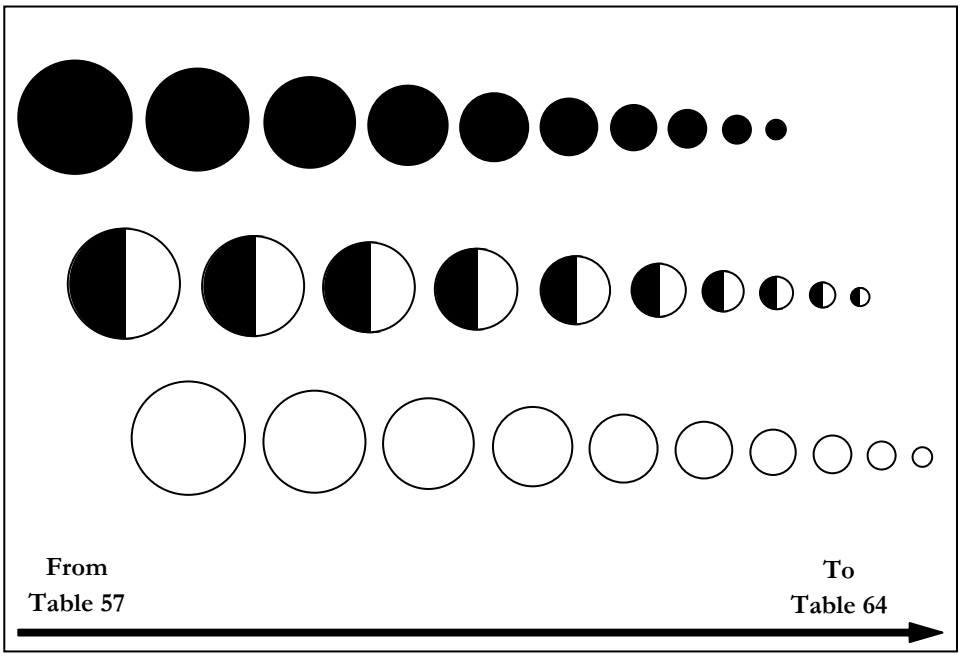

Figure 25. Sketch of classification and pre-enrichment within the hydrosizer.

The result of this process is that the Cr_2O_3 enrichment from feed to concentrate (ΔCr_2O_3) of each table strongly differs, with a minimum of 3.44 Cr_2O_3 wt% increase for table 60 to a maximum of 22.67 Cr_2O_3 wt% increase for table 63 (Figure 26).

Similar considerations can be done for the wastes as ΔCr_2O_3 between feeds and wastes ranges from 15.03 to 31.75 wt%. Finally mixes compared to the feeds show a Cr_2O_3 wt% content decrease, which is again strongly variable for each table.

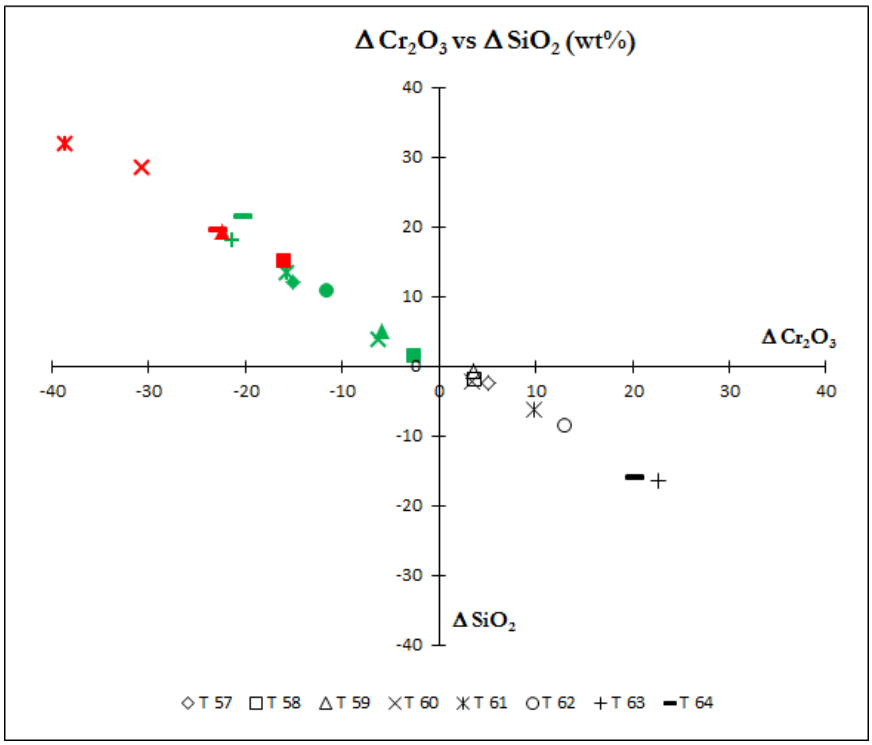

Figure 26. ΔCr_2O_3 vs ΔSiO_2 wt% content between feeds and each other type of material. Black symbols = concentrates, green symbols = mixes and red symbols = wastes.

Two kinds of setting changes can be envisaged to improve plant efficiency. First change, involving modification of table setting, requires a more detailed study of table efficiency to find out the reason of the differences between tables enlightened here. This can be done through the application of Separation Efficiency (SE) formula and is developed in Paragraph 5.5.5.

A second easier change that was operated effectively at Brieville plant is based on a change of destination of different products by simply changing pipe settings.

The strong pre-enrichment in chromite operated by hydrosizer produce some feeds, i.e. 58 F, 59 F and 60 F, that could already be used for special steel chromite market without undergoing shaking tables beneficiation (Figure 27).

The best concentrate is from table 61 with 52.44 Cr_2O_3 wt% content and 2.42 SiO_2 wt% content while the worst is from table 64 with 47.31 Cr_2O_3 wt% content and 5.35 SiO_2 wt% content (Figure 28). All concentrates of tables and also final product have however Cr_2O_3 and SiO_2 wt% contents that satisfied chemical parameters of special steel chromite market.

On the other hand no mixes can be used for special steels market even if Cr_2O_3 and SiO_2 wt% contents of mix from table 58 are very close to the market limits (Figure 29). Moreover mix from table 58, together with mixes from tables 59 and 60, should be added to concentrates rather than be re-worked with spirals and another shaking tables series, having a quite high Cr_2O_3 wt% content and a quite low SiO_2 wt% content. Instead mixes with very low Cr_2O_3 wt% content, as 63 M and 64 M, should be discharged with wastes. These solutions should reduce the processing cost of plant.

A reduction of total plant costs can be also achieved by decreasing of waste amount. It is possible to add some wastes from tables to the mixes that are subjected to the re-working with spirals and another shaking table series. For example wastes from tables 58 and 59 have a quite good Cr_2O_3 wt% content, respectively of 31.08 and 24.91 wt% (Figure 30). In fact these values are very similar to those of some mixes (Table 3).

Some of the changes here proposed were effectively applied in Brieville plant after a discussion of results with the engineers responsible for the plant. In detail mix of table 58 was moved to concentrate and mixes from tables 63 and 64 were moved to waste.

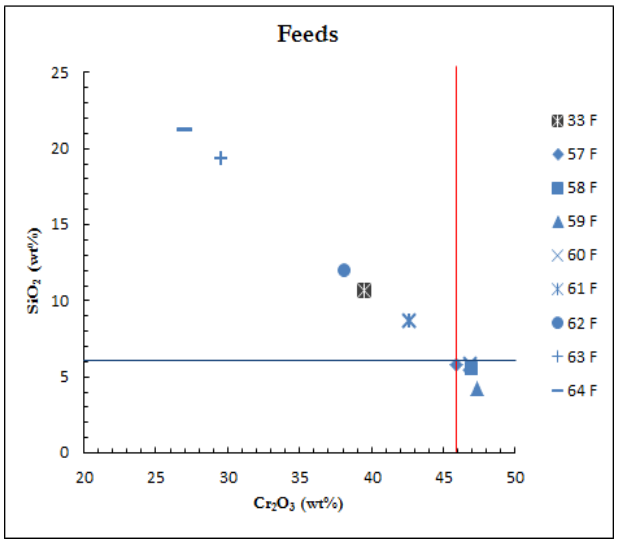

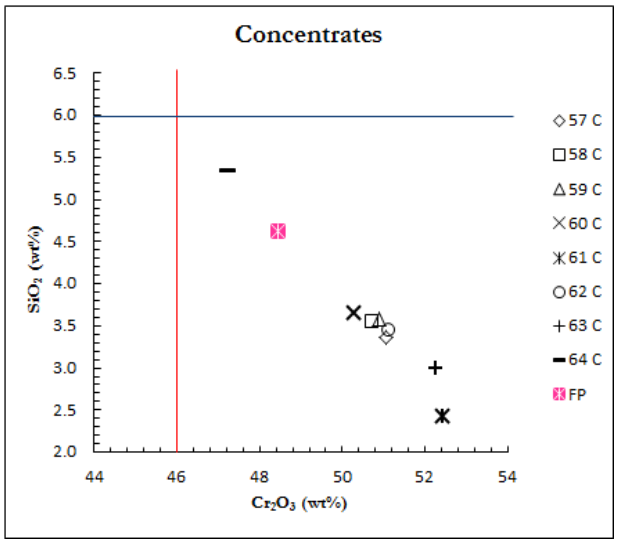

Figures 27 & 28. Cr_2O_3 vs SiO_2 wt% content of feeds (on the left) and concentrates (on the right) of each shaking table. Red and blue continuous lines indicate respectively Cr_2O_3 and SiO_2 content limits fixed at 46 wt% and 6 wt%, for chromite use in the special steels market.

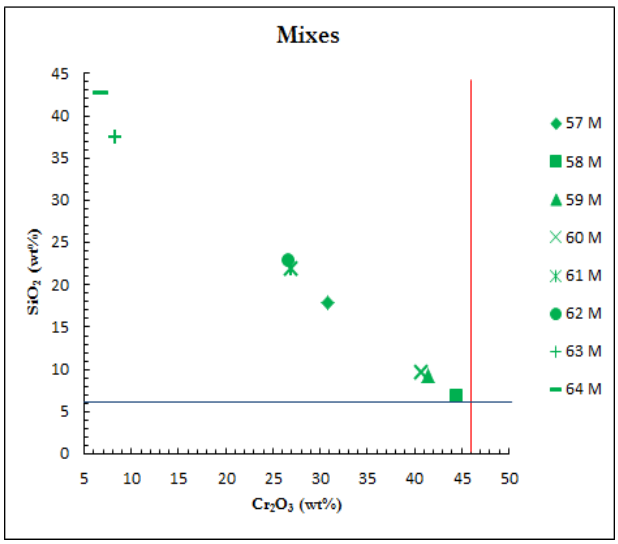

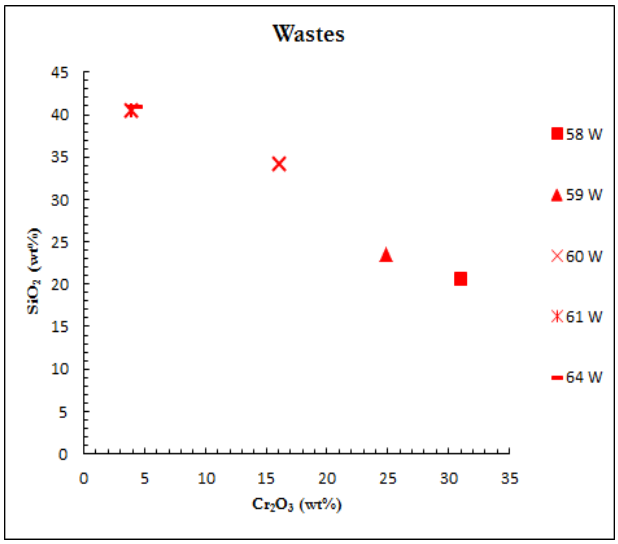

Figures 29 & 30. Cr_2O_3 vs SiO_2 wt% content of mixes (on the left) and wastes (on the right) of each shaking table. Red and blue continuous lines indicate respectively Cr_2O_3 and SiO_2 content limits fixed at 46 wt% and 6 wt%, for chromite use in the special steels market.

5.5.4 Flow rate calculation

At Brieville plant it was not easy to measure flow rate of shaking tables due to the lack of UNI flow measuring instruments, i.e. flowmeters. In fact the flow rates of water and of water-material mixture into pipes are not mechanically regulated, but the adjustment is carried out manually by Malagasy workers, based on their experience.

Then measurement of shaking tables flow rates were carried out with rudimental method trying to perform measurements as reliable as possible. A bucket and a stopwatch are used because there is an analogy for the operation of a positive displacement meter. The stopwatch is started when the flow starts, and stopped when the bucket reaches its limit. The volume divided by the time gives the flow rate. Results are shown in Table 4, some tables are set in a way that does not give any waste as output.

Table 4. Different products flow rate of each table and overall flow rate of tables. Measures are given in kg/s and converted into percentage (%). C = concentrate, M = mix and W =waste.

	Flow rate (kg/s)			Flow rate (%)		
	C	**M**	**W**	**C**	**M**	**W**
T 57	0.073	0.048	/	60.33	39.67	0.00
T 58	0.051	0.074	0.012	37.23	54.01	8.76
T 59	0.092	0.033	0.014	66.19	23.74	10.07
T 60	0.091	0.051	0.017	57.23	32.08	10.69
T 61	0.120	0.065	0.018	59.11	32.02	8.87
T 62	0.071	0.080	/	47.02	52.98	0.00
T 63	0.064	0.065	/	49.61	50.39	0.00
T 64	0.115	0.058	0.022	58.97	29.74	11.28
Total tables	0.677	0.474	0.083	54.86	38.41	6.73

Comparisons between flow rates of different products for each table are plotted in Figure 31.

Comparisons show that some tables receive much more material to be processed, irrespective of their distance from the source of flow. Moreover the proportions between the three different products flow rates are generally variable, while it should be constant in order to have an equal efficiency of shaking tables.

In fact some tables do not produce waste, i.e. tables 57, 62 and 63, while some tables produce more mix than concentrate, i.e. tables 58, 62 and 63 (Figure 31).

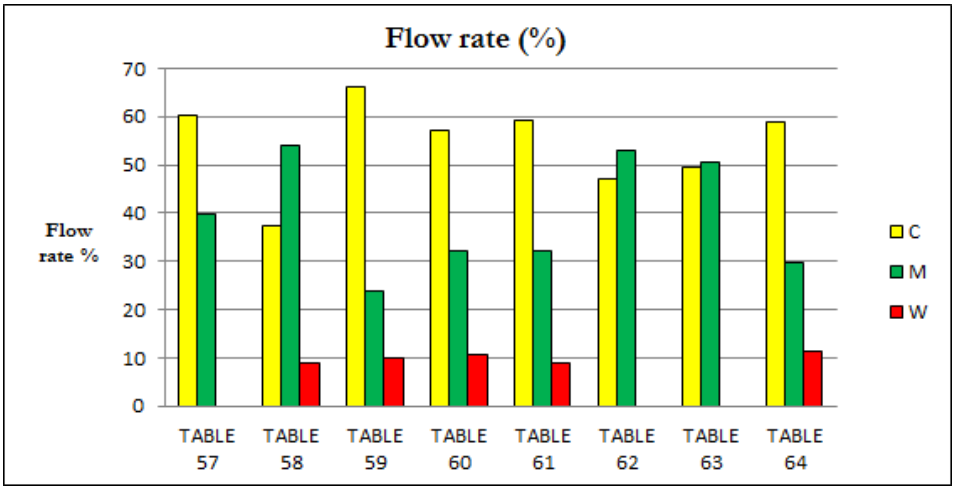

Figure 31. Comparisons between flow rates of different products for each table. C = concentrate, M = mix and W = waste.

Overall flow rate of tables also show a remarkable disparity between different products. As a matter of fact concentrate flow rate is about 55 % and it is greater than sum of mix and waste (Figure 32).

Flow rate data together with XRF analyses results question good working of hydrosizer and also good efficiency of shaking tables.

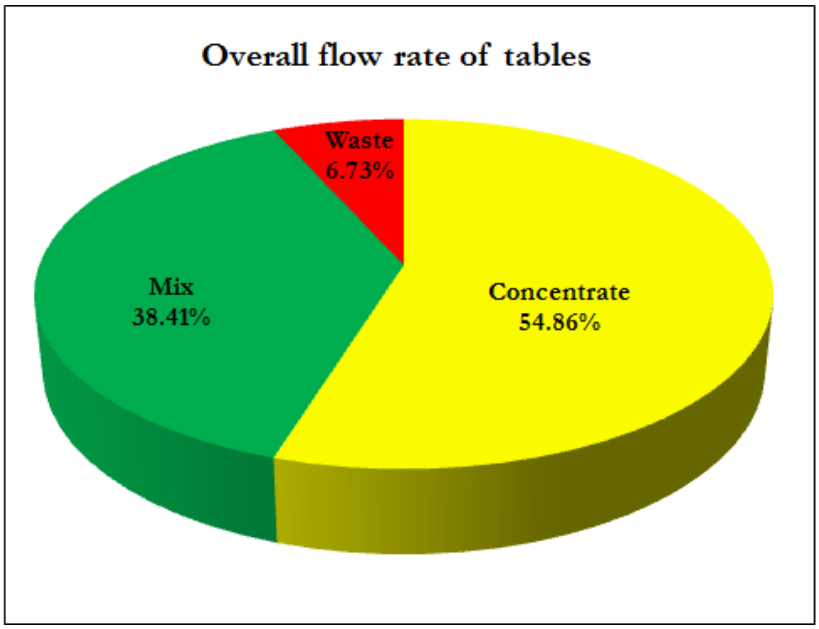

Figure 32. Overall flow rate of tables for each product: concentrate, mix and waste.

5.5.5 Separation efficiency (SE) of shaking tables and plant

X-ray Fluorescence (XRF) whole-rock analyses, flow rates measurements and Electron Microprobe (EMP) microanalyses of chromite crystals allow determining separation efficiency (SE) of shaking tables and plant using Wills' equation (1979), already explained in Chapter 2 and applied in Chapter 4.

Equation used is:

$$SE = \frac{100Cm(c-f)}{(m-f)f}$$

where C is the fraction of the total feed weight that reports to the concentrate, m is the percentage metal content of the valuable mineral, c is the metal % of the concentrate and f is the metal % of the feed.

The C values were calculated as ratio between the concentrate flow rate and the total flow rate of each table.

The m value is Cr_2O_3 wt% content of chromite crystals and was calculated as the average Cr_2O_3 wt% detected with EMP microanalyses (Table 5 in Appendix II). The average of thirteen analyses was chosen as m value, showing low standard deviation value of 0.80.

The f and c values respectively feed and concentrate Cr_2O_3 wt% content, were obtained by XRF analysis.

Values of parameters used to calculate separation efficiency (SE) and SE results are shown in Table 6.

Table 6. Parameters used to calculate separation efficiency (SE) and separation efficiency results of each table, total tables and plant. F = feed, C = concentrate, 33F = overall feed and TC = overall tables concentrate.

	Material type	f or c (wt%)	C	m (wt%)	SE (%)	c*C (wt%)
TABLE 57	57F	45.90	0.603	53.03	50.25	30.78
	57C	51.04				
TABLE 58	58F	47.02	0.372	53.03	25.82	18.87
	58C	50.72				
TABLE 59	59F	47.31	0.662	53.03	46.44	33.69
	59C	50.89				
TABLE 60	60F	46.86	0.572	53.03	36.09	28.77
	60C	50.30				
TABLE 61	61F	42.65	0.591	53.03	69.30	30.99
	61C	52.44				
TABLE 62	62F	38.15	0.470	53.03	56.99	24.03
	62C	51.13				
TABLE 63	63F	29.59	0.496	53.03	85.98	25.92
	63C	52.26				
TABLE 64	64F	26.95	0.590	53.03	90.18	27.85
	64C	47.21				
TABLES	33F	39.51	0.549	53.03	60.45	27.77
	TC	50.62				
PLANT	33F	39.51	0.650	53.03	57.66	31.49
	FP	48.44				

Separation efficiency of shaking tables is strong variable at Brieville plant and ranges between a minimum of 25.82% of table 58 and a maximum of 90.18% of table 64 (Figure 33).

The malfunctioning of some tables, testified by low SE of four of them, decreases separation efficiency of the overall tables that is fixed at 60.45%.

Separation efficiency of plant (57.66%) is lower than separation efficiency of the overall tables (60.45%) due to the low efficiency of the gravity plant (spirals + shaking tables) re-working mix. In fact it should be noted that at Brieville marketed final product is composed of about 85 wt% primary concentrate, achieved by tabling process and about 15 wt% of second concentrate achieved by re-working mix with spirals and tables.

Separation efficiency variability of shaking tables is caused by the difference of separation efficiency parameters of each table. In fact tables working coarser feeds pre-enriched in chromite have low separation efficiency, while those that work finer feeds pre-depleted in chromite have very high separation efficiency (Figure 33). This fact confirms hypothesis that hydrosizer, the device providing the overall feed to shaking tables, hides a strongly different efficiency of the tables. As the huge difference in SE of different tables is strictly correlated to the grain size of the sand they work. An evaluation of the degree of liberation in selected tables was performed in order to understand if the difference in SE can be due to a low degree of liberation (see Paragraph 5.5.6).

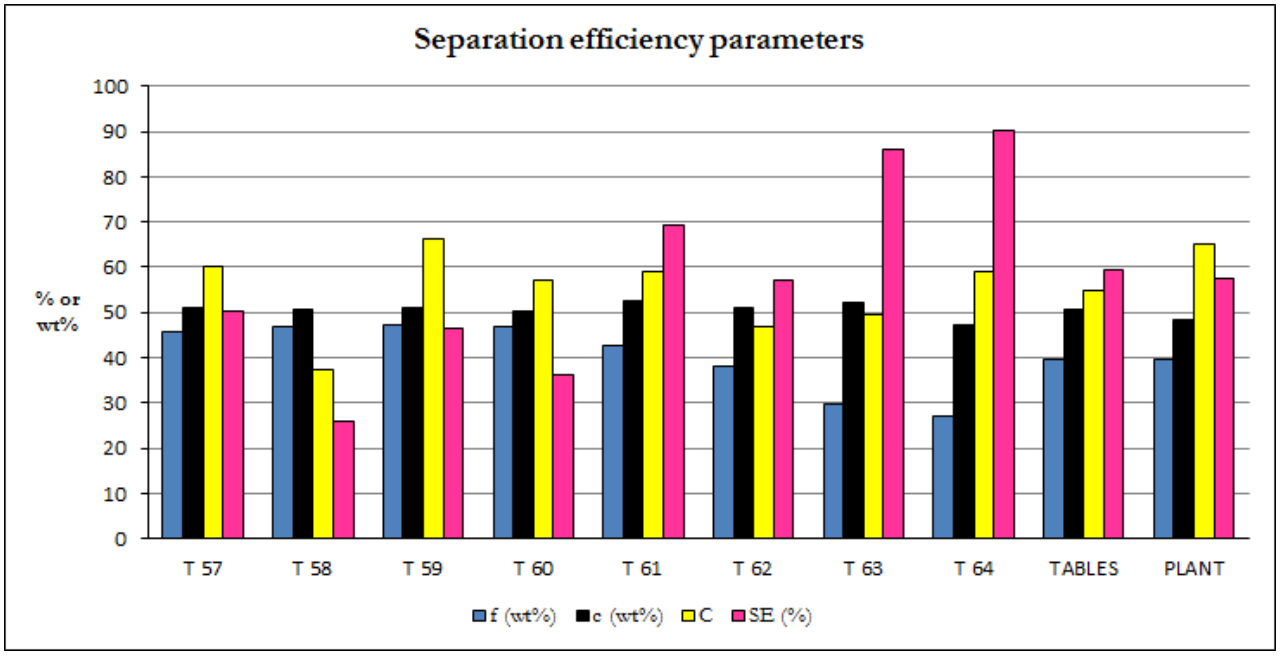

Figure 33. Separation efficiency parameters and separation efficiency values of each table, overall tables (TABLES) and enrichment plant (PLANT).

Although the value of separation efficiency can be useful in comparing the performance of different operating conditions on selectivity, it takes no account of economic factors, and, as it will become apparent, a high value of separation efficiency does not necessarily lead to the most economic return (Wills and Napier-Munn, 2006).

Since the purpose of mineral processing is to increase the economic value of the ore, the importance of the recovery-grade relationship is in determining the most economic combination of recovery and grade which will produce the greatest financial return per ton of ore treated in the plant. This will depend primarily on the current price of the valuable product, transportation costs to the smelter, refinery, or other further treatment plant, and the cost of such further treatment, the latter being very dependent on the grade of concentrate supplied. A high grade concentrate will incur lower smelting costs, but the lower recovery means lower returns of final product. A low grade concentrate may achieve greater recovery of the values, but incurs greater smelting and transportation costs due to the included gangue minerals (Wills and Napier-Munn, 2006).

The arithmetic product of concentrate Cr_2O_3 content (c parameter) and recovery (C parameter) gives an economic value to the material. The relationship between arithmetic product (c * C) and separation efficiency (SE) allows a rational evaluation of cost effective work at Brieville enrichment plant (Figure 34).

In general at Brieville plant there is not a clear correlation between c * C and SE again because of the pre-enrichment effect operated by hydrosizer. Tables 57, 59 and 61 show the highest values of c * C that do not correspond to the highest SE because in spite of giving an abundant and good quality concentrate they lose much chromite in the mix and in the waste.

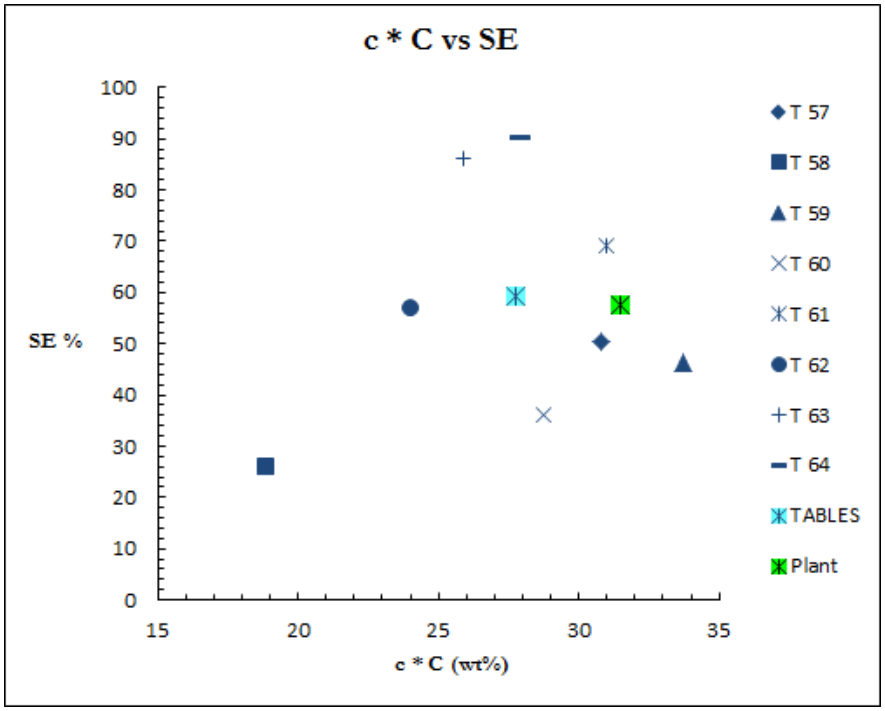

Figure 34. c * C vs SE of each table, overall tables (light blue symbol) and enrichment plant (green symbol).

5.5.6 Grain counting and liberation degree (LD)

One of the major purposes of comminution is the liberation of the valuable minerals from the associated gangue minerals at the coarsest possible particle size. In practice, complete liberation is seldom achieved, even if the ore is ground down to the grain size of the desired mineral particles. The particles of "locked" mineral and gangue are known as middlings, and further liberation from this fraction can only be achieved by further comminution.

Many researchers have tried to quantify degree of liberation with a view to predicting the behavior of particles in a separation process (Barbery, 1991).

The first attempt at the development of a model for the calculation of liberation was made by Gaudin (1939); King (1982) developed an exact expression for the fraction of particles of a certain size that contained less than a prescribed fraction of any particular mineral. These models, however, suffered from many unrealistic assumptions that must be made with respect to the grain structure of the minerals in the ore, in particular that liberation is preferential, and in 1988 Austin and Luckie concluded that "there is no adequate model of liberation of binary systems suitable for incorporation into a mill model". For this reason liberation models have not found much practical application.

However, some fresh approaches by Gay, allowing multi-mineral systems to be modeled (not just binary systems) free of the assumptions of preferential breakage, have recently demonstrated that there may yet be a useful role for such models (Gay, 2004a,b). The quantification of liberation is now routinely possible using the dedicated scanning electron microscope MLA and QEMSCAN systems and concentrators are increasingly using such systems to monitor the degree of liberation in their processes.

Due to the existence of few research facilities in the world having the MLA instrumentation and due to expensive analysis, this advanced analysis technique can be replaced by hand labor grain counting, that requires a long time but is a low-cost technique.

At Brieville previous results show that a study of the degree of liberation is pivotal to understand the difference in efficiency between tables and especially the low efficiency of tables working coarser sand.

Degree of liberation of chromite from silicate gangue was evaluated on selected samples from Brieville enrichment plant by grain counting under transmitted light microscope, where middlings were defined as grains

containing 10 to 90% chromite. Each datum refers to 500 grains counted on a thin polished section and relative number of grains is transformed into wt% by using average density of phases. Liberation degree is also affected by materials grain size and then grain counting was also performed on four different grain size of each product: +1000 μm; -1000 +600 μm; -600 +300 μm and -300 +150 μm. Grain counting was limited to grain sizes coarser than 150 μm due to the difficult identification of finer grains under transmitted microscope and due to expected concentration of middlings into coarser grain sizes.

The total distribution of grains each product was then calculated as the average of each grain size weighted for the relative amount of each grain size class.

Grain counting was focused on each product of the table that works the coarsest grain size, i.e. 57F, 57M and 57C, comparing the values with the overall feed (33F), the feed of the table that works a finer grain size (62 F) and with the final product (FP).

On the basis of concepts expressed by Wills (2006), who says that the degree of liberation refers to the percentage of the mineral occurring as free particles in the ore in relation to the total content, two different equations are below proposed in order to calculate liberation degree:

$$LD = \frac{100\,Nchr}{Nchr + \frac{1}{2}\,Nmid} \qquad (1)$$

where *Nchr* is the number of chromite grains transformed into wt% and *Nmid* is the number of middlings transformed into wt%. This equation calculates LD as the ratio between chromite in chromite grains and total chromite, where total chromite is the sum of chromite in chromite grains and chromite in middlings, with the approximation that middlings in average contain 50% chromite.

$$LD = \frac{100\,(Nchr + Nsil)}{Nchr + Nsil + Nmid} \qquad (2)$$

where *Nchr*, *Nsil* and *Nmid* are respectively the number of chromite, silicate and middling grains transformed into wt%. This equation calculates LD as the ratio between the weight of liberated grains (either chromite or silicate) and the total weight of all the grains.

Results of grain counting and liberation degree of selected samples are shown in Table 7.

Table 7. Grain counting and liberation degree results of selected samples. 33F = overall feed, FP = final product, F = feed, M = mix and C = concentrate.

Sample	Grain size (μm)	Chromites (wt%)	Middlings (wt%)	Silicates (wt%)	Liberation eq. (1)	Liberation eq. (2)
33 F	+1000	16.56	32.69	50.75	50.33	67.31
	-1000 +600	62.60	14.80	22.60	89.43	85.20
	-600 +300	60.60	21.20	18.20	85.11	78.80
	-300 +150	66.00	6.40	27.60	95.38	93.60
	Total	**58.99**	**17.43**	**23.58**	**87.13**	**82.57**
57 F	+1000	33.92	38.25	27.83	63.94	61.75
	-1000 +600	63.60	31.60	4.80	80.10	68.40
	-600 +300	68.40	23.80	7.80	85.18	76.20
	-300 +150	67.60	13.00	19.40	91.23	87.00
	Total	**63.11**	**27.40**	**9.49**	**82.16**	**72.60**
57 C	+600	84.20	14.40	1.40	92.12	85.60
	-600 +300	82.60	13.80	3.60	92.29	86.20
	-300 +150	76.60	7.20	16.20	95.51	92.80
	Total	**82.34**	**13.32**	**4.34**	**92.52**	**86.68**
57 M	+1000	14.29	59.05	26.67	32.61	40.95
	-1000 +600	25.00	37.80	37.20	56.95	62.20
	-600 +300	40.60	30.40	29.00	72.76	69.60
	-300 +150	33.40	11.00	55.60	85.86	89.00
	Total	**19.93**	**49.02**	**31.05**	**44.85**	**50.98**
61 F	+600	24.40	16.20	59.40	75.08	83.80
	-600 +300	47.20	21.20	31.60	81.66	78.80
	-300 +150	70.80	13.60	15.60	91.24	86.40
	Total	**54.06**	**17.78**	**28.17**	**85.88**	**82.22**
FP	+600	78.40	19.20	2.40	89.09	80.80
	-600 +300	68.95	24.73	6.32	84.79	75.27
	-300 +150	68.40	16.20	15.40	89.41	83.80
	Total	**69.95**	**21.47**	**8.59**	**86.70**	**78.53**

In general, as expected, the amount of middlings decreases with decrease in grain size for all the products, as well as the liberation degree increases with decrease of grain size.

Overall feed (33F) is strongly enriched in silicate grains and middlings in the coarsest grain size, while the highest concentration of chromite grains is in the finest grain size (Figure 35). Totally gravity separation plant works a feed that has about 59 wt% chromite grains, 17.5 wt% middlings and 23.5 wt% silicate grains (Table 7).

A strict direct correlation between decreasing of middlings and grain size occurs in the feed of table 57 (57F). Therefore, even in the case of 57 F, the lowest middling content is in the grain size that ranges from 300 to 150 μm, as for the overall feed (Figure 35).

The concentrate of the table 57 (57C) has a very high percentage of chromite grains, middlings decrease with the grain size decreasing and on the other hand silicates increase with the grain size decreasing (Figure 35).

The mix of the table 57 (57M) is characterized by a considerable amount of middlings mainly into coarser grain sizes. In fact in the grain size class above 1000 μm middlings are about 60 wt% while in the grain size class between 300 and 150 μm are only 11 wt% (Table 7).

The feed of table 61 (61F) shows a different trend if compared to other products, in fact most middlings stay into intermediate grain size that ranges between 600 and 300 µm (Figure 35).

Final product (FP) has the same middlings trend of the table 61 (61F), while silicate grains increase with grain size decreasing, the opposite is for chromite grains which decrease with grain size decreasing (Figure 35).

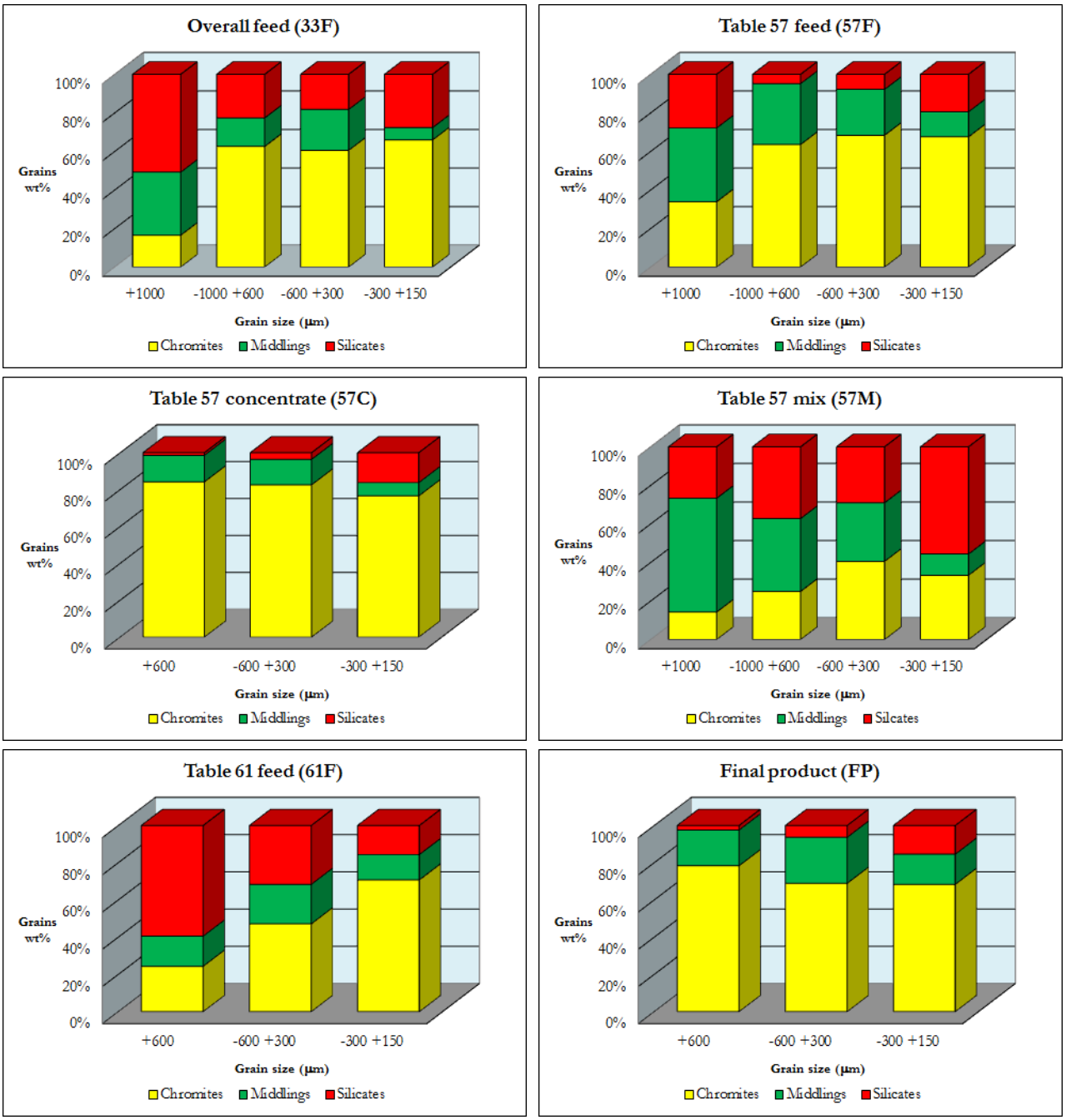

Figure 35. Selected samples grain counting of different grain sizes.

Samples comparison for each grain size is shown in Figure 36 and highlights other important features of shaking tables work.

Samples having a significant amount of sand coarser than 1000 µm are only the overall feed (33F), feed of table 57 (57F) and mix of table 57 (57M). The absence of table 57 concentrate (57C) at grain size coarser than 1000 µm

means that almost all grains feeding into table 57 report to the mix (57M). As a matter of fact sample 57M has a very high amount of middlings (about 60 wt%).

For the grain size ranging between 1000 and 600 µm the best product is the concentrate of table 57 (57C) due to the high percentage of chromite grains and thereby due to low amount of middlings and silicates. The sample 57M shows also into this grain size the highest middlings amount, which is similar to silicates (Table 7).

Concentrate of the table 57 (57C) has an excellent amount of chromite grains compared to the other samples even in the grain size ranges between 600 and 300 µm, while the mix of table 57 (57M) is always the sample with the highest middlings amount.

Grain size ranging between 300 and 150 µm is depleted in middlings compared to all other grain sizes and the highest middlings amount is into the final product (FP) with about 16 wt%. Moreover this grain size shows that mix of the table 57 (57M) is very rich in silicates, with about 55 wt%.

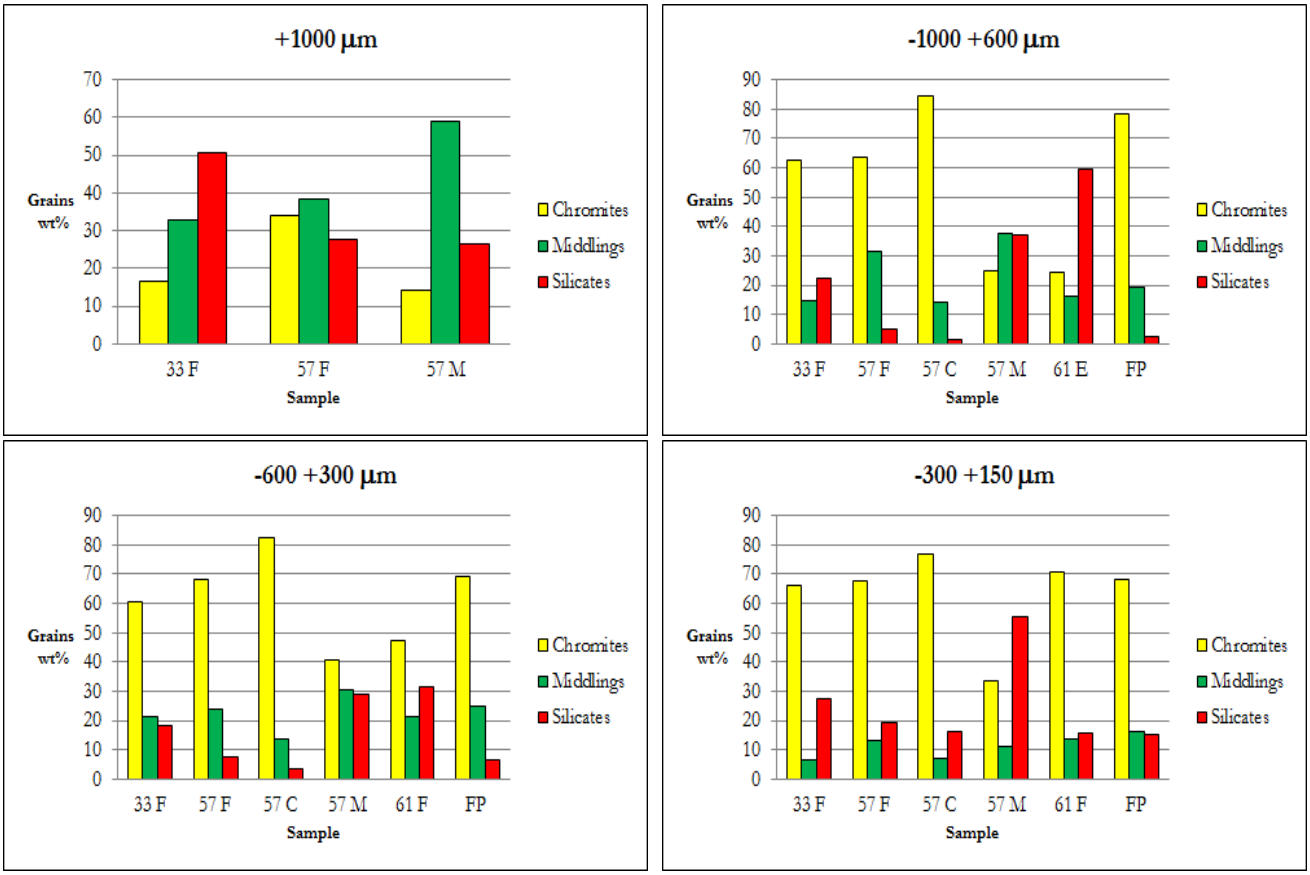

Figure 36. Samples comparison to each grain size.

Figure 37 shows the distribution of grains for different products regardless of grain size. The pre-concentration at hydrosizer is clearly visible in the very different grain distribution between feed of tables 57 (57F, with 65 wt% chromite grains) and 61 (61F, with 53 wt% chromite grains).

The residual SiO_2 content of concentrates (57C and FP) is mainly due to their high amount of middlings (respectively 13.32 and 21.47 wt%), while the amount of silicate grains is quite low respectively 4.34 and 8.59 wt%). If we assume that the average chromite content of middlings is 50 wt% the previous data mean that about two thirds of SiO_2 within concentrate is found in middlings and only about one third in silicate grains.

The high content of middlings in the mix (57M) shows that setting of the table is correct as it correctly separates grains according to their density, with chromite grains mainly reporting to the concentrate, middlings to the mix

and silicate grains to the waste. On the other hand as the mix is so high in middlings it cannot be efficiently re-worked. This can explain the lower SE of the whole plant compared with that of tables (Figure 33).

The final product (FP) compared to overall feed (33F) shows that the chromite increase is 10.9 wt% and the silicate decrease is 14.5 wt%, results that can be very well compared with Cr_2O_3 increase and SiO_2 decrease for the same products. Finally the middlings content is increased by 4 wt% (Table 7).

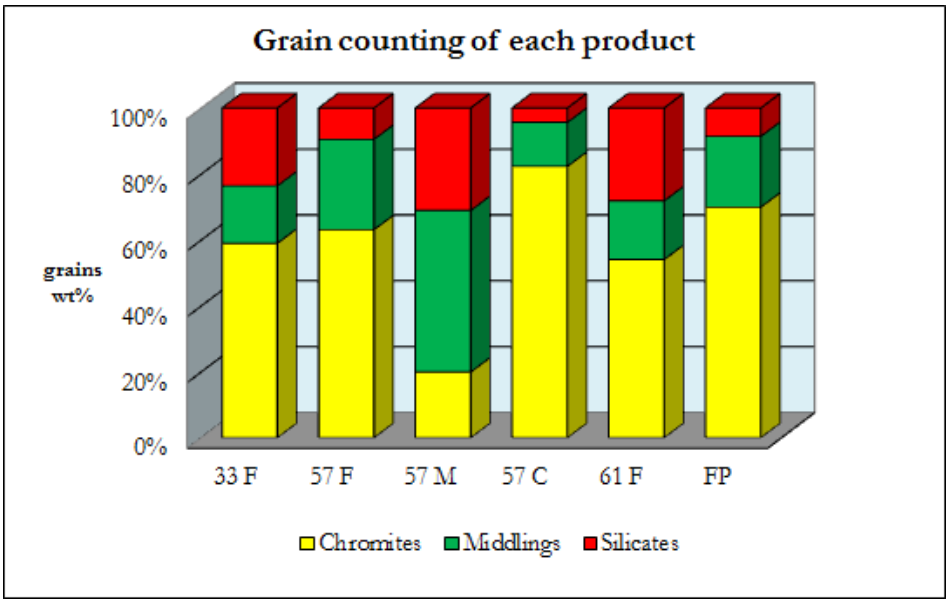

Figure 37. Grain counting of each selected samples regardless of grain size.

Grain counting allowed defining the liberation degree of selected samples at Brieville plant. Degree of liberation was calculated with two different equations As a matter of fact comparison between the two different equations used to calculate liberation degree (LD) shows that liberation degree evaluated with Eq. 2 is generally lower than that evaluated with Eq. 1 (Figure 38). There is only one case in which the Eq. 2 gives a result higher than Eq. 1, i.e. the case of sample 57M, where middlings are more abundant than silicate grains, especially into the coarsest grain size with about 60 wt% content.

LD calculated with Eq. 2 better describes the behavior of the tables during separation and is more strictly correlated to SE. Lower LD of table 57 can well explain its lower SE compared to Table 61.

Considering table 57, LD results show that in spite of the low SE value of this table it well separates grains according to their density as concentrate is strongly enriched in chromite grains (82.34 wt%), while mix is strongly depleted in chromite grains (19.93 wt%). The main reason why the table has a very low SE is the high middlings content of the feed and hence its low LD (72.60 wt% Eq. 2). Such high middlings content causes a high chromite loss into the mix and results in a low LD value according to Eq. 1 (82.16 wt%) that shows the percentage of chromite that reports to the concentrate.

Table 61, that works much finer sand, has a much higher LD (82.22, Eq. 2) that results in a much better SE, again due to the middlings content that in this case is much lower than in Table 57.

LD of overall feed is quite good, even if, when we consider its value for the different grain size classes, it sharply decreases for the coarsest class (+1000 μm).

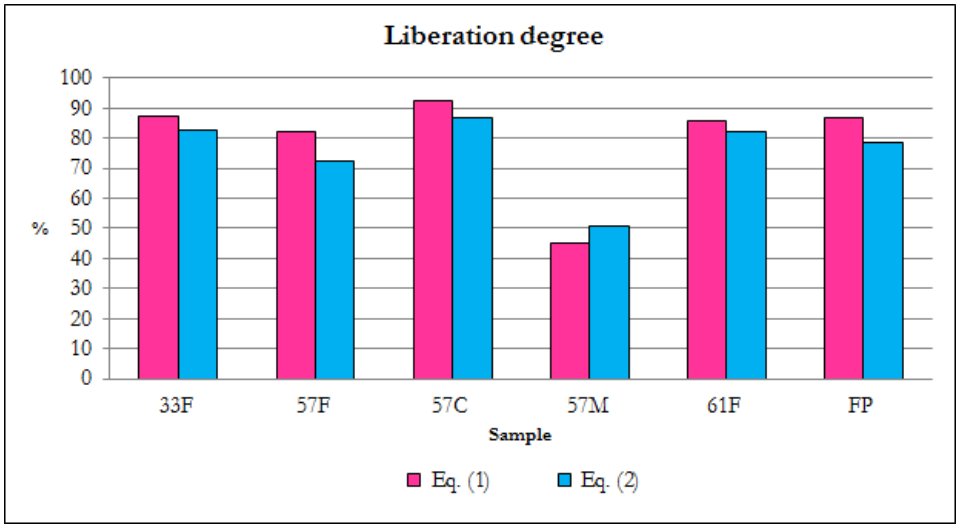

Figure 38. Liberation degree of selected samples at Brieville plant. Results were obtained with two different equations.

The results suggest a possible strategy to improve shaking tables efficiency. The low LD of overall feed for grain size +1000 μm (67.31 wt% Eq. 2) together with the absence of this grain size class in all the concentrates and in the final product are clear clues that feeding sand should be grinded to -1.0 mm instead of -1.5 mm.

A second change that can improve the whole plant efficiency is related to the high middlings content of mix that prevent an efficient separation in the re-cycling of mix itself. The only way to get a good efficiency in re-cycling is to grind mix to -600 μm before re-using it as the feed of the re-cycling spirals and tables.

These changes anyway require a detail economic study to compare the benefits of increasing SE of the plant and the additional costs of new grinding operations.

5.6 Conclusions

The results of grain size, XRD, XRF, EMP and grain counting analyses together with separation efficiency (SE) and liberation degree (LD) evaluation allow the following conclusions:

- ✓ Brieville overall feed chromite sand has a very heterogeneous mineralogy, comprising primary and secondary minerals, but devoid of olivine. Differential separation of gangue minerals could reasonably occur.
- ✓ Hydrosizer operates a pre-selection of chromite sand and, as a consequence, tables are fed with sands different not only in grain size but also in mineralogy and chemistry.
- ✓ The main parameter affecting the quality of the final product is the degree of liberation of chromite, as more than half of SiO_2 content of final product is hosted in middlings.
- ✓ Low sorting of sands feeding tables negatively affects their separation efficiency.
- ✓ Re-cycling of mix cannot efficiently separate chromite due to its very high middlings content.

Plant efficiency and quality of final product can be improved according to the previous conclusions by:

1. Moving the Cr_2O_3-enriched mixes to the concentrate and the Cr_2O_3-depleted mixes to the waste.
2. Grinding the overall feed to -1 mm instead of -1.5 mm.
3. Grinding mixes that will be re-cycled to -600 μm.
4. Substituting of hydrosizers with screens that would increase shaking tables efficiency.

The first change, that does not involve any additional operational cost, has been effectively applied to the plant just after publication of the present study. The last three changes, on the other hand, involve additional operational costs and require a detailed economic analysis before being applied to the plant.

Chapter 6

Enrichment test: application of an innovative beneficiation technique to Krasta chromite ore (Albania) for the production of high grade – low silica chromite sand

6.1 Introduction

This work deals with disseminated chromite ore samples collected at Krasta Mine, located in the central southern part of the Bulqiza Massif (Mirdita ophiolite, Albania). First of all the samples, having an average Cr_2O_3 content of 23.66 wt%, were enriched using spirals and shaking tables at Krasta plant. The first chromite sand concentrate has 46.58 wt% Cr_2O_3 and 10.35 wt% SiO_2. In order to meet the very demanding chemical parameter requirements for refractory market chromite first concentrate sand was re-enriched using a combination of dry magnetic and gravity separation at the pilot plant of Omega Foundry Machinery LTD. in Peterborough (UK). In a second step sand was enriched using a drum magnet. New concentrate was then enriched in a third step by means of an Inclined Fluidised Separator (IFS) that works in dry conditions using an air cushion as fluidisation agent.

Preliminary results show that the pilot plant is able to strongly re-enrich the primary concentrate sand, producing a final concentrate sand with up to 60.01 wt% Cr_2O_3 and as low as 2.43 wt% SiO_2 with a tail that is still suitable for the steel market.

6.2 Geology of the Mirdita ophiolite

The Albanian ophiolites occur within the Dinaride–Hellenide segment of the Alpine orogenic system and represent the remnants of the MesozoicNeo-Tethyan ocean (e.g., Shallo and Dilek, 2003; Dilek and Furnes, 2009).

The Mirdita ophiolite is located in the northern ophiolite belt of Albania (Figure 1). Based on differences in the internal stratigraphy and chemical composition of the crustal unit, two types of ophiolites have been recognized in the Mirdita ophiolite, namely the Western Mirdita Ophiolite (WMO) and the Eastern Mirdita Ophiolite (EMO) (Beccaluva et al., 1994; Bortolotti et al., 1996; Dilek et al., 2008; Shallo, 1990; Shallo et al., 1987, 1990). Boninitic dikes and lavas crosscut and/or overlie earlier extrusive rocks in the EMO (Beccaluva et al., 1994; Dilek et al., 2008; Shallo et al., 1987). The crustal section of the WMO has MORB affinities, whereas that of the EMO shows predominantly SSZ geochemical affinities. The extrusive sequence in the EMO consists of pillowed to massive flows ranging in composition from basalt and basaltic andesite in the lower section to andesite, dacite, and rhyodacite in the upper part (Bortolotti et al., 1996; Dilek et al., 2008). Large peridotite massifs are exposed at the western and eastern ends of the Mirdita ophiolite. Plagioclase-bearing peridotites are frequently observed in the WMO, whereas harzburgite is dominant in the EMO (Beccaluva et al., 1994, 1998; Beqiraj et al., 2000; Hoxha and Boullier, 1995).

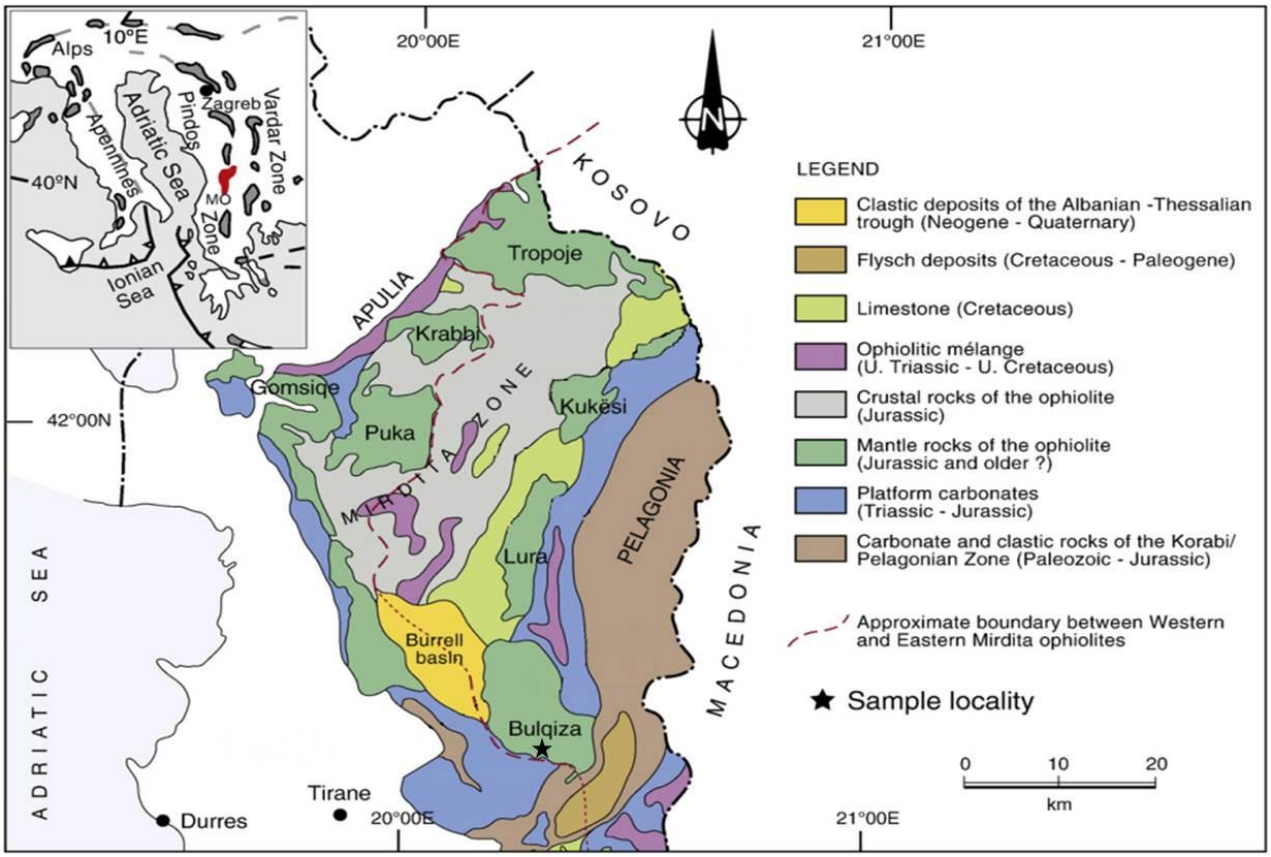

Figure 1. Simplified geological map of the Mirdita ophiolite in north-central Albania (modified from Dilek et al., 2007). Inset map shows the distribution of a part of the Tethyan ophiolites in the Balkan Peninsula, with the Mirdita ophiolite in red.

6.3 Bulqiza Massif and Krasta chromite deposit

Bulqiza Massif is located about 40 km north-east of Tirana (Figure 1) and it is the most important ultrabasic complex hosting chromite ores of the EMO. It covers an area of 370 km^2 and chromite reserves are currently estimated around 12 million tons.

Systematic lithological variations in the mantle section with proximity to the crustal section have previously been recognized (Beccaluva et al., 1998; Beqiraj et al., 2000; Hoxha and Boullier, 1995). We also confirmed systematic lithological variations in the mantle section: clinopyroxene porphyroclast-bearing harzburgites (Cpx-harzburgites hereafter, Figure 2a) are sometimes observed in the eastern margin of massifs, i.e. the basal part of the mantle section, whereas harzburgite and dunite are dominant in the upper parts of the mantle section (Beccaluva et al., 1998; Beqiraj et al., 2000; Dilek and Morishita, 2009; Hoxha and Boullier, 1995). Cpx-harzburgites have a porphyroclastic texture. Clinopyroxene occurs as both porphyroclastic grains and their recrystallized fine grains. The lithological boundary between dunites and harzburgites is usually sharp and is sometimes nearly parallel to the foliation plane defined by mineral orientations. Dunite also frequently occurs as small bodies with complicated irregular boundaries with harzburgites (Figure 2b). Harzburgite shows granular to porphyroclastic textures.

Orthopyroxenite dikes/layers a few cm to 3 m wide are frequently observed in the uppermost section of the mantle sequence (Beccaluva et al., 1998; Dilek and Morishita, 2009) (Figure 2d). They rarely occur as layers nearly parallel to the foliation and lithological boundaries in the host peridotites, and more frequently occur as dike-like features cutting all lithological boundaries at high angles (Figure 2b), indicating that they are related to late melt migration through the mantle section. Fewer deformation textures are observed in orthopyroxenites.

Orthopyroxenites mainly consist of coarse-grained orthopyroxene (up to 10 cm across) with small amounts of spinel and olivine. Olivines sometimes show resorbed textures in large orthopyroxene grains (Figure 3b). Large

orthopyroxenes have many clinopyroxene exsolution lamellae. Dark brown spinel is commonly included in large orthopyroxene grains. Orthopyroxenites locally contain amphibole and/or clinopyroxene. Clinopyroxene sometimes occurs as veins along orthopyroxenites. Amphibole occurs as an interstitial phase along the grain boundaries of orthopyroxene and also as poikilitic phases including orthopyroxene grains (Figure 3c).

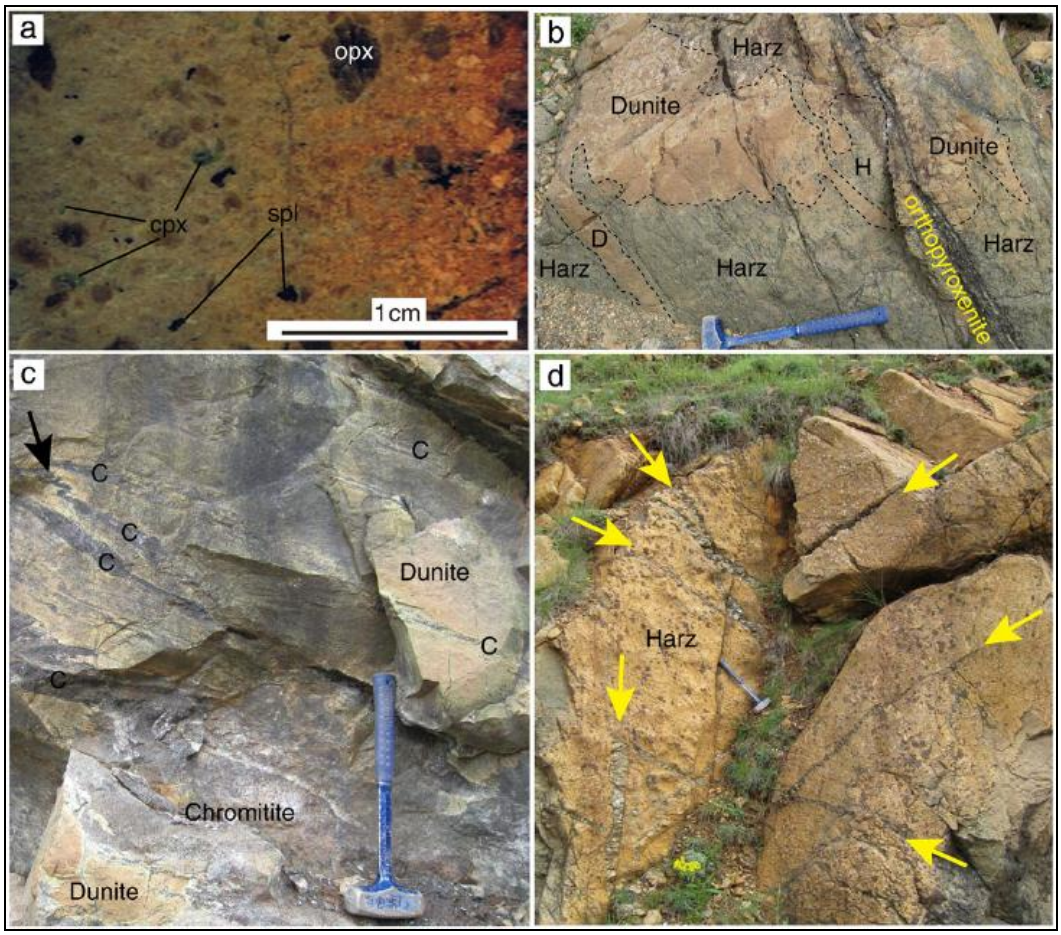

Figure 2. (a) Polished surface of a clinopyroxene porphyroclast-bearing harzburgite. (b) Field relationships between dunite, harzburgites and orthopyroxenite. (c) Occurrence of chromitite layers in dunite. Chromitite is sometimes tightly folded (arrow). (d) Orthopyroxenite network (yellow arrows) in harzburgites.
C = chromitite, cpx = clinopyroxene, D = dunite, H or Harz =harzburgite.

Harzburgites and minor dunitic layers and lenses, with different degree of serpentinization, host Krasta chromite ore that is located in the central southern part of the Bulqiza Massif (black star in Figure 1). Outcropping chromitite layers a few cm thick are frequently observed in dunite and usually occur parallel to each other and to the lithological boundary between dunite and harzburgite (Figure 2c). Chromitite layers are occasionally tightly folded in dunites (Figure 2c). It is interesting to note that inclusions of silicate minerals, such as amphibole, orthopyroxene, clinopyroxene, and their secondary minerals (e.g., chlorite and serpentine), are commonly found within chromian spinels in harzburgites near dunite (Figure 3a).

Several chromite lumpy from Krasta mine stock (Figure 4) were collected and XRF whole rock analysis reveals an average Cr_2O_3 content of 23.66 wt%.

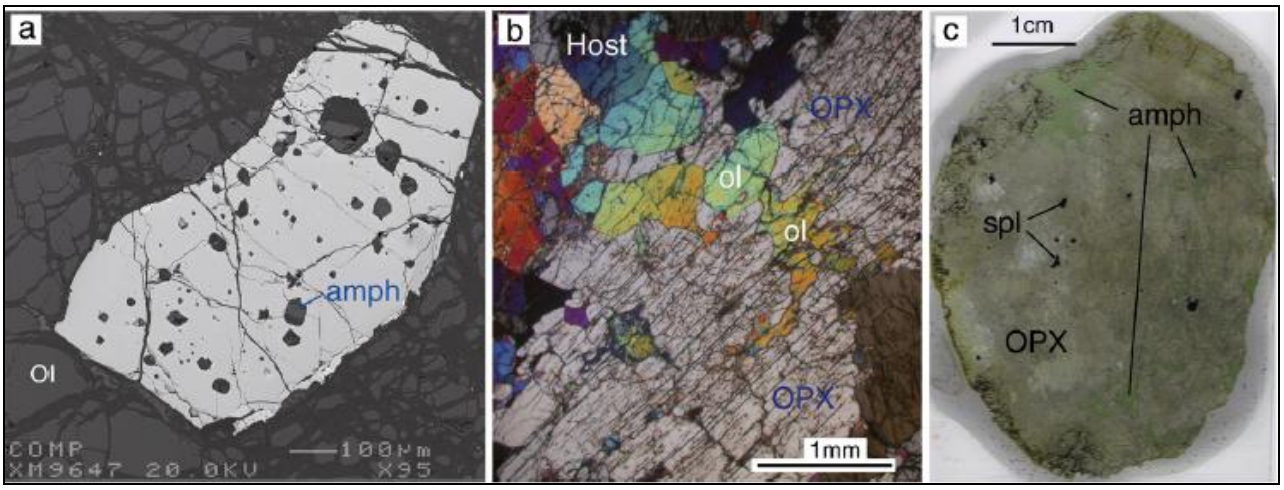

Figure 3. (a) Back-scattered electron image of a spinel grain with silicate mineral inclusions in harzburgites close to dunite. (b) Resorbed olivine in a large orthopyroxene grain in an orthopyroxenite. (c) Poikilitic amphibole (light green phase) in orthopyroxenite. amph = amphibole, ol = olivine, OPX = orthopyroxene, spl = spinel.

Figure 4. Panoramic view of Krasta mine with a chromite lumpy stock on the right.

6.4 Krasta enrichment plant

The Krasta mine has been exploited mainly in underground but also in open pit since 1971. Chromite sand (grain size -1.5 mm) is produced at the Krasta enrichment plant, located in an optimum logistic position, being only a few meters from underground working adits.

Chromite sand enrichment is achieved by crushing and gravity separation, according to the flow sheet shown in Figure 5.

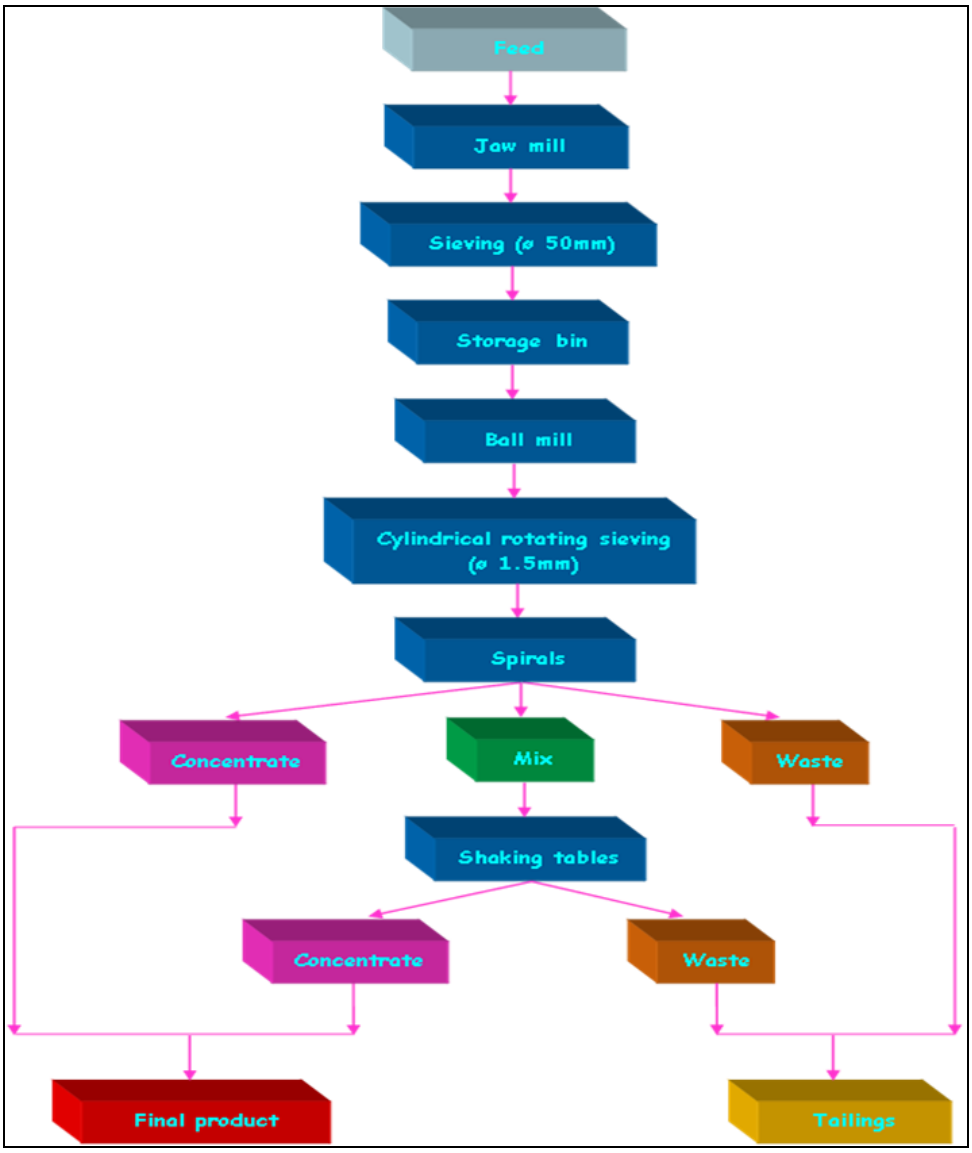

Figure 5. Flow sheet of Krasta enrichment plant.

Crushing and grinding plant is composed of jaw and ball mills, with associated sieves and cylindrical rotating sieve, that reduce feed in the first step to -50 mm grain size and finally to -1.5 mm grain size.

Gravity separation plant is made up of spirals and shaking tables. Several pipes send feed to a series of spirals comprising 32 spirals (Figure 6a). Each spiral produces three types of materials: concentrate, mix and waste. The mix material coming out from spirals is re-enriched by 8 shaking tables (Figure 6b) that produce concentrate and waste materials.

Concentrate sands obtained from spirals and shaking tables are blended in order to achieve the chromite final product that is stocked close to the plant (Figure 6c) while wastes from spirals and tables form tailings that are disposed in a dump.

About 200 kilograms of chromite concentrate sand were collected following UNI462800-1976 norm in order to have a big amount of material for making new enrichment tests at the pilot plant of Omega Foundry Machinery LTD. in Peterborough (UK).

The portion of the concentrate sand from Krasta enrichment plant used for later enrichment tests has 48.51 wt% Cr_2O_3 content and 9.09 wt% SiO_2 content.

Figure 6. Photos taken at Krasta enrichment plant. (a) Spirals. (b) Shaking tables. (c) Stock of chromite concentrate sand.

6.5 Chromite ore chemical parameters for different markets

Chromite is commercially used in three different market types, which require strict chemical and technical parameters (as shown in the Table 1). The refractory market is very limited due to the high chromite purity (SiO_2 < 2.5 wt%) and therefore chromite sand assumes a high economic value. Nowadays the only country that produces chromite for refractories is South Africa thanks to its several stratiform chromite deposits with low SiO_2 content.

In this work, we focus on the possibility to reduce SiO_2 content of Krasta chromite concentrate sand performing tests by means of an innovative beneficiation technique.

Table 1. Chemical and technical chromite parameters for three different market types. AFS-GFN =grain fineness number.

Market type	Cr_2O_3 (wt%)	SiO_2 (wt%)	Ratio Cr/Fe	AFS-GFN	Melting point
Special steels	> 46	< 6	> 2	40 - 60	/
Ferro-chromium alloys	42 - 46	< 15	1.5 - 2	/	/
Refractories	> 38	< 2.5	/	40 - 60	> 2180 °C

6.6 An innovative beneficiation technique (DM + IFS)

In order to meet the very demanding chemical parameter requirements for refractory market chromite first concentrate sand, purified from fraction +1 mm and -150 μm grain sizes due to proper machineries working, was re-enriched using a combination of dry magnetic and gravity separation at the pilot plant of Omega Foundry Machinery LTD. in Peterborough (UK).

Re-enrichment was carried out using a Drum Magnet (DM) that works with a field intensity of 10,000 gauss (Figure 7a). New concentrate was then processed by means of an Inclined Fluidised Separator (IFS) that works in dry conditions using an air cushion as fluidization agent (Figure 7b).). IFS was designed for re-cycling of foundry sands and has not been applied yet to mine concentrates. Its high performance is due to the use of an air cushion as fluidizing agent that enhances the specific weight contrast between the grains in the sand.

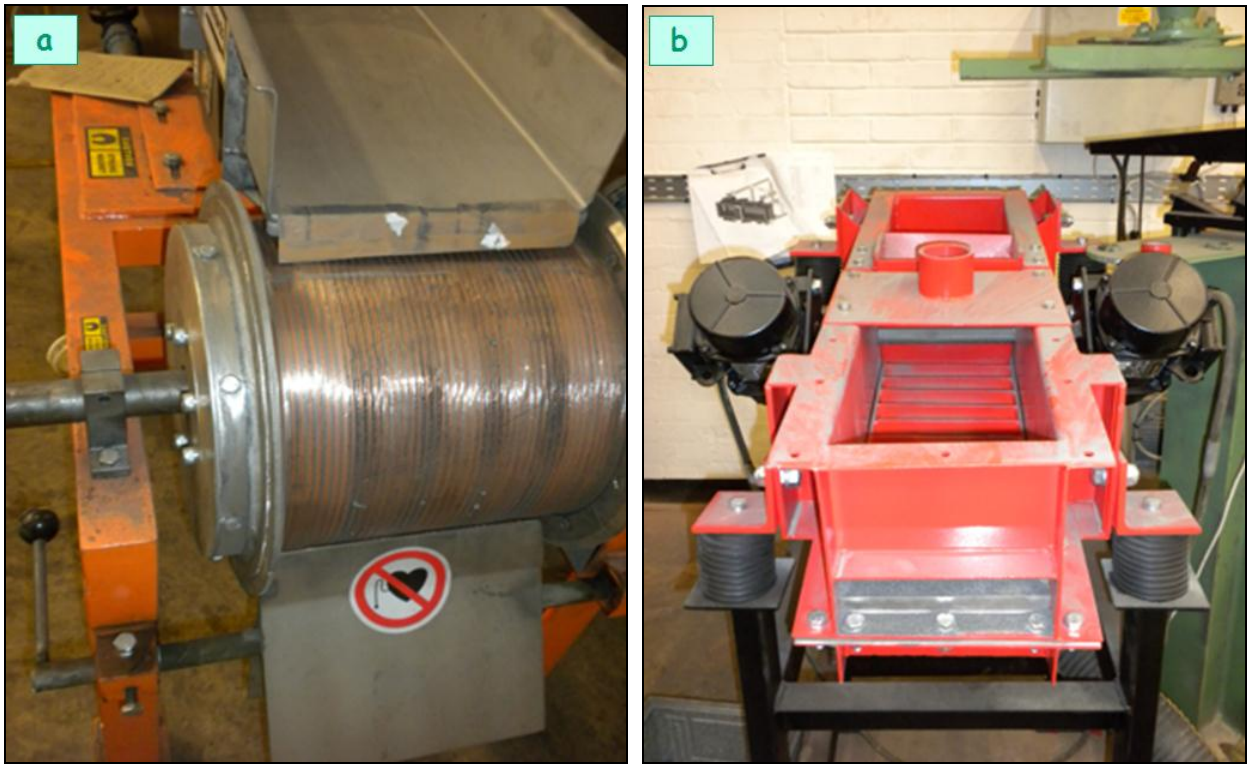

Figure 7. Photos taken at the pilot plant in Peterborough (UK). (a) Drum magnet (DM). (b) Inclined fluidised separator (IFS).

6.7 Enrichment test results: XRF analysis, grain size (AFS-GFN) and XRD analysis

At pilot plant in Peterborough (UK) a three steps enrichment test was performed:

- DM first step: Krasta feed was enriched using Drum Magnet and a concentrate (C DM) and a waste (W DM) were obtained;
- IFS second step: concentrate (C DM) was re-enriched using Inclined Fluidised Separator and a concentrate (C1 IFS) and a waste (W1 IFS) were obtained;
- IFS third step: waste (W1 IFS) was re-runned into Inclined Fluidised Separator and a concentrate (C2 IFS) and a waste (W2 IFS) were obtained.

XRF and grain size analysis, with grain finesse number (AFS-GFN) calculation, were carried out on each product achieved from enrichment test (as shown in Table 2).

The AFS Grain Fineness Number (AFS-GFN) is one means of measuring the grain fineness of a sand. GFN is a measure of the average size of the particles (or grains) in a sand sample. AFS-GFN gives the metal casting facility a means to verify its molding sand.

The grain fineness of sand is measured using a test called sieve analysis, which is performed as follows:

1. A representative sample of the sand is dried and weighed, then passed through a series of progressively finer sieves (screens) while they are agitated and tapped for a 15 minute test cycle.

2. The sand retained on each sieve (grains that are too large to pass through) is then weighed and recorded.

3. The weight retained on each sieve is divided by the total sample weight to arrive at the percent retained on each screen.

4. The percentage of sand retained is then multiplied by a factor, or multiplier, for each particular screen. (Table 1). The factors reflect the fact that the sand retained on a particular sieve (e.g. 50 mesh) is not all 50 mesh in size, but rather smaller than 40 mesh (i.e. it passed through a 40 mesh screen) and larger than 50 mesh (it won't pass through 50 mesh screen).

5. The individual screen values then are added together to get the AFS-GFN of the sand, representing an average grain fineness.

Table 2. XRF analyses (wt%) of chromite enrichment test at Peterborough pilot plant and grain fineness number (AFS-GFN) of each product.

SAMPLES	FEED	C DM	W DM	C1 IFS	W1 IFS	C2 IFS	W2 IFS
Cr_2O_3	51.33	55.40	38.35	60.01	44.33	58.72	23.30
SiO_2	7.47	5.39	14.92	2.43	11.75	3.00	25.54
Al_2O_3	7.21	7.49	5.62	7.96	5.44	7.47	3.36
CaO	0.07	0.04	0.15	0.03	0.07	0.03	0.23
Fe_2O_3	14.08	14.95	10.63	15.61	12.32	14.01	7.31
K_2O	0.00	0.00	0.00	0.00	0.00	0.00	0.00
MnO	0.16	0.17	0.13	0.17	0.16	0.16	0.11
MgO	19.22	17.14	25.91	14.38	22.81	14.91	34.78
Na_2O	0.22	0.23	0.16	0.26	0.17	0.23	0.06
P_2O_5	0.02	0.02	0.01	0.02	0.02	0.02	0.01
TiO_2	0.10	0.11	0.08	0.11	0.09	0.11	0.05
LOI	0.12	/	4.04	/	2.84	1.34	5.26
Total	100.00	100.94	100.00	100.98	100.00	100.00	100.00
RATIO Cr/Fe	3.57	3.62	3.53	3.76	3.52	4.10	3.12
AFS-GFN	66	56	78	42	83	41	88

These results highlight that C1 IFS is the best chromite concentrate obtained thanks to the first and second steps of the enrichment test, and it reaches chemical and technical parameters for refractory market (as shown in Figure 8 by blue triangle falling in R field) having Cr_2O_3 content of 60.01 wt%, SiO_2 content of 2.43 wt% and AFS-GFN of 42.

It is worth to notice that both C1 IFS and C2 IFS have a higher AFS-GFN than the feed. The increase in grain size of concentrate relative to feed is the opposite of what happens in shaking tables and is attained by the Inclined Fluidised Separator (IFS) thanks to its air cushion that favors flotation and hence discharge of finer grains. As usually concentrates from chromite beneficiation plants, like that of Krasta plant, are too fine for refractory market this property of IFS is pivotal for its use in production of refractory sands.

It is also important to observe that also some other enrichment test products can be commercialized.

As a matter of fact concentrate C DM, extracted from drum magnet first step enrichment, falls inside special steels market field (pink triangle falling in SS field, Figure 8) and has a suitable AFS-GFN (56). On the other hand concentrate C2 IFS, obtained from inclined fluidised separator third step enrichment, can certainly be used for special steel market and perhaps it can also be used for refractory market even if SiO_2 content is 3.00 wt% (yellow triangle in Figure 8).

Finally even the waste product of inclined fluidised separator second step enrichment test (W1 IFS) can be used for ferro-chromium alloy market (blue circle falling in A field, Figure 8), although it has a high AFS-GFN of 83, which anyway is not an important parameter for this kind of product.

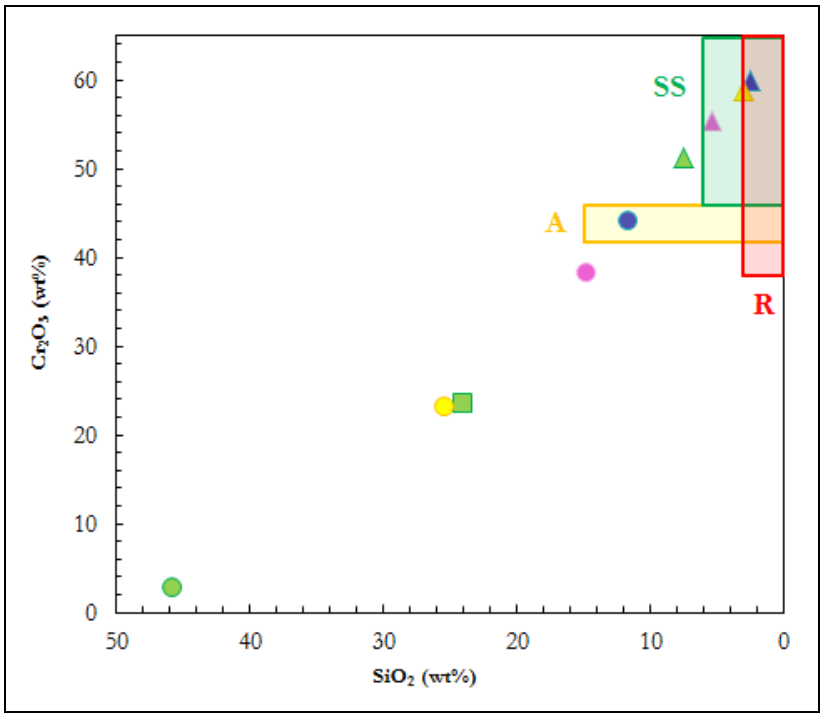

Figure 8. Krasta chromite ore enrichment: products at Krasta plant (green symbols), DM first step (pink symbols), IFS second step (blue symbols) and IFS third step (yellow symbols) at Peterborough pilot plant.
Square = feed, triangles = concentrates and circles = wastes. Green triangle is the feed of pink triangle, which is the feed of blue triangle, while blue circle is the feed of yellow triangle. Colored rectangles show the compositional fields of commercial chromite. A = ferro-chromium alloys, R = refractories and SS = special steels.

X-ray powder diffractometer (XRD) analyses were carried out on feed and on six different products obtained by three steps enrichment test in order to understand the mineralogical phases (chromite, olivine and serpentine) distribution into concentrates and wastes after magnetic and gravity enrichment.

Results show that drum magnet (DM) first step enrichment reports olivine to the waste (W DM) and chromite and serpentine to the concentrate (C DM) (as shown in compared XRD patterns, Figure 9a), due to different magnetic susceptibility of mineralogical phases.

Instead chromite is separated from serpentine during inclined fluidised separator (IFS) second step enrichment because of its different density. In fact concentrate (C1 IFS) XRD pattern shows only chromite peaks while waste (W1 IFS) XRD pattern has a high intensity serpentine peak (Figure 9b).

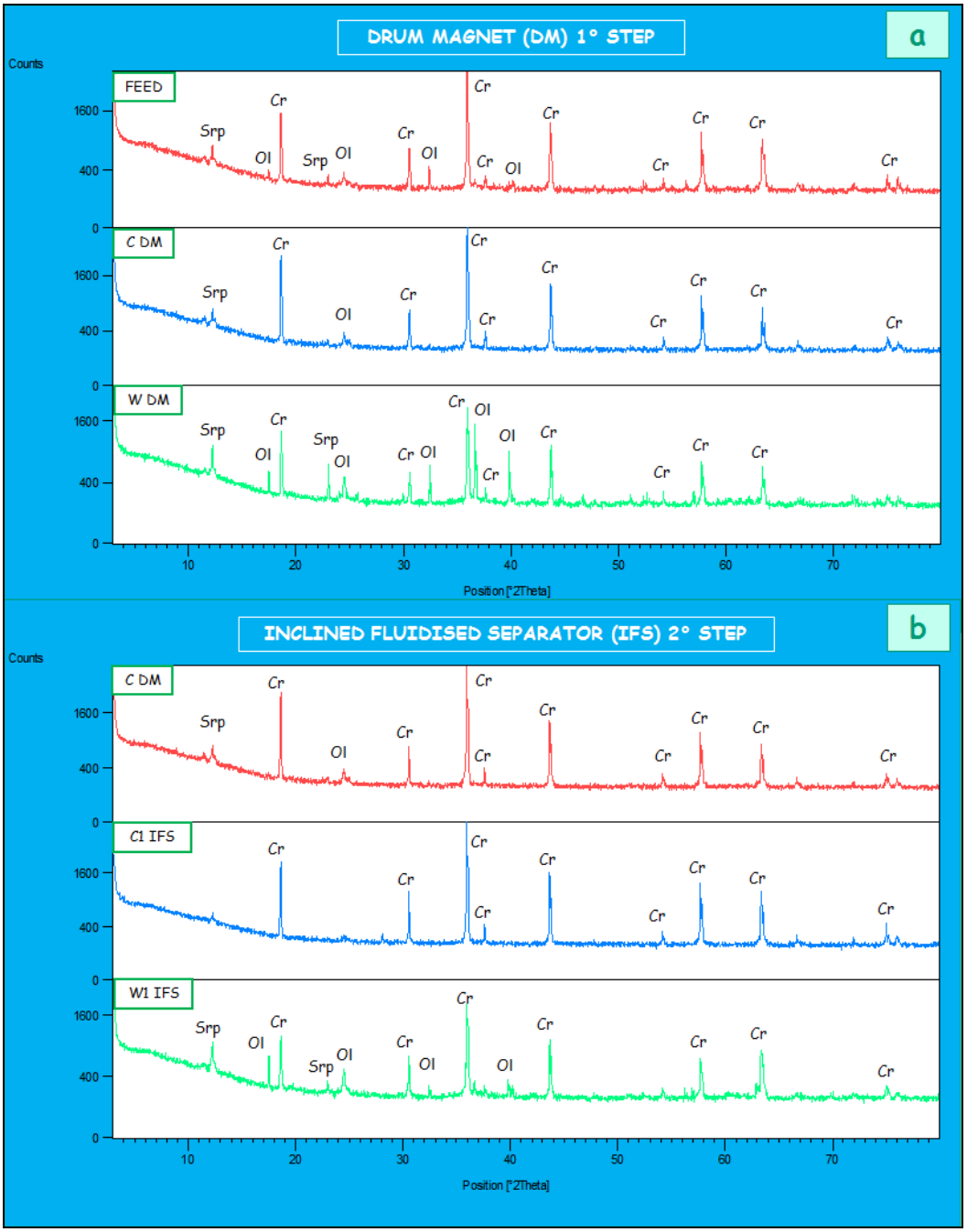

Figure 9. Comparison between XRD patterns of different enrichment test products.

6.8 Separation Efficiency (SE) and SiO_2 recovery

At Peterborough (UK) Separation Efficiency (SE) was calculated for three steps enrichment test and total pilot plant using the equation described in Chapter 2 and in Chapter 5.

$$SE = \frac{100Cm(c-f)}{(m-f)f}$$

where C is the fraction of the total feed weight that reports to the waste, m is the wt% SiO_2 content of the gangue minerals, c is the SiO_2 wt% of the waste and f is the SiO_2 wt% of the feed.

Separation efficiency was calculated using SiO_2 content as values of m, c and f, instead Cr_2O_3 content like in the previous chapters, because in this case the beneficiation aim is the chromite purification (decreasing SiO_2) and is not the chromite enrichment (increasing Cr_2O_3).

Parameters for calculation of separation efficiency (SE) are shown in Table 3, where recovery values (C) refer for each step to its specific feed.

Table 3. . Separation Efficiency (SE) results of three steps chromite enrichment test and total plant SE.

Parameters	DM 1°step	IFS 2°step	IFS 3°step	Total
C	0.28	0.35	0.59	0.53
m (wt%)	40.09	40.09	40.09	40.09
c (wt%)	14.92	11.75	25.54	13.16
f (wt%)	7.47	5.39	14.92	7.47
SE (%)	34.3	47.7	66.9	49.8

SiO_2 recovery is the fraction of silica in the feed that reports to the waste, while total SiO_2 recovery is the fraction of the total feed weight that reports to the waste and provides information on the amount of silica that can be removed from feed chromite sand (Table 4).

The SiO_2 recovery increases during each step of enrichment test and it reaches the remarkable value of 92.5 wt% in the inclined fluidised separator (IFS) third step, as shown in Figure 10.

The best product is C1 IFS because further purification in the third step is attained at the expenses of a decrease in the recovery of concentrate as total recovery after each step is the product of the recoveries of all step performed.

Purification processes like that performed in this test are characterized by low SE values due to the necessity to maintain high total recoveries. Separation efficiency for the Peterborough pilot plant of 49.8 % can be considered very good for a product that has already undergone an intensive enrichment treatment like that performed at Krasta plant.

IFS second step provides a high quality concentrate for refractory market at a relatively high cumulate recovery of 46.8 wt% (Table 4). Moreover W1 IFS at a cumulate recovery of 25.2 wt% is a product that can be used for the iron-chromium alloy market and only 28 wt% of the feed is discharged.

IFS third step adds, with C2 IFS, 10.3 wt% more product that could be useful for the refractory market while W2 IFS is added to the discharge. In total performing all three steps we can get a 57.1 wt% of excellent concentrate for refractory market and 42.9 wt% discharge. An economic analysis of costs and market values can discriminate between this option and the alternative option of performing only first and second steps.

Table 4. Total recovery of concentrate (C) and waste (W) products and SiO_2 recovery results.

Test type	Samples	Partial recovery (wt%)	Cumulate total recovery after 2° step (wt%)	Cumulate total recovery after 3° step (wt%)	SiO_2 recovery (wt%)
DM 1° STEP	C DM	72	/	/	51.8
	W DM	28	28.0	28.0	
IFS 2° STEP	C1 IFS	65	46.8	46.8	72.3
	W1 IFS	35	25.2	/	
IFS 3° STEP	C2 IFS	41	/	10.3	92.5
	W2 IFS	59	/	14.9	
TOTAL TEST	CONC	57	/	/	83.2
	WASTE	43	/	/	

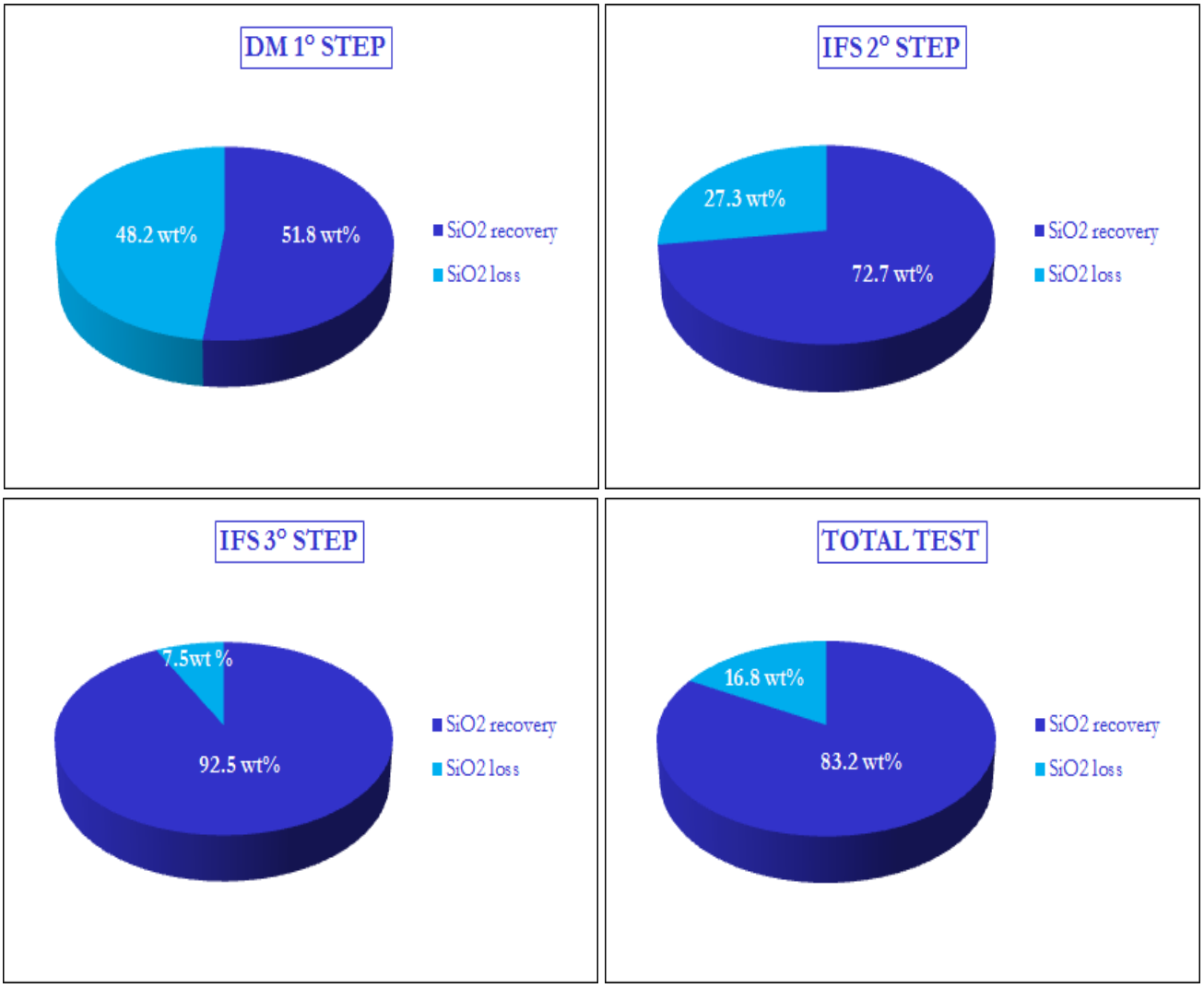

Figure 10. Graphs showing SiO_2 recovery results of three steps enrichment test and total plant SiO_2 recovery.

6.9 Conclusions

Refractory chromite sand chemical and technical requirements are very demanding and no chromite ore can attain them by simple crushing. On the other hand usual enrichment methodologies either cannot meet the required parameters or have a very low refractory sand recovery.

The combination of Drum Magnet (DM) and Inclined Fluidised Separator (IFS) in the Omega Foundry Machinery LTD. pilot plant not only produces a good quality refractory sand, but the result is reached with an high recovery, making of this plant an optimal solution for the production of refractory chromite sand.

The Inclined Fluidised Separator is particularly performing as it combines a very high recovery of silica in the waste with an increase of the grain size of concentrate.

Albanian chromite ore is suitable for production of refractory sand with the new beneficiation technique and it has two more minor benefits: the high olivine/serpentine ratio in the gangue and the high Cr_2O_3 content of chromite.

The high Cr_2O_3 content of Albanian ore chromite allows also the use of part of the wastes produced for the iron-chromium alloys and the special steels industries.

Appendix I - Chapter 3

Table 3. Representative EMP analyses of chromite.

	Andriamena					North Befandriana					North Toamasina				
Sample	**1**	**2**	**3**	**4**	**5**	**1**	**2**	**3**	**4**	**5**	**1**	**2**	**3**	**4**	**5**
TiO_2	0.05	0.15	0.13	0.10	0.09	0.20	0.18	0.15	0.21	0.16	0.54	0.50	0.53	0.43	0.46
Al_2O_3	21.83	16.91	16.89	19.37	18.09	13.12	10.21	12.78	13.16	9.80	11.93	11.68	14.93	14.06	14.68
Cr_2O_3	46.01	49.84	50.20	47.20	48.03	58.50	62.04	53.01	57.44	61.43	43.38	43.75	39.37	45.95	45.41
Fe_2O_3	4.11	4.79	4.86	3.45	4.02	0.00	0.00	2.39	2.33	1.97	13.94	13.87	14.61	8.39	8.41
FeO	13.98	16.66	16.93	22.82	22.71	15.47	15.13	16.59	13.53	14.91	21.76	22.12	21.50	22.00	21.76
MnO	0.04	0.10	0.12	0.23	0.19	0.05	0.09	0.23	0.14	0.09	0.42	0.38	0.37	0.50	0.42
NiO	0.16	0.11	0.03	0.06	0.05	0.09	0.11	0.08	0.12	0.16	0.11	0.05	0.12	0.09	0.10
MgO	13.97	11.80	11.77	8.18	8.12	11.39	11.43	10.39	13.50	12.32	7.78	7.57	8.23	7.62	7.94
Total	**100.14**	**100.36**	**100.92**	**101.42**	**101.30**	**98.82**	**99.19**	**95.62**	**100.44**	**100.84**	**99.86**	**99.93**	**99.66**	**99.04**	**99.19**
Ti	0.00	0.00	0.00	0.00	0.00	0.00	0.00	0.00	0.01	0.00	0.01	0.01	0.01	0.01	0.01
Al	0.79	0.63	0.63	0.73	0.68	0.50	0.40	0.51	0.49	0.37	0.47	0.46	0.58	0.55	0.57
Cr	1.11	1.25	1.25	1.19	1.22	1.51	1.62	1.42	1.44	1.57	1.15	1.16	1.03	1.21	1.19
Fe^{3+}	0.09	0.11	0.12	0.08	0.10	0.00	0.00	0.06	0.06	0.05	0.35	0.35	0.36	0.21	0.21
Fe^{2+}	0.36	0.44	0.45	0.61	0.61	0.42	0.42	0.47	0.36	0.40	0.61	0.62	0.59	0.61	0.60
Mn	0.00	0.00	0.00	0.01	0.01	0.00	0.00	0.01	0.00	0.00	0.01	0.01	0.01	0.01	0.01
Ni	0.00	0.00	0.00	0.00	0.00	0.00	0.00	0.00	0.00	0.00	0.00	0.00	0.00	0.00	0.00
Mg	0.64	0.56	0.55	0.39	0.39	0.55	0.56	0.52	0.64	0.59	0.39	0.38	0.41	0.38	0.39
Cr/(Cr+Al)	0.59	0.66	0.67	0.62	0.64	0.75	0.80	0.74	0.75	0.81	1.20	1.20	1.07	1.47	1.46
$Fe^2/(Fe^2+Mg)$	0.36	0.44	0.45	0.61	0.61	0.43	0.43	0.47	0.36	0.40	0.71	0.72	0.64	0.69	0.67
$Mg/Mg+Fe^2$	0.64	0.56	0.55	0.39	0.39	0.57	0.57	0.53	0.64	0.60	0.61	0.62	0.59	0.62	0.61

Table 5. Continued

	North Belobaka					Antanimbary					
Sample	**1**	**2**	**3**	**4**	**5**	**1**	**2**	**3**	**4**	**5**	**6**
TiO_2	0.53	0.41	0.48	0.55	0.63	1.06	0.35	0.69	0.59	1.27	0.47
Al_2O_3	12.01	16.89	15.32	13.74	12.71	3.39	16.40	6.78	11.48	13.93	11.91
Cr_2O_3	46.13	38.01	45.34	46.68	47.23	33.73	41.23	38.09	43.46	35.59	42.99
Fe_2O_3	9.45	11.27	6.95	7.49	7.81	29.67	7.58	21.72	10.88	14.64	11.92
FeO	27.04	28.36	25.50	25.40	25.40	29.60	32.08	30.01	30.98	31.60	31.63
MnO	0.19	0.36	0.17	0.20	0.20	0.40	0.35	0.93	0.50	0.73	0.53
MgO	4.46	3.87	5.93	5.85	5.80	2.04	1.51	1.55	1.66	1.72	1.49
Total	**99.86**	**99.23**	**99.71**	**99.99**	**99.80**	**99.93**	**99.67**	**99.82**	**99.59**	**99.54**	**100.99**
Ti	0.01	0.01	0.01	0.01	0.02	0.03	0.01	0.02	0.02	0.03	0.01
Al	0.48	0.67	0.60	0.54	0.51	0.15	0.66	0.29	0.48	0.57	0.49
Cr	1.25	1.02	1.20	1.24	1.26	0.98	1.12	1.09	1.21	0.98	1.18
Fe^{3+}	0.24	0.29	0.17	0.19	0.20	0.82	0.20	0.59	0.29	0.38	0.31
Fe^{2+}	0.77	0.80	0.71	0.71	0.72	0.91	0.92	0.90	0.91	0.92	0.92
Mn	0.01	0.01	0.00	0.01	0.01	0.01	0.01	0.03	0.01	0.02	0.02
Mg	0.23	0.20	0.30	0.29	0.29	0.11	0.08	0.08	0.09	0.09	0.08
Cr/(Cr+Al)	0.72	0.60	0.67	0.70	0.71	0.87	0.63	0.79	0.72	0.63	0.71
$Fe^2/(Fe^2+Mg)$	0.77	0.80	0.71	0.71	0.71	0.89	0.92	0.92	0.91	0.91	0.92
$Mg/Mg+Fe^2$	0.23	0.20	0.29	0.29	0.29	0.11	0.08	0.08	0.09	0.09	0.08

Table 6. Representative EMP analyses of orthopyroxenes.

	Andriamena					North Befandriana					North Toamasina			
Sample	**1**	**2**	**3**	**4**	**5**	**1**	**2**	**3**	**4**	**5**	**1**	**2**	**3**	**4**
SiO_2	58.39	58.76	57.92	57.25	57.36	58.76	58.85	58.81	56.45	56.13	57.46	56.97	57.81	56.94
TiO_2	0.02	0.03	0.10	0.07	0.07	0.06	0.08	0.02	0.04	0.08	0.12	0.07	0.10	0.10
Al_2O_3	0.71	0.76	1.02	1.05	1.28	0.23	0.28	0.27	0.70	0.42	0.94	1.23	0.95	0.84
Cr_2O_3	0.35	0.25	0.43	0.50	0.48	1.40	1.53	1.29	3.54	1.85	0.39	0.38	0.33	0.51
Fe_2O_3	0.56	0.34	0.00	0.00	0.39	0.00	0.00	0.00	0.00	0.00	0.00	0.42	0.71	0.39
FeO	2.61	2.91	2.89	3.06	2.74	2.48	2.40	2.63	2.83	2.48	5.49	5.00	4.70	5.03
MnO	0.06	0.10	0.10	0.07	0.11	0.09	0.05	0.10	0.10	0.08	0.23	0.26	0.33	0.23
NiO	0.10	0.14	0.12	0.12	0.08	0.11	0.12	0.12	0.10	0.12	0.11	0.10	0.05	0.06
MgO	37.46	37.24	36.76	36.73	36.17	38.29	37.51	37.88	37.51	36.41	35.79	35.44	35.67	35.51
CaO	0.12	0.18	0.26	0.27	0.34	0.07	0.07	0.14	0.07	0.06	0.17	0.17	0.15	0.15
Total	**100.40**	**100.71**	**99.60**	**99.13**	**99.04**	**101.51**	**100.88**	**101.28**	**101.37**	**97.63**	**100.70**	**100.04**	**100.80**	**99.77**
Si	1.98	1.98	1.97	1.96	1.97	1.97	1.98	1.97	1.91	1.96	1.96	1.96	1.97	1.96
Ti	0.00	0.00	0.00	0.00	0.00	0.00	0.00	0.00	0.00	0.00	0.00	0.00	0.00	0.00
Al	0.03	0.03	0.04	0.04	0.05	0.01	0.01	0.01	0.03	0.02	0.04	0.05	0.04	0.03
Cr	0.01	0.01	0.01	0.01	0.01	0.04	0.04	0.03	0.09	0.05	0.01	0.01	0.01	0.01
Fe^{3+}	0.01	0.01	0.00	0.00	0.01	0.00	0.00	0.00	0.00	0.00	0.00	0.01	0.02	0.01
Fe^{2+}	0.07	0.08	0.08	0.09	0.08	0.07	0.07	0.07	0.08	0.07	0.16	0.14	0.13	0.15
Mn	0.00	0.00	0.00	0.00	0.00	0.00	0.00	0.00	0.00	0.00	0.01	0.01	0.01	0.01
Ni	0.00	0.00	0.00	0.00	0.00	0.00	0.00	0.00	0.00	0.00	0.00	0.00	0.00	0.00
Mg	1.89	1.87	1.87	1.88	1.85	1.91	1.88	1.90	1.90	1.89	1.82	1.82	1.81	1.83
Ca	0.00	0.01	0.01	0.01	0.01	0.00	0.00	0.00	0.00	0.00	0.01	0.01	0.01	0.01
$Mg/(Mg+Fe^{2+})$	0.96	0.96	0.96	0.96	0.96	0.96	0.97	0.96	0.96	0.96	0.92	0.93	0.93	0.93

Table 4. Continued.

	North Belobaka					Antanimbary				
Sample	**1**	**2**	**3**	**4**	**5**	**1**	**2**	**3**	**4**	**5**
SiO_2	55.76	55.44	56.13	55.7	55.36	56.11	56.73	56.41	56.28	56.51
TiO_2	0.03	0.04	0.01	0.04	0.10	0.09	0.04	0.00	0.06	0.00
Al_2O_3	0.26	0.52	0.41	0.45	0.94	1.12	0.51	0.98	0.31	0.84
Cr_2O_3	0.08	0.09	0.16	0.1	0.46	0.28	0.09	0.17	0.37	0.13
Fe_2O_3	1.84	1.54	1.82	1.51	1.02	0.00	0.00	0.00	0.00	0.00
FeO	8.08	9.93	7.72	8.5	9.39	16.41	15.79	15.86	16.99	15.31
MnO	0.19	0.23	0.23	0.23	0.22	0.43	0.49	0.38	0.51	0.40
MgO	32.66	31.37	32.83	32.3	31.65	22.62	23.53	23.07	22.59	23.97
CaO	0.15	0.13	0.41	0.19	0.21	0.50	0.69	1.01	0.66	0.48
Na_2O	0.00	0.00	0.00	0.00	0.00	0.13	0.02	0.06	0.00	0.04
Total	**99.05**	**99.3**	**99.74**	**99.04**	**99.34**	**97.69**	**97.89**	**97.95**	**97.78**	**97.68**
Si	1.97	1.97	1.97	1.97	1.96	2.11	2.12	2.11	2.12	2.11
Ti	0.00	0.00	0.00	0.00	0.00	0.00	0.00	0.00	0.00	0.00
Al	0.01	0.02	0.02	0.02	0.04	0.05	0.02	0.04	0.01	0.04
Cr	0.00	0.00	0.00	0.00	0.01	0.01	0.00	0.01	0.01	0.00
Fe^{3+}	0.05	0.04	0.05	0.04	0.03	0.00	0.00	0.00	0.00	0.00
Fe^{2+}	0.24	0.29	0.23	0.25	0.28	0.52	0.49	0.50	0.54	0.48
Mn	0.01	0.01	0.01	0.01	0.01	0.01	0.02	0.01	0.02	0.01
Mg	1.72	1.66	1.71	1.70	1.67	1.27	1.31	1.29	1.27	1.33
Ca	0.01	0.00	0.02	0.01	0.01	0.02	0.03	0.04	0.03	0.02
Na	0.00	0.00	0.00	0.00	0.00	0.01	0.00	0.00	0.00	0.00
$Mg/(Mg+Fe^{2+})$	0.88	0.85	0.88	0.87	0.86	0.71	0.73	0.72	0.70	0.74

Appendix II - Chapter 5

Table 5. Representative EMP analyses of Bemanevika chromites.

Sample	1	2	3	4	5	6	7	8	9	10	11	12	13	Average
SiO_2	0.03	0.00	0.00	0.01	0.02	0.00	0.00	0.00	0.01	0.00	0.00	0.02	0.00	0.01
TiO_2	0.12	0.19	0.10	0.17	0.13	0.15	0.13	0.15	0.18	0.17	0.17	0.13	0.11	0.15
Al_2O_3	16.43	16.74	15.36	16.76	17.22	16.49	15.62	14.61	17.54	18.19	15.07	17.43	17.75	16.55
Cr_2O_3	52.83	53.64	53.16	54.01	52.93	52.73	53.96	53.83	51.76	52.12	53.08	53.71	51.69	**53.03**
Fe_2O_3	3.40	2.32	4.08	1.76	3.21	2.41	3.16	3.19	2.76	2.49	4.69	2.11	3.21	2.98
FeO	15.82	14.43	15.91	14.41	13.92	18.31	13.93	18.15	14.44	14.32	13.77	13.67	14.53	15.05
MnO	0.10	0.04	0.14	0.00	0.00	0.12	0.11	0.14	0.18	0.11	0.09	0.02	0.15	0.09
MgO	12.57	13.50	12.29	13.43	13.93	10.92	13.41	10.75	13.35	13.72	13.55	14.14	13.41	13.00
CaO	0.00	0.00	0.01	0.00	0.01	0.00	0.00	0.00	0.00	0.00	0.00	0.01	0.00	0.00
Na_2O	0.00	0.00	0.00	0.02	0.02	0.00	0.04	0.00	0.00	0.00	0.02	0.00	0.00	0.01
K_2O	0.01	0.00	0.00	0.00	0.00	0.00	0.00	0.00	0.00	0.00	0.00	0.00	0.00	0.00
Total	**101.31**	**100.86**	**101.05**	**100.58**	**101.39**	**101.13**	**100.36**	**100.82**	**100.22**	**101.12**	**100.44**	**101.24**	**100.85**	**100.87**
Si	0.00	0.00	0.00	0.00	0.00	0.00	0.00	0.00	0.00	0.00	0.00	0.00	0.00	0.00
Ti	0.00	0.00	0.00	0.00	0.00	0.00	0.00	0.00	0.00	0.00	0.00	0.00	0.00	0.00
Al	0.61	0.61	0.57	0.62	0.63	0.62	0.58	0.55	0.65	0.66	0.56	0.63	0.65	0.61
Cr	1.31	1.32	1.33	1.33	1.29	1.32	1.34	1.36	1.28	1.27	1.32	1.31	1.27	1.31
Fe^{3+}	0.08	0.05	0.10	0.04	0.07	0.06	0.07	0.08	0.06	0.06	0.11	0.05	0.08	0.07
Fe^{2+}	0.41	0.38	0.42	0.38	0.36	0.49	0.37	0.49	0.38	0.37	0.36	0.35	0.38	0.39
Mn	0.00	0.00	0.00	0.00	0.00	0.00	0.00	0.00	0.00	0.00	0.00	0.00	0.00	0.00
Mg	0.59	0.63	0.58	0.63	0.64	0.52	0.63	0.51	0.62	0.63	0.64	0.65	0.62	0.61
Ca	0.00	0.00	0.00	0.00	0.00	0.00	0.00	0.00	0.00	0.00	0.00	0.00	0.00	0.00
Na	0.00	0.00	0.00	0.00	0.00	0.00	0.00	0.00	0.00	0.00	0.00	0.00	0.00	0.00
K	0.00	0.00	0.00	0.00	0.00	0.00	0.00	0.00	0.00	0.00	0.00	0.00	0.00	0.00

References

Agakayak, T., Zedef, V., Aydogan, S. (2007) *Beneficiation of low-grade chromite ores of abandoned mine at Topraktepe, Beysehir, SW Turkey*. Acta. Mont. Slovaca 12(4), 323–327.

Arai, S. & Yurimoto, H. (1994) *Podiform chromitites of the Tari-Misaka ultamafic complex, southwestern Japan, as mantle-melt interaction products*. Economic Geol. **89**, 1279-1288.

Arai, S., Shimizu, Y., Ismail, S.A., Ahmed, A.H. (2006) *Low-T formation of high-Cr spinel with apparently primary chemical characteristics within podiform chromitite from Rayat, northeastern Iraq*. Mineral. Mag. 70(5), 499–508.

Augé, T., Genna, A. &Legendre, O. (2005) *Primary platinum mineralisation in the Nizhny Tagil and Kachkanar ultramafic complexes, Urals, Russia: a genetic model for PGE concentration in chromite-rich zones*. Economic Geol. 100, 707-732.

Austin, L.G. and Luckie, P.T. (1988) *Problems of quantifying mineral liberation*: A review, Particle & Particle Systems Characterisation, 5(3), Sep., 122-129.

Barbery, G. (1991) *Mineral liberation*. Les Edition GB, Quebec.

Barnes, S.J. (2000) *Chromite in Komatiites, II Modification during Greenschist to Mid-Amphibolite facies metamorphism*. J. Petrol. 41, 387–409.

Barnes, S.J. & Roeder, P.L. (2001) *The range of spinel composition in terrestrial mafic and ultramafic rocks*. J. Petrol., 42(12), 2279-2302.

Baum, W., Lotter, N.O., and Whittaker, P.J. (2004) *Process mineralogy - A new generation for ore characterization and plant optimization*. 2003 SME Annual Meeting (Feb.), Denver, Preprint 04-12.

Beccaluva, L., Coltorti, M., Premti, I., Saccani, E., Siena, F., Zeda, O. (1994) *Mid-ocean ridge and suprasubduction affinities in the ophiolitic belts of Albania***.** Ofioliti 19, 77–96.

Beccaluva, L., Coltorti, M., Ferrini, V., Saccani, E., Siena, F., Zeda, O. (1998) *Petrological modeling of Albanian Ophiolites with particular regard to the Bulqiza chromite ore deposits*. Periodico di Mineralogia 67, 7–23.

Beqiraj, A., Masi, U., Violo, M. (2000) *Geochemical characterization of podiform chromite ores from the ultramafic massif of Bulqiza (Eastern Ophiolitic Belt, Albania) and hints for exploration.* Exploration and Mining Geology 9, 149–156.

Bésairie, H. (1966) *Gites Minéraux de Madagascar. Annales Géologiques de Madagascar*. Volume 2, Fascicule 34, 117-127.

Bésairie, H. (1970) *Déscription géologique du massif ancien de Madagascar. Dèuxieme volume: la region cotière orientale entre le Mangoro et Vangaindrano*. Documentation du Bureau Geologique. Service Geologique de Madagascar, Tananarive, 67 pp.

Bésairie, H. (1971) *Carte géologique à 1/2000000 et notice explicative*. Docum. Bur. Geol. Madagascar, No. 184.

Blott, S.J & Pye, K. (2001) *Gradistat: a grain size distribution and statistics package for the analysis of unconsolidated sediments. Earth Surf. Process. Landforms 26, 1237–1248*.

Boccaletti, M., Manetti, P., Peccerillo, A. (1974) *The Balkandis a san instance of back arc thrust belt: possible relation to Hellenides*. Geol. Soc. Am. Bull. 85, 1077–1084.

Bonavia, F.F., Diella V., Ferrario, A. (1993) *Precambrian podiform chromitites from Kenticha Hill, Southern Ethiopia.* Econ. Geol., 88, 198-202.

Bonsu, A.K. (1983) *Influence of pulp density and particle size on spiral concentration efficiency*. M.Phil. Thesis, Camborne School of Mines.

Bortolotti, V., Kodra, A., Marroni, M., Mustafa, F., Pandolfi, L., Principi, G., Saccani, E., (1996) *Geology and Petrology of ophiolitic sequences in the Mirdita region. (Northern Albania).* Ofioliti 21, 3–20.

BSG–USGS–GLW (2008) *Republique de Madagascar Ministre de L'energie et des Mines*. British Geological Survey, Research Report, 78, 1049 pp.

Burt, R.O. (1985*)* *Gravity Concentration Technology*. Elsevier, Amsterdam.

Cawthorn, R.G. (2005b) *Pressure fluctuations and the formation of the PGE-rich Merensky and chromitite reefs, Bushveld Complex*. Miner. Deposita, 40, 231-235.

Cazzaniga, A. (2009) *Studio della mineralizzazione a Cr-PGE del giacimento di Ranomena (Tamatave, Madagascar)*. In italian, Master Thesis, 194 pp.

Ceuleener, G. & Nicolas, A. (1985) *Structures in podiform chromite from the Maqsad district (Sumail ophiolite, Oman)*. Miner. Deposita 20, 177-184.

Ceuleener, G., Monnereau, M. & Amri, I. (1996) *Thermal structure of a fossil mantle diaper inferred from the distribution of mafic cumulates*. Nature 379, 149-153.

Christofides, G., Thimiatis, G., Koroneos, A., Sklavounos, S., Eleftheriadis, G. (1994) *Mineralogy and chemistry of Cr-chlorites associated with chromites from Vavdos and Vasilika complexes (Chalkidiki, Macedonia, N. Greece)*. Chem. Erde 54, 151–166.

Collins, A.S. (2000) *The tectonic evolution of Madagascar: its place in the East African Orogen*. Gondwana Research (Gondwana Newsletter Section), 3(4), 549-552.

Collins, A.S. (2006) *Madagascar and the amalgamation of Central Gondwana.* Gondwana Research, 9, 3-16.

Collins, A.S., Kröner, A., Fitzsimons, I.C.W., Razakamanana, T. (2003) *Detrital footprint of the Mozambique ocean: U–Pb SHRIMP and Pb evaporation zircon geochronology of metasedimentary gneisses in eastern Madagascar*. Tectonophysics 375, 77–99.

Collins, A.S. & Pisarevsky, A.S. (2005) *Amalgamating eastern Gondwana: the evolutions of the circum-Indian orogens*. Earth-Science Reviews, 71, 229-270.

Collins, A.S., Windley, B.F. (2002) *The tectonic evolution of central and northern Madagascar and its place in the final assembly of Gondwana.* J. Geol., 110, 325–339.

Dahlin D.C., Brown L.L., Kinney J.J. (1983) *Podiform chromite occurrences in the Caribou Mountain and lower Kanuti River areas, Central Alaska*. Bureau of Mines Information Circula 8916, United States Department of the Interior, 1983, p. 15.

De Waele, B., Horstwood, M.S.A., Pitfield, P.E.J., Thomas, R.J., Key, R.M., Rabarimana, M., Rafahatelo, J.-M., Ralison, V., Randriamananjara, T. (2009) *The architecture of the "Betsimisaraka Suture Zone": a record of oceanic arcs and associated metasedimentary successions between the "Indian" and "African" parts of Madagascar*. In: International

Conference on Island Arc, Continent Collisions, The Macquarie Arc Conference, Orange, Australia, April 2009. Orange, Australia, 56-57.

De Waele, B, Thomas, R, Macey, P. et al. (2011) *Provenance and tectonic significance of the Palaeoproterozoic metasedimentary successions of central and northern Madagascar*. Precambrian Research, 2011, 189, 1-2, 18-42.

Dilek, Y., Furnes, H. (2009) *Structure and geochemistry of Tethyan ophiolites and their petrogenesis in subduction rollback systems*. Lithos 113, 1–20.

Dilek, Y., Morishita, T. (2009) *Melt migration and upper mantle evolution during incipient arc construction: Jurassic Eastern Mirdita ophiolite, Albania*. Island Arc 19, 551–554.

Dilek, Y., Furnes, H., Shallo, M. (2008) *Geochemistry of the Jurassic Mirdita Ophiolite (Albania) and the MORB to SSZ evolution of a marginal basin oceanic crust*. Lithos 100, 174–209.

Ferrario, A. & Garuti, G. (1988) *Platinum group minerals in chromiterich horizons of the Niquelandia complex (Central Goias, Brazil)*. In: Prichard, H.M., Potts, P.J., Bowles, J.F.W., Cribb, S.J. (Eds.), Geo-platinum, vol. 87. Elsevier Applied Sciences, London, pp. 261–272.

Folk, R.L. & Ward, W.C. (1957). *Brazos River bar: a study in the significance of grain size parameters. Journal of Sedimentary Petrology 27: 3–26*.

Garuti, G., Proenza, J.A., Zaccarini, F. (2007) *Distribution and mineralogy of platinum-group elements in altered chromitites of the Campo Formoso layered intrusion (Bahia State, Brazil): control by magmatic and hydrothermal fluids*. Mineral. Petrol. 89, 159–188.

Gaudin, A.M. (1939) *Principles of Mineral Dressing*. McGraw-Hill, London.

Gay, S.L. (2004a) *A liberation model for comminution based on probability theory*. Minerals Engng., 17(4), Apr., 525-534.

Gay, S.L., (2004b) *Simple texture-based liberation modelling of ores*. Minerals Engng., 17(11-12), Nov/Dec., 1209-1216.

Gence, N. (1999) *Beneficiation of Elazig-Kefdag chromite by multi gravity separator*. Tr. J. of Engineering and Environmental Science, 23, 473-475.

Gilchrist, J.D. (1989) *Extraction Metallurgy*. 3rd edn, Pergamon Press, Oxford.

Gonzalez-Jimenez, A., Kerestedjian, T., Proenza, J.A., Gervilla, F. (2009) *Metamorphism on chromite ores from the Dobromirtsi ultramafic massif Rhodope mountains (SE Bulgaria)*. Geol. Acta 7(4), 413–430.

Gray, P.M.J. (1984) *Metallurgy of the complex sulphide ores*. Mining Mag. (Oct), 315.

Grieco, G., Diella, V., Chaplygina, N.L., Savelieva, G.N. (2007) *Platinum group elements zoning and mineralogy of chromitites from the cumulate sequence of the nurali massif (Southern urals, Russia)*. Ore Geol.Rev., 30, 2007, 257-276.

Grieco G., Merlini M. (2010) *Chromites from Vourinos complex mines and their alteration. Geologica Balcanica. In: XIX congress of Carpathian-Balkan Geological Association (CBGA)*. Abstracts, pp. 143–144.

Grieco G., Pedrotti M., Moroni M. (2011) *Metamorphic redistribution of Cr within chromitites and its influence on chromite ore gravity enrichment*. Minerals Engng., 24, 2, 102-107.

Grieco, G., Merlini, A., Cazzaniga, A. (2012) *The tectonic significance of PGM-bearing chromitites at the Ranomena mine, Toamasina chromite district, Madagascar*. Ore Geol. Rev., 44, 70-81.

Guerney, P.J., Laplante, A.R., and O'Leary, S. (2003) *Gravity recoverable gold and the Mineral Liberation Analyser.* Proc. 35th Annual Meeting of the Canadian Mineral Processors, CMP, CIMMP, Ontario (Jan.), 401-416.

Guney, A., Onal, G., Atmaca, T. (2001) *New aspect of chromite gravity tailings reprocessing.* Miner. Eng. 11, 1527–1530.

Hamada, M., Seto, S., Akasaka, M., Takasu, A. (2008) *Chromian pumpellyite and associated chromian minerals from Sangun metamorphic rocks, Osayama, southwest Japan.* J. Miner. Petrol. Sci. 103, 390–399.

Hausen, D.M. (1991) *The role of mineralogy in mineral beneficiation, in Evaluation and Optimization of Metallurgical Performance.* Ed. D. Malhotra et al., SME Inc., Chapter 17.

Hoxha, M., Boullier, A.M. (1995) *The peridotites of the Kukës ophiolite (Albania): structure and kinematics.* Tectonophysics 249, 217–231.

Hubbard, J.S., Humphreys, I.B. and Brown, E.W. (1953) *How Humphreys spiral concentrator is used in modem dressing practice.* Mining Worm (May).

Khalil, K.I. (2007) *Chromite mineralization in ultramafic rocks of the Wadi Ghadir area, Eastern Desert, Egypt: mineralogical, microchemical and genetic studies.* N. Jb. Miner. Abh. 183(3), 283–296.

King, R.P. (1982) *The prediction of mineral liberation from mineralogical textures.* XIVth International Mineral Process Congress, paper VII-1, CIM, Toronto, Canada.

Kinnaird, J.A., Kruger, F.J., Nex, P.A.M. & Cawthorn, R. (2002) *Chromitite formation – a key to understanding processes of platinum enrichment.* Trans. Instn. Min. Metall. B 111, 23-35.

Kimball, K.L. (1990) *Effects of hydrothermal alteration on the composition of chromian spinels.* Contrib. Mineral. Petrol. 105, 337–346.

Kröner, A., Hegner, E., Collins, A.S., Windley, B.F., Brewer, T.S., Razakamanana, T., Pidgeon, R.T. (2000) *Age and magmatic history of the Antananarivo Block, Central Madagascar, as derived from zircon geochronology and Nd isotopic systematics.* American J. Sci., 300, 251– 288.

Leblanc, M. & Nicolas, A. (1992) *Les chromitites ophiolitiques.* Chronique de la Recherche Minière, 507, 3–25.

Lyman, G.J. (1992) *Review of jigging principles and control.* Coal Preparation, 11(3-4), 145.

Malitch, K.N., Thalhammer, O.A.R., Knauf, V.V., Melcher, F. (2003) *Diversity of platinum-group mineral assemblages in banded and podiform chromitite from the Kraubath ultramafic massif, Austria: evidence for an ophiolitic transition zone?* Mineralium Deposita, 38, 282–297.

Mathez, E.A. & Mey, J.L. (2005) *Charachter of the UG2 chromitite and host rock and petrogenesis of its pegmatoidal footwall, Northeastern Bushveld Complex.* Econ. Geol., 100, 1617-1630.

Matveev, S. & Ballhaus, C. (2002) *Role of water in the origin of podiform chromitite deposits.* Earth Planet. Sci. Lett. 203, 235-243.

Mellini, M., Rumori, C., Viti, C. (2005) *Hydrothermally reset magmatic spinels in retrograde serpentinites, formation of "ferritchromit" rims and chlorite aureoles.* Contrib. Mineral. Petrol. 149, 266–275.

Merlini, A., Grieco, G., Diella, V. (2009) *Ferritchromite and Cr–chlorite formation in Kalkan serpentinitic melange (Southern Urals, Russia).* Am. Mineral. 94, 1459–1467.

Mohanty, J.K., Sahoo, R.K., Paul, A.K. (1996) *Chromite alteration at Boula-Nausahi igneous complex, Orissa*. J. Geol. Soc. India 48, 265–276.

Mondal, S.K. & Mathez, E.A. (2007) *Origin of the UG2 chromitite layer, Bushveld Complex*. J. Petrol., 48, 495-510.

Muller, B.G.J., Ashwal, L.D., Tucker, R.D., Rambeloson, R.A. (1997) *The Ranotsara Shear Zone, central Madagascar*. In: Cox R. and Ashwal L.D. (Eds.) Abstracts to IGCP 348/368, Proterozoic Geology of Madagascar. Gondwana Research Group Misc. Publ., 5, 60-61.

Naldrett, A.J., Kinnarid, J., Wilson, A., Yudovskaya, M., McQuade, S., Chunnett, G. and Stanley, C. (2009) *Chromite composition and PGE content of Bushveld chromitites*: Part 1 – the Lower and Middle Groups. Institution of Mining and Metallurgy, Transactions, Section B: Applied Earth Science: 118, 3/4, 131-161.

Nafziger, R.H. (1982) *A review of the deposits and beneficiation of lower-grade chromite*. J. South African Inst. Mining and Metallurgy, 205–226.

Naldrett, A.J., Wilson, A., Kinnaird, J. & Chunnet, G. (2009) *PGE tenor and metal ratios within and below the Merensky Reef, Bushveld Complex: Implications for its genesis*. Journal of Petrology, 50, 625-659.

Pagé, P. & Barnes, S.J. (2009) *Using trace elements in chromites to constrain the origin of podiform chomitites in the Thetford mines ophiolite, Québec, Canada*. Economic Geol. 104, 997-1018.

Papp, J.F. (2001) *Chromium*. Pages 44-45 in Mineral Commodity Summaries 2001. Reston, VA: USGS.

Papp, J.F. (2005) *Chromium*. Minerals Yearbook 2003. Volume 1.

Papp, J.F. (2011) *Chromium in metals and minerals*. U.S. Geological Survey Mineral Yearbook 2009, v. I, p. 17-22.

Pascoe, R.D., Power, M.R., Simpson, B. (2007) *QUEMSCAN analysis as a tool for improved understanding of gravity separator performance*. Miner. Eng. 20, 487–495.

Prendergast, M.D. (2008) *Archean komatiitic sill-hosted chromite deposits in the Zimbabwe Craton*. Economic Geol. 103, 981-1004.

Raharimahefa, T. & Kusky, T.M. (2009) *Structural and remote sensing analysis of the Betsimisaraka Suture in northeastern Madagascar*. Gondwana Research, 15, 14-27.

Ravelonandro, V.M.G. (2011) *Etude des intrusions basiques et ultrabasiques chromiferes d'Anosibe, commune rurale de Belobaka, District de Tsiroanomandidy*. Unpublished PhD thesis, Université d'Antananarivo, Ecole Superieure Polytechnique, 90 pp.

Roeder, P.L. (1994) *Chromite: from the fiery rain of chondrules to the Kilauea Iki lava lake*. Canad. Mineral., 32, 729-746.

Rollinson, H. (1997) *The Arkean komatiite-related Inyala chromitite, Southern Zimbabwe*. Economic Geol. 92, 98-107.

Schofield, D.I., Thomas, R.J., Goodenough, K.M., De Waele, B., Pitfield, P.E.J., Key, R.M., Bauer, W., Walsh, G., Lidke, D., Ralison, A.V., Rabarimanana, M., Rafahatelo, J.M., Randriamananjara, T. (2010) *Geological evolution of the Antongil Craton, NE Madagascar*. Precambrian Research, 182, 187–203.

Schulz, N.F. (1970) *Separation efficiency*. TRANS. SME-AIME. 247, 56.

Service Geologique de Madagascar (SIGM) (1984) *Chromite de Madagascar*. Ministère de l'energie et des mines. Rapport. Antananarivo, 1984.

Shallo, M. (1990) *Volcanic glasses of the Albanian ophiolite belts.* In: Malpas, J., Moores, E.M., Panayiotou, A., Xenophontos, C. (Eds.), Ophiolites: Oceanic Crustal Analogues: Geological Survey Department, Cyprus, pp. 271–278.

Shallo, M., Dilek, Y. (2003) In: Dilek, Y., Newcomb, S. (Eds.) *Development of the ideas on the origin of Albanian ophiolites: Ophiolite Concept and the Evolution of Geological Thought***.** Geological Society of America Special Paper, vol. 373, pp. 351–364.

Shallo, M., Kote, D., Vranai, A. (1987) *Geochemistry of the volcanics from ophiolitic belts Albanides.* Ofioliti 12, 125–136.

Shallo, M., Kodra, A., Gjata, K. (1990) *Geotectonics of the Albanian ophiolites.* In: Malpas, J., Moores, E.M., Panayiotou, A., Xenophontos, C. (Eds.), Ophiolites: Oceanic Crustal Analogues: The Geological Survey Department, Cyprus, pp. 265–270.

Spandler, C. Mavrogenes, J., Arculus, R. (2005*) Origin of chromitites in layered intrusions: Evidence from chromite-hosted melt inclusions from the Stillwater Complex.* Geology, 33, 893-896.

Stowe, C.W. (1994) *Compositions and tectonic settings of chromite deposits through time*. Economic Geol. 89, 528-546.

Thayer, T.P. (1969) *Gravity differentiation and magmatic replacement of podiform chromite deposits*. Economic Geol. Monograph, 4, 132-146.

Traore, A., Conil, P., Houot, R., Save, M. (1995) *An evaluation of the Mozley MGS for fine particle gravity separation.* Miner. Eng. 8(7), 767–778.

Tucker, R.D., Roig, J.Y., Delor, C., Amelin, Y., Goncalves, P., Rabarimanana, M.H., Ralison, A.V., Belcher, R.W. (2010) *Neoproterozoic Extension in the Greater Dharwar Craton: a reevaluation of the "Betsimisaraka Suture‖" in Madagascar.* Canadian Journal of Earth Science, 48, 389–417.

Tucker, R.D., Roig, J.Y., Macey, P.H., Delor, C., Amelin, Y., Armstrong, R.A., Rabarimanana, M.H., Ralison, A.V. (2011) *A new geological framework for south-central Madagascar, and its relevance to the "out-of-Africa" hypothesis.*

UT (2009) *Relazione finale Befandriana.* In italian, United Technologies internal report, 15 pp.

Vantongeren, J.A., Mathez, E.A., Kelemenn, P.B. (2010) A Felsic end to Bushveld Differentiation. Journal of Petrol, 51, 9, 1891-1912.

Vermaak, C.F. (1986) *Summary aspects of the economics of chromium with special reference to Southern Africa*. Mineral deposits of Southern Africa. Volume 2. Pages 1155-1182.

Wills, B.A. (1979) *Mineral processing technology.* Pergamon Books Inc., Elmsford , 650 pp.

Wills, B.A. & Napier-Munn (2006) *Wills' mineral processing technology.* Butterworth-Heinemann, Oxford, 444 pp.

Wills, B.A. & Atkinson, K. (1991) *The development of mineral engineering in the 20th century.* Minerals Engng., 4(7-11), 643.

Wills, B.A. and Atkinson, K. (1993) *Some observations on the fracture and liberation of mineral assemblies*. Minerals Engng., 6(7), 697.

Zhou, M.F. & Robinson, P.T. (1997) *Origin and tectonic environment of podiform chromite deposits*. Economic Geol. 92, 259-262.

Acknowledgements

Grazie a chi mi ha aiutato con passione e professionalità ad acquisire conoscenze, capacità e competenze scientifiche di cui farò sicuramente tesoro.

Grazie a chi mi ha dato la possibilità di viaggiare molto. Ho visitato Paesi splendidi e luoghi impensabili, incontrando persone di diverse nazionalità, persone incredibili e talvolta stravaganti. Ho conosciuto usi, costumi e tradizioni che sono agli antipodi rispetto alla mia vita quotidiana. Ho sviluppato un intenso spirito di adattamento vivendo in situazioni sia psicologicamente sia fisicamente difficoltose e riuscendo a cavarmela anche da sola. Ho imparato ad apprezzare e ad ascoltare il silenzio durante i momenti di solitudine.

Grazie a chi mi ha dato l'opportunità di vivere e studiare nella Grande Mela. Non riesco a descrivere con le parole le emozioni provate, ma posso solamente dire che è stata l'esperienza più bella della mia vita. Attraversare in solitaria il Brooklyn Bridge al tramonto è da brivido!

Grazie a chi mi ha supportato e sopportato restando sempre al mio fianco nel momento del bisogno.

Grazie al mio fidanzato Luca che con sincero amore e profonda stima mi ha spronato a dare il meglio di me stessa in questi ultimi mesi durante i quali lo sconforto e la demotivazione hanno prevalso a causa della difficile e finora vana ricerca del lavoro.

Grazie alla mia famiglia (terrestri e celesti) e specialmente alla Mamma perché: "per arrivare alla fine della scalata ci vogliono i giusti appigli ed io li ho trovati in voi che ogni giorno mi confermate un affetto che va al di là del quotidiano contatto ma è semplicemente quel "tocco di cuore" che dà voce alla mia forza di continuare a crederci!!!"

Lo studio della geologia, dei giacimenti minerari, dell'ingegneria mineraria e delle innovative tecniche analitiche mi ha permesso di vivere esperienze uniche e di provare fortissime emozioni sia positive sia negative, che resteranno per sempre impresse nella mia mente come fossero delle fotografie istantanee.

Grazie di cuore a tutte le persone che hanno reso questi tre anni di dottorato di ricerca speciali e indimenticabili.

"É molto semplice: non si vede bene che col cuore. L'essenziale è invisibile agli occhi"
(Il Piccolo Principe)